Electronic Supplementary Material (ESI) for Green Chemistry.
This journal is © The Royal Society of Chemistry 2024

Supporting information

Mechanochemical Aerobic Oxidative Heck Coupling by Polymer-Assisted Grinding: Cyclodextrin Additive Facilitating Regioselectivity Control

Keyu Xiang[a], Haowen Shou[a,b], Chenhui Hu[a], Weike Su[a], Jingbo Yu[a]*

[a] *Laboratory of Pharmaceutical Engineering of Zhejiang Province, Key Laboratory for Green Pharmaceutical Technologies and Related Equipment of Ministry of Education, Collaborative Innovation Center of Yangtze River Delta Region Green Pharmaceuticals, Zhejiang University of Technology. Hangzhou. 310014, P. R. China. E-mail: yjb@zjut.edu.cn*

[b] *State Key Laboratory of Drug Research, Shanghai Institute of Materia Medical, Chinese Academy of Sciences. Shanghai, 201203, P.R. China.*

Table of Contents

1. General information

Unless otherwise stated, all reagents were purchased from commercial suppliers and used without further purification. All of the ball-milling reactions were conducted in a Mixer mill (MM 400 RetschGmbh, Hann, Germany) with 25/50 mL stainless-steel grinding jars (custom-built stainless jar) with stainless-steel balls (d_{MB} = 1.2 cm), if not mentioned otherwise. Reactions were monitored by Thin Layer Chromatography (TLC) using UV light (254/365 nm) for detection. Flash chromatography was carried out using silica gel (200-300 mesh). ^{1}H, ^{13}C and ^{19}F NMR spectra were recorded on Bruker 400, 500 or 600 MHz spectrometer in $CDCl_3$ or d_6-DMSO with tetramethylsilane (TMS) as internal standard. The following abbreviations were used to explain multiplicities: s = singlet, brs = broad singlet, d = doublet, t = triplet, dd = doublet of doublets, m = multiplet and the *J* coupling constants were reported in Hertz unit (Hz). Melting points were measured using an SRS OptiMelt MPA100 apparatus and were uncorrected. High Resolution Mass spectra (HRMS) and Electron Impact mass spectrometry (EI) were recorded on Bruker micrOTOF-Q II 10366, Agilent 6890-GCT Premier or Agilent 8890 GC / 7250 Q-TOF MS. Inductively Coupled Plasma-Mass Spectrometry (ICP-MS) was record on Agilent 7700. X-ray photoelectron spectroscopy (XPS) was measured by Thermo Scientific K-Alpha+. Transmission Electron Microscope (TEM) experiments were recorded with Hitachi HT7700 EXALENS. Scanning Electron Microscope (SEM) experiments were recorded with Zeiss Gemini 500.

2. General procedures for the synthesis of substrates

The olefin derivatives were synthesized according to Ref 1-8. (Table S1)

Table S1 The synthesis of known olefins derivatives

Substrates	Ref		Ref
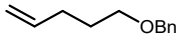 **2c**	1	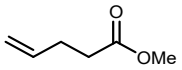 **2e**	2
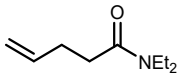 **2f**	3	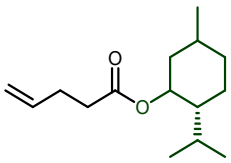 **2q**	4
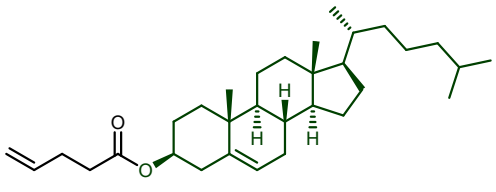 **2r**	5	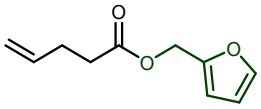 **2s**	6
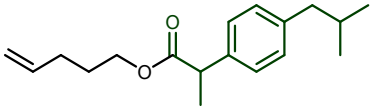 **2u**	7	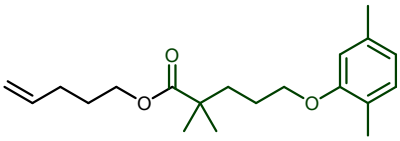 **2v**	8

N-(adamantan-1-yl)pent-4-enamide (**2t**) was prepared by modified approach according to Ref[3] from the amantadine. The product was purified by flash column chromatography on silica gel.

White solid, mp 76–78 °C; **^{1}H NMR** (600 MHz, Chloroform-*d*) δ 5.86 – 5.78 (m, 1H), 5.13 (s, 1H), 5.08 – 5.04 (m, 1H), 5.02 – 4.97 (m, 1H), 2.39 – 2.31 (m, 2H), 2.17 (t, *J* = 7.4 Hz, 2H), 2.06 (s, 3H), 1.98 (d, *J* = 2.8 Hz, 6H), 1.67 (s, 6H). **^{13}C NMR** (150 MHz, Chloroform-*d*) δ 171.3, 137.3, 115.4, 51.9, 41.8 (3C), 36.9, 36.4 (3C), 29.7, 29.5 (3C).

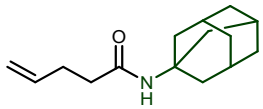

2t

3. Reaction optimization & typical procedures

Table S2. Optimization of the reaction conditions[a]

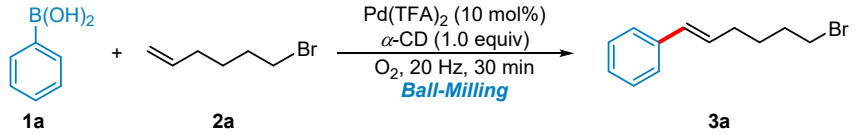

1a **2a** **3a**

Entry	Variation	Yield%[d]
1	none	30
2	$Pd(OAc)_2$ instead of $Pd(TFA)_2$	22
3	$Pd[O_2C(CH_3)_3]_2$ instead of $Pd(TFA)_2$	trace
4	β-CD instead of α-CD	20
5	γ-CD instead of α-CD	17
6	α-CD (2.0 equiv.)	trace
7	α-CD (0.8 equiv.)	51
8	α-CD (0.6 equiv.)	57
9	α-CD (0.4 equiv.)	63
10	α-CD (0.2 equiv.)	50
11	α-CD (0.1 equiv.)	37
12	without CD	10
13	$Pd(TFA)_2$ (5 mol%), α-CD (0.4 equiv.)	22
14	$Pd(TFA)_2$ (7 mol%), α-CD (0.4 equiv.)	46
15	$Pd(TFA)_2$ (10 mol%), methyl α-*D*-glucopyranoside (0.4 equiv)	trace
16	$Pd(TFA)_2$ (10 mol%), α-lactose monohydrate (0.4 equiv.)	trace
17	$Pd(TFA)_2$ (10 mol%), starch soluble (0.4 equiv.)	21
18[b]	$Pd(TFA)_2$ (10 mol%), α-CD (0.4 equiv.)	9
19[c]	$Pd(TFA)_2$ (10 mol%), α-CD (0.4 equiv.)	trace

[a] Reaction conditions: **1a** (0.5 mmol), **2a** (1.0 mmol), $Pd(TFA)_2$ (10 mol%) and an additive were placed in a custom-built stainless-steel vessel with two stainless-steel balls ($\varnothing$ = 1.2 cm) milling at 20 Hz for 30 min under an oxygen atmosphere.

[b] Comparative experiment: **1a** (0.5 mmol), **2a** (1.0 mmol), $Pd(TFA)_2$ (10 mol%), α-CD (0.4 equiv) and DMF (5 mL), 50 °C, 24 h under an oxygen atmosphere.

[c] Comparative experiment: **1a** (0.5 mmol), **2a** (0.5 mmol), $Pd(TFA)_2$ (10 mol%) and α-CD (0.4 equiv.) were placed in a stainless-steel jar without agitation for 4 h under an oxygen atmosphere, then aging in an flask for 7 days under an oxygen atmosphere.

[d] Isolated yields.

3.1 Influence of the milling time and frequency on the oxidative Heck reaction

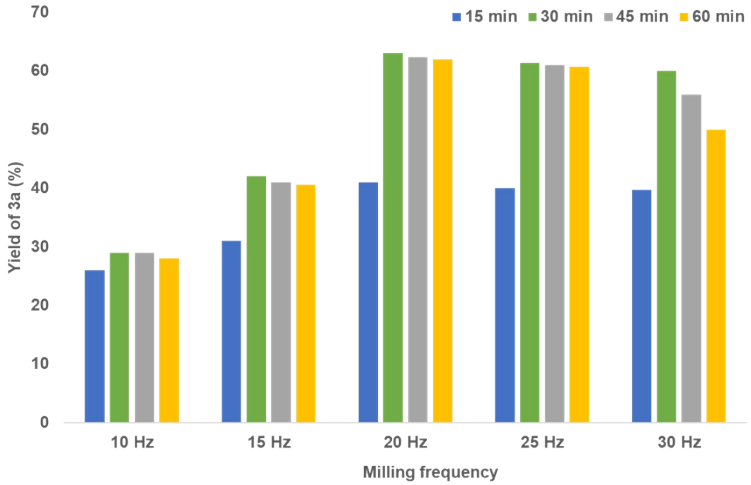

Figure S1. Effect of milling time and frequency on the reaction yield. Reaction condition: **1a** (0.5 mmol), **2a** (0.5 mmol), $Pd(TFA)_2$ (10 mol%)and α-CD (0.4 eq.) were grinded for a certain time at a certain frequency, using two stainless-steel balls ($\varnothing$ = 1.2 cm) in a 25 mL custom-built stainless jar under O_2 atmosphere.

3.2 Influence of the oxygen flow rate on the oxidative Heck reaction

A gas flowmeter was utilized to precisely monitor and regulate the oxygen flow rate.

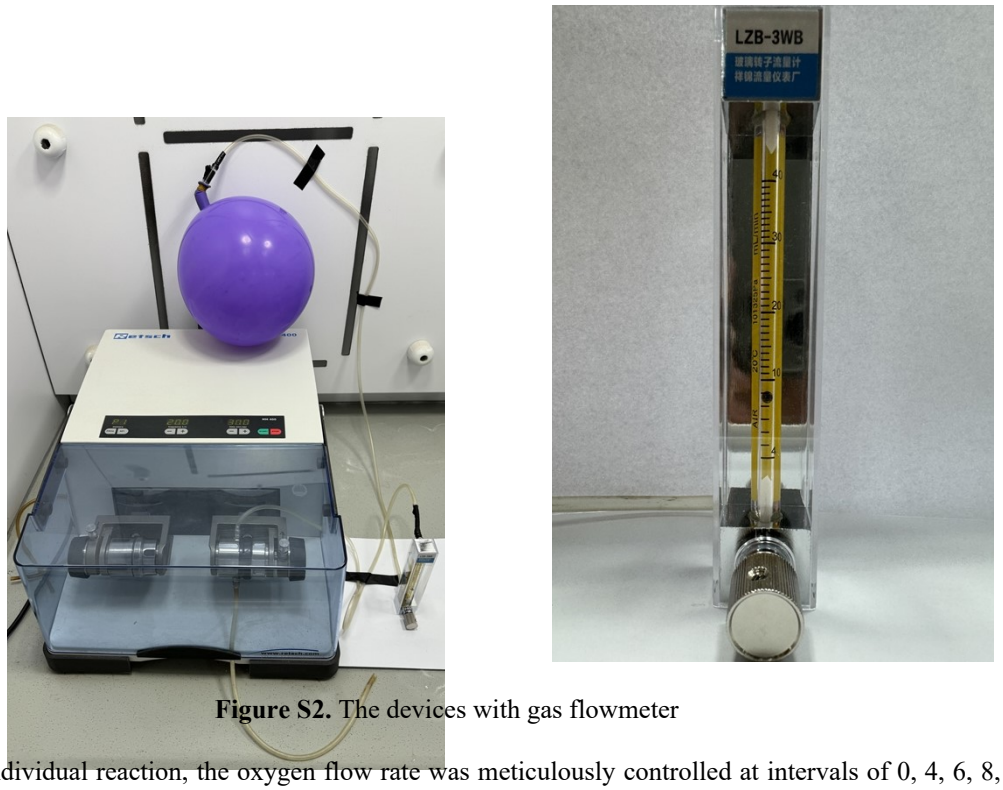

Figure S2. The devices with gas flowmeter

In each individual reaction, the oxygen flow rate was meticulously controlled at intervals of 0, 4, 6, 8, 10, and 15 $mL \cdot min^{-1}$, ensuring constant surveillance through the use of a gas flowmeter. The influence of these flow rates on the product yields was graphically illustrated in Figure S3. Our findings revealed

the presence of a critical threshold value around 6 mL·min^{-1} for this particular reaction process. Below this threshold (at flow rates less than 6 mL·min^{-1}), the reaction yield was notably suppressed. Upon reaching the optimal flow rate of 6 mL·min^{-1}, the reaction yield attained its maximum level. Subsequently, escalating the oxygen flow rate beyond this point did not result in any further enhancement of the reaction yield.

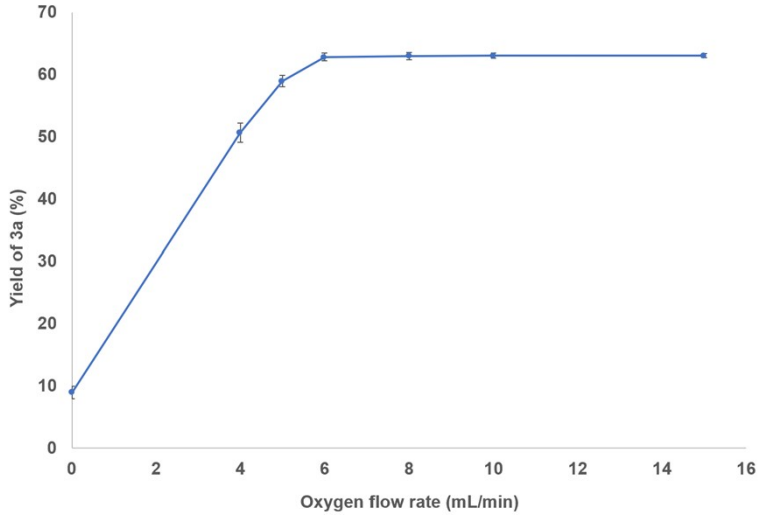

Figure S3. Effect of O_2 flow rate on the reaction yield. Reaction condition: **1a** (0.5 mmol), **2a** (0.5 mmol), $Pd(TFA)_2$ (10 mol%) and α-CD (0.4 eq.) were milled for 30 min at 20 Hz, using two stainless-steel balls ($\varnothing$ = 1.2 cm) in a 25 mL custom-made stainless jar under O_2 atmosphere with a certain O_2 flow rate. Experimental data were performed in triplicate.

3.3 Influence of the jar and ball sizes on the oxidative Heck reaction

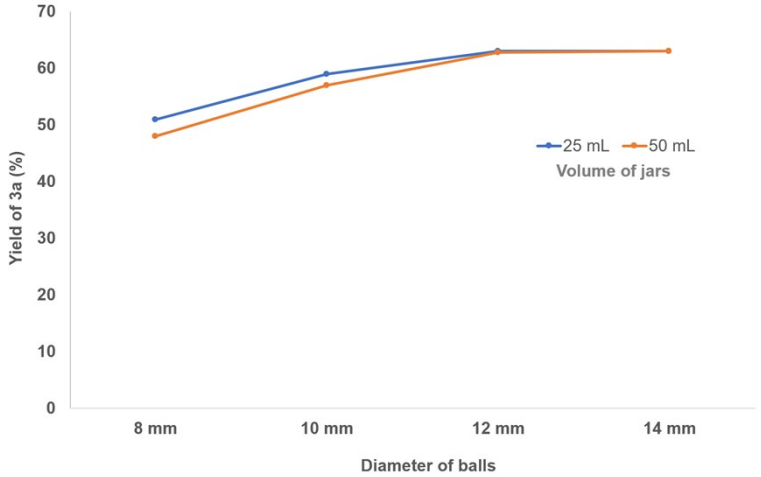

Figure S4. Effect of jar and ball sizes on the reaction yield. Reaction condition: **1a** (0.5 mmol), **2a** (0.5 mmol), $Pd(TFA)_2$ (10 mol%) and α-CD (0.4 eq.) were milled for 30 min at 20 Hz, using two stainless-steel balls (with different size) in a 25/50 mL custom-made stainless jar under O_2 atmosphere.

We have conducted this reaction in a custom-made, ventilated 25/50 mL stainless jar, using milling balls of various size. The graphical representation in Figure S4 elucidates the effects of both jar and ball sizes

on the product yields. Using smaller ball with diameters of ø 0.8 or ø 1.0 cm results in reduced mechanical force exerted on the material, causing inadequate dispersion of reagents and heightened aggregation. This issue becomes more pronounced in larger jars, leading to a more significant decline in yield. Conversely, using larger balls with a diameter of ø1.4 cm did not prove beneficial in enhancing the reaction performance.

3.4 The morphology of the reaction mixtures with different amount of *α*-CD

Figure S5. The status of the reaction mixtures after ball milling using different amounts of *α*-CD (a 2.0 equiv. *α*-CD, b 0.4 equiv. *α*-CD, c 0.1 equiv. *α*-CD)

The investigation of the amount of *α*-CD showed that 0.4 eq *α*-CD gave the best performance. Lowering its usage to 0.1 equiv. resulted in poor substrate dispersion and thereby low yield. Conversely, using an excess of *α*-CD (2.0 eq) also led to decreased yield, which was probably raised by the dilution of reagents.

3.5 Influence of different CDs on the oxidative Heck reaction

(a) The influence of CDs on the reaction of 6-bromohex-1-ene and phenylboronic acid

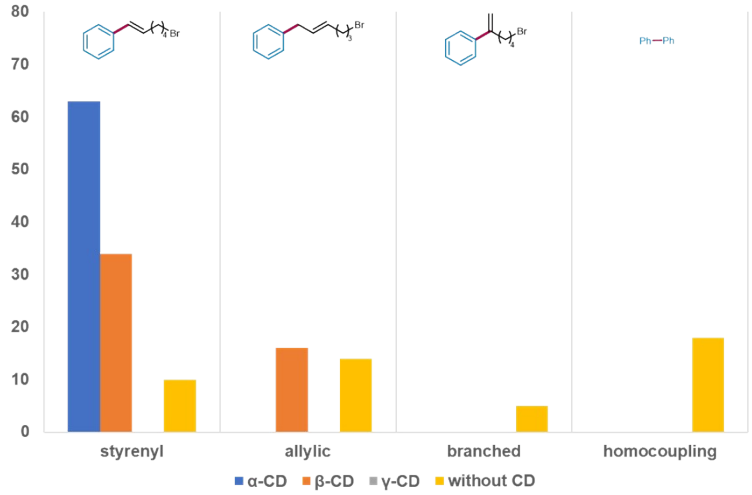

Figure S6. The influence of CDs on the reaction of 6-bromohex-1-ene and phenylboronic acid. Reaction condition: **1a** (0.5 mmol), **2a** (0.5 mmol) and CDs (0.4 eq.) were milled for 30 min at 20 Hz, using two stainless-steel balls (*ø* = 1.2 cm) in a 25 mL custom-made stainless jar under O_2 atmosphere.

When *α*-CD was used as PLOAGs, only the styrenyl product was formed, whereas the used of *β*-CD led to a mixture of styrenyl and allylic products. No products were detected when *γ*-CD was utilized. In the absence of PLOAGs, the reaction afforded a mixture of styrenyl, allylic, branched,

and homocoupling products, highlighting the significant role of CD in regulating the selectivity for this oxidative Heck reaction.

(b) The influence of CDs on the reaction of cyclopentene and phenylboronic acid

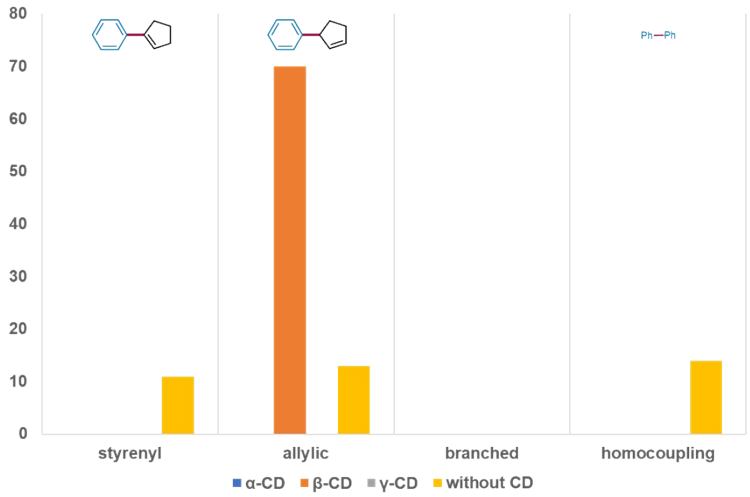

Figure S7. The influence of CDs on the reaction of cyclopentene and phenylboronic acid. Reaction condition: **1a** (0.5 mmol), **4l** (1.0 mmol) and CDs (0.4 eq.) were milled for 30 min at 20 Hz, using two stainless-steel balls ($\varnothing$ = 1.2 cm) in a 25 mL custom-made stainless jar under O_2 atmosphere.

The use of α-CD and γ-CD did not lead to the formation of any product, with only the allylic product being detected when employing β-CD as POLAGs. Milling the reactants in the absence of POLAGs resulted in a mixture of styrenyl/allylic/homocoupling products.

(c) The influence of CDs on the reaction of cyclooctene and phenylboronic acid

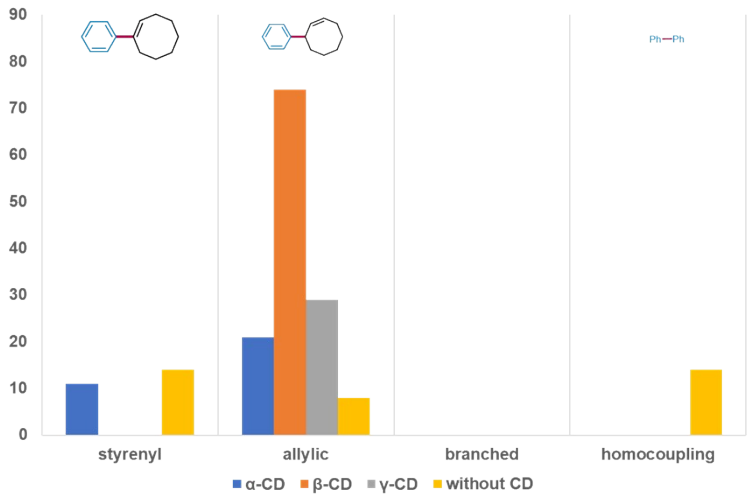

Figure S8. The influence of CDs on the reaction of cyclooctene and phenylboronic acid. Reaction condition: **1a** (0.5 mmol), **4n** (1.0 mmol) and CDs (0.4 eq.) were milled for 30 min at 20 Hz, using two stainless-steel balls ($\varnothing$ = 1.2 cm) in a 25 mL custom-made stainless jar under O_2 atmosphere.

When α-CD was used as a POLAGs, a mixture of styrenyl/allylic products was obtained in relatively low yield. In sharp contrast, β-CD resulted in a good yield of allylic product exclusively, while a substantial decrease in yield was observed when using γ-CD. Milling the reactants in the absence of POLAGs gave a mixture of styrenyl/allylic/homocoupling products.

(d) The influence of CDs on the reaction of camphene and phenylboronic acid

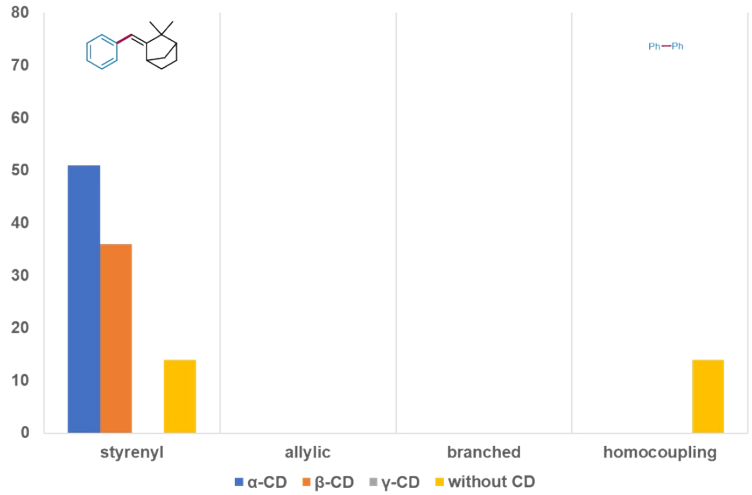

Figure S9. The influence of CDs on the reaction of camphene and phenylboronic acid. Reaction condition: **1a** (0.5 mmol), **4i** (0.5 mmol) and CDs (0.4 eq.) were milled for30 min at 20 Hz, using two stainless-steel balls ($\varnothing$ = 1.2 cm) in a 25 mL custom-made stainless jar under O_2 atmosphere.

When α-CD and β-CD were employed as POLAG additives, only the styrenyl product was detected. no products were obtained when using γ-CD. Milling the reactants in the absence of POLAGs gave a mixture of styrenyl/homocoupling products.

Note: plausible mechanisms are hypothesized in Section 4.

3.6 Typical procedures for the oxidative Heck reaction

Typical procedures for the oxidative Heck reaction in ball-milling: A mixture of phenylboronic acid (0.5 mmol, 1.0 equiv.), olefins **2** or **4** (0.5 mmol, 1.0 equiv.), $Pd(TFA)_2$ (10 mol%) and α-CD (0.2 mmol, 0.4 equiv.) were placed in a custom-made stainless-steel jar (25 mL) with two stainless-steel balls ($\varnothing$ = 1.2 cm). The jar was connected to a balloon filled with oxygen and milling at 20 Hz for 30 min (Figure S10, also see the video in ESI). After the milling was finished, the contents were scratched off the jar and purified by column chromatography on silica gel using hexane to give the desired products.

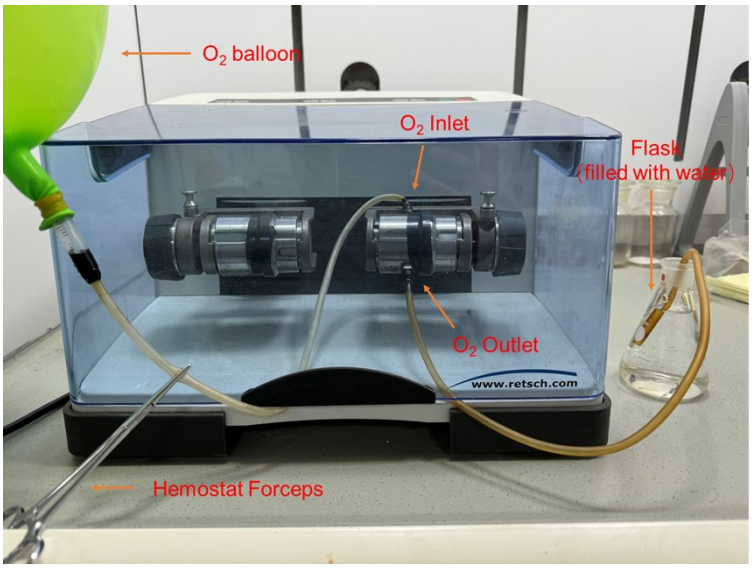

Figure S10. The device of gas-assisted ball-milling reaction (custom-made stainless-steel jar). An O_2 balloon was employed to provide a continuous supply of oxygen, hemostat forceps were used to control the oxygen flow rate, and a flask filled with water served to monitor the flow of oxygen.

Typical procedures for the oxidative Heck reaction with volatile olefins in ball-milling: A mixture of phenylboronic acid (0.5 mmol, 1.0 equiv.), olefins **4** (1 mmol, 2.0 equiv.), $Pd(TFA)_2$ (10 mol%) and CDs (0.2 mmol, 0.4 equiv.) were placed in a custom-made stainless-steel jar (25 mL) with two stainless-steel balls ($ø$ = 1.2 cm). The jar was connected to a balloon filled with oxygen and milling at 20 Hz for 30 min. After the milling was finished, the contents were scratched off the jar, then *purified by rinsing with cyclohexane, followed by filtration to collect the filtrate. Next the cyclohexane and excess volatile olefins were removed via vacuum distillation.*

The volatile olefins (bp. < 130 ℃) including 1-octene, neohexene, 2,4,4-trimethyl-1-pentene, 1-vinylcyclohexene, cyclopentene, cyclohexene, cyclooctene.

Typical procedure for the oxidative Heck reaction in solution: A mixture of phenylboronic acid (0.5 mmol, 1.0 equiv.), 6-bromohex-1-ene **2a** (0.5 mmol, 2.0 equiv.), $Pd(TFA)_2$ (10 mol%), α-CD (0.2 mmol, 0.4 equiv.) and DMF (5 mL) were placed in a round-bottomed flask, then stirred at 50 ℃ for 24 h under an oxygen atmosphere.

3.7 The oxidative Heck reaction of substituted arylboronic acids

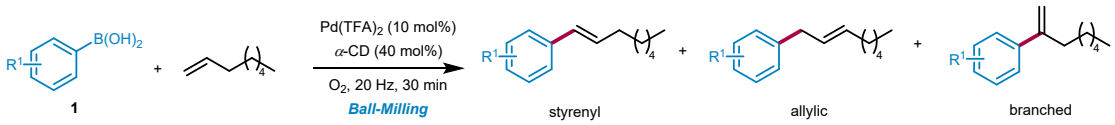

R^1 = 2,4-Me		45%	45%	10%
R^1 = 4-Br		53%	29%	18%
R^1 = 4-^{i}Pr		41%	43%	16%
R^1 = H *	* silica gel instead of α-CD	27%	62%	11%

Scheme S1. The oxidative Heck reaction of substituted arylboronic acids. Determined by ^{1}H NMR spectroscopy.

Unfortunately, in this reaction system, some arylboronic acids with different substituents exhibited bad performance when coupling with an alternative olefin (octylene), resulting in poor regioselectivity. However, in the absence of α-CD, a lower selectivity of 27/73 for styrenyl/other isomers was obtained, highlighting the key role of α-CD in regulating the regioselectivity for the oxidative Heck reaction. *A plausible mechanism will be hypothesized in Section 4.*

3.8 Recycling of CDs

After the reaction was completed, the mixtures were placed to the Buchner funnel, rinsing with cyclohexane. The filter residue could be directly used for the next reaction after drying under reduced pressure. (The dried residue is what we called Pd/CD)

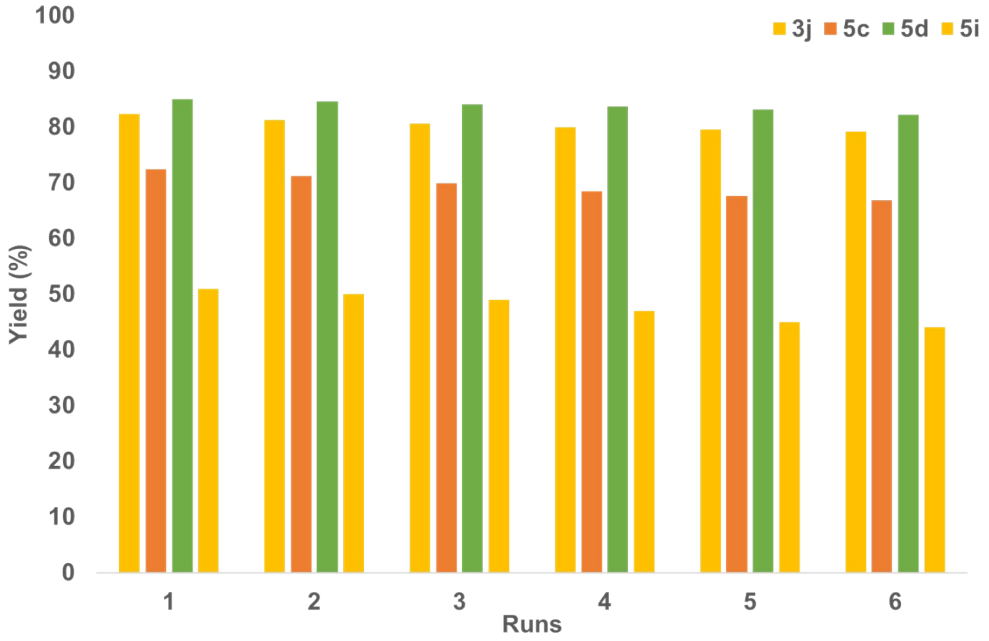

Figure S11. Recycling of Pd/α-CD for the synthesis of **3j**/**5c**/**5d**/**5i**

3.9 Determination of palladium traces in Pd/CD sample using ICP-MS analysis

Table S3. ICP-MS analysis of Pd/CD

Sample	Pd content (%)
Pd/CD after 1st run	1.49
Pd/CD after 3rd run	1.32
Pd/CD after 5th run	0.92

3.10 X-ray photoelectron spectroscopy (XPS) analysis

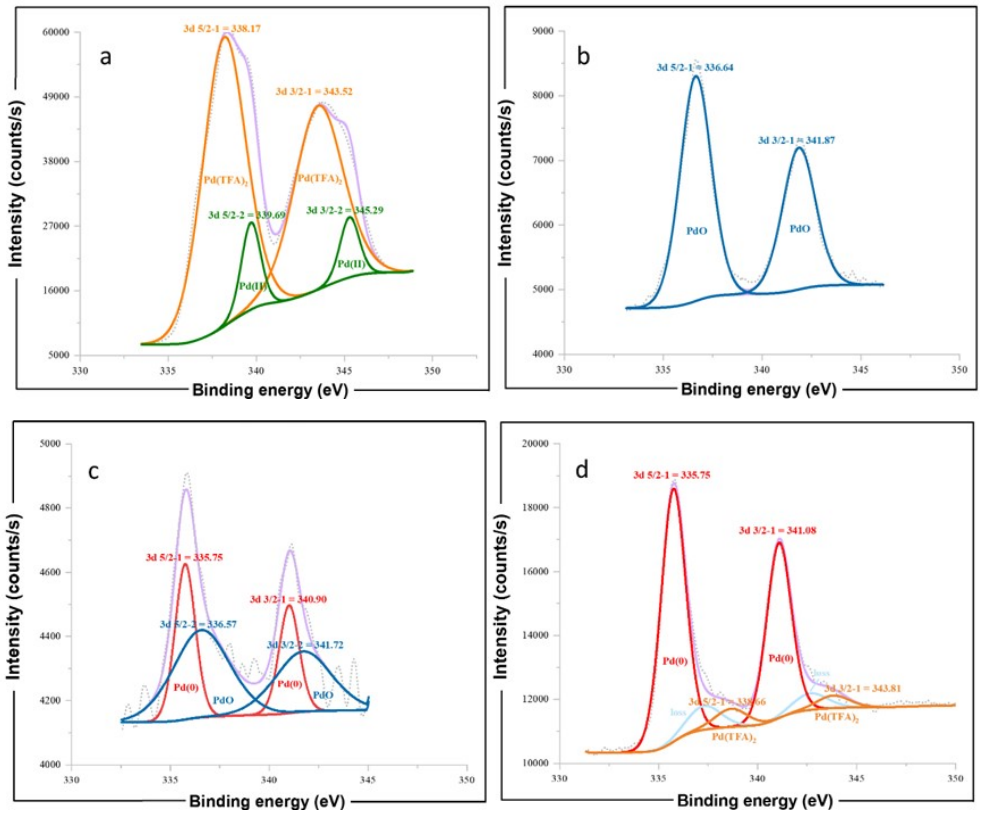

Figure S12. X-ray photoelectron spectroscopy of the mixtures after the reaction

Commercial $Pd(TFA)_2$: Fresh, untreated, commercial $Pd(TFA)_2$

$Pd(TFA)_2$/α-CD (Sample A): The mixture of $Pd(TFA)_2$ and α-CD after 30 min ball-milling at 20 Hz.

Reaction mixture with α-CD (Sample B): The mixture of $Pd(TFA)_2$, olefin, phenylboronic acid and α-CD after 30 min ball-milling at 20 Hz, followed by rising with cyclohexane and drying. (Pd/CD)

Reaction mixture without α-CD (Sample C): The mixture of $Pd(TFA)_2$, olefin and phenylboronic acid after 30 min ball-milling at 20 Hz, followed by rising with cyclohexane and drying.

The values of 338.17 eV (3d 5/2) and 343.52 eV (3d 3/2) are reported for $Pd(TFA)_2$ in the literature[9]. Additional peaks (339.69 and 345.29 eV) for Pd 3d might be assigned to the impurity in commercial $Pd(TFA)_2$.

3.11 Comparative experiments with jars fabricated from diverse materials

To definitively rule out the potential catalytic behavior of leached metals such as Fe, Co and Ni during the milling process, it was imperative to conduct a comparative study using jars made from diverse materials. Since commercially available, ventilated jars constructed from non-metallic substances are currently lacking, we devised an alternative strategy for control experiments. In this setup, we exposed various material jars and balls to an oxygen atmosphere for a sufficient duration to guarantee that the jars became saturated with oxygen as much as practicable, as depicted in Figure S13.

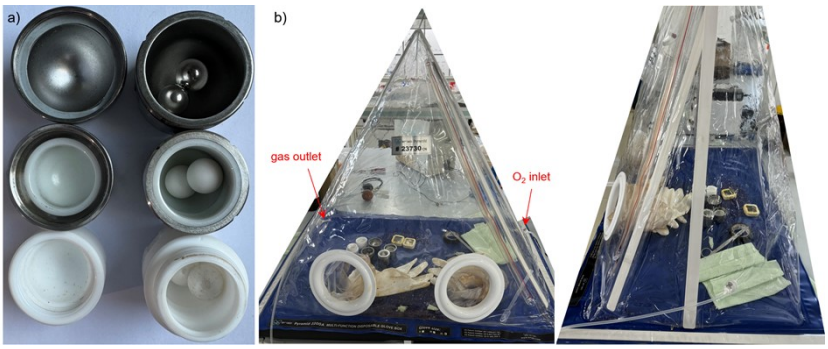

Figure S13. a) The stainless/zirconium oxide/Teflon jars. b) The jars in pyramid glove box under oxygen atmosphere.

To minimize the volatilization of olefins during the oxygen purging process, solid camphene (**4i**) was used as a model substrate. Initially, experiments were carried out in stainless steel (SS) jars with different sizes under ambient air conditions; however, only a marginal amount of product was detected, as the limited oxygen (in air) present in the jar proved insufficient to reoxidize the Pd(0) species effectively. Upon enhancing the oxygen content within the jar, a marked increase in yield was observed. Significantly, no considerable discrepancies were found between the reactions executed in non-metallic material jars and those in SS jars (Table S4, entries 2-4), thus eliminating the likelihood of potential catalytic behavior stemming from leached metals during the mechanochemically activated process. It should be noted that when using the Teflon jar, the yields were relatively low. This reduction can primarily be attributed to the decreased mechanical force imparted by the lighter weight of the Teflon jar.

Table S4. The influences of the jar and balls material on the yield of **5i**[a]

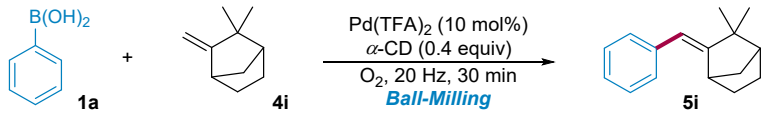

Entry	Material of jars/balls	Size of jars (mL)	Atmosphere	Yield (%)
1	SS/SS	50/25/5	air	14/11/8[b]
2	SS/SS	50/25	O_2	40/34
3	ZrO/ZrO	25	O_2	36
4	Teflon/ZrO	25	O_2	27

[a] Reaction conditions: **1a** (0.5 mmol), **4i** (1.0 mmol), $Pd(TFA)_2$ (10 mol%) and α-CD (0.4 eq.) were added in a jar with two balls ($\varnothing$ = 1.2 cm) following placing them under air/oxygen atmosphere for 1 h, then sealing the jars with electric tape and milling at 20 Hz for 30 min. SS = stainless steel.

[b] One ball is used.

4. The plausible effect of CDs on the reaction

4.1 The influence of CDs on the reaction of 6-bromohex-1-ene and phenylboronic acid

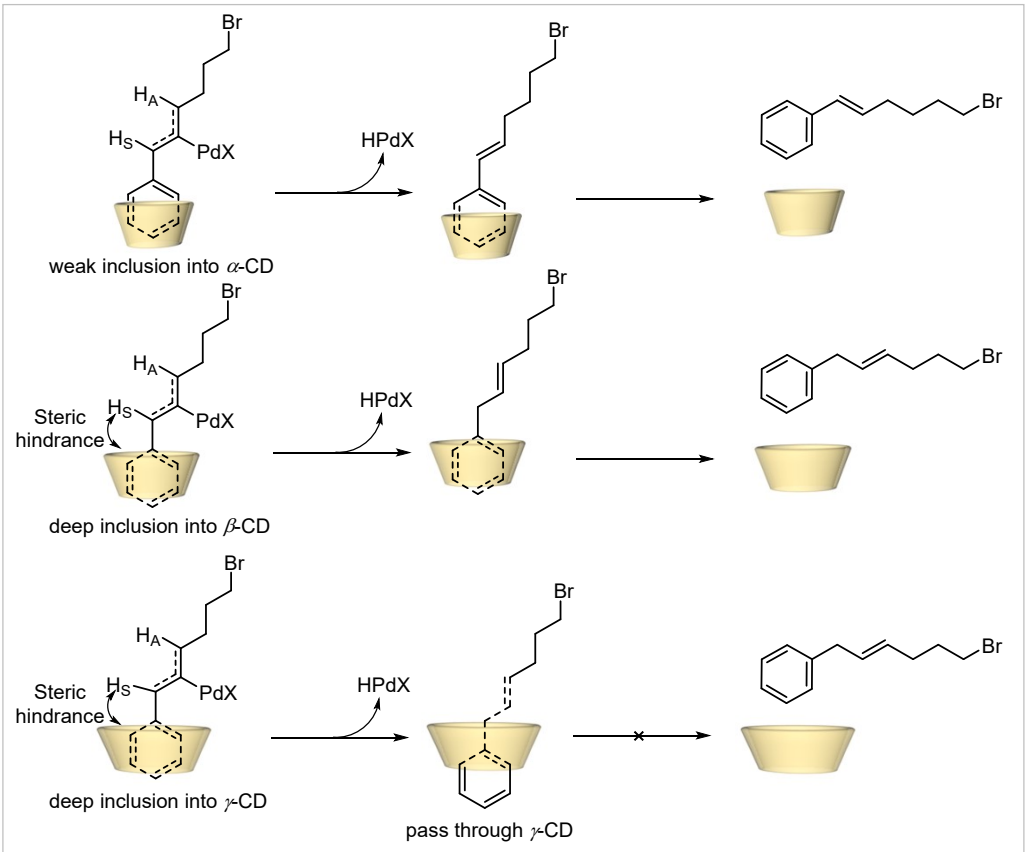

Figure S14. The plausible effect of CDs on the reaction of 6-bromohex-1-ene and phenylboronic acid

The aromatic ring of phenylboronic acid fails to fully enter the cavity of α-CD, and there is almost no steric hinderance during the β-H_S elimination, which lead to the formation a thermodynamically stable styrene type product. The excessive formation of allylic isomer (see Figure S6) can be attributed to a deeper penetration of the aromatic ring into the cavity of β-CD. Upon inclusion of phenylboronic acid, the bulky rigid structure of β-CD and H_S repelled the PdX towards the less hindered H_A to align them coplanar, thereby weakening the β-H_S elimination and leading to the formation of allylic isomer. When the reaction was performed with γ-CD, the intermediate product was well adapted to the CD cavity and was difficult to detach from the cavity, thus inhibiting the formation of product.

4.2 The influence of CDs on the reaction of cyclopentene and phenylboronic acid

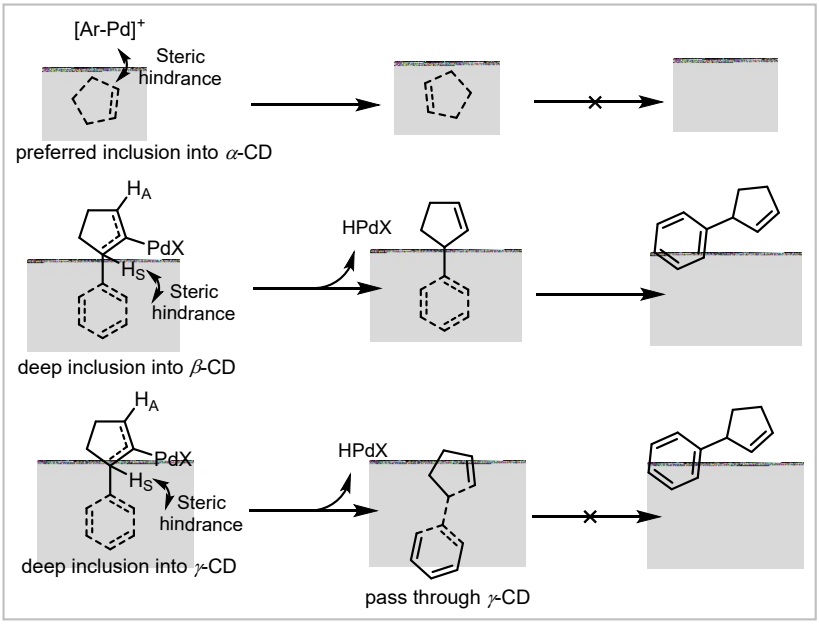

Figure S15. The plausible effect of CDs on the reaction of cyclopentene and phenylboronic acid

The cyclopentene may have good compatibility with the cavity of α-CD, making it difficult to detach once inside, thereby impeding the migration insertion of $[Ar\text{-}Pd]^+$ to olefin and resulting in the absence of product formation. A deeper insertion of the aromatic ring into the cavity of β-CD causes steric hindrance between H_S and CD, favoring the elimination of β-H_A over β-H_S. In the reaction performed with γ-CD, the intermediate product is well accommodated in the CD cavity and proved challenging to detach, leading to no product formation.

4.3 The influence of CDs on the reaction of cyclooctene and phenylboronic acid

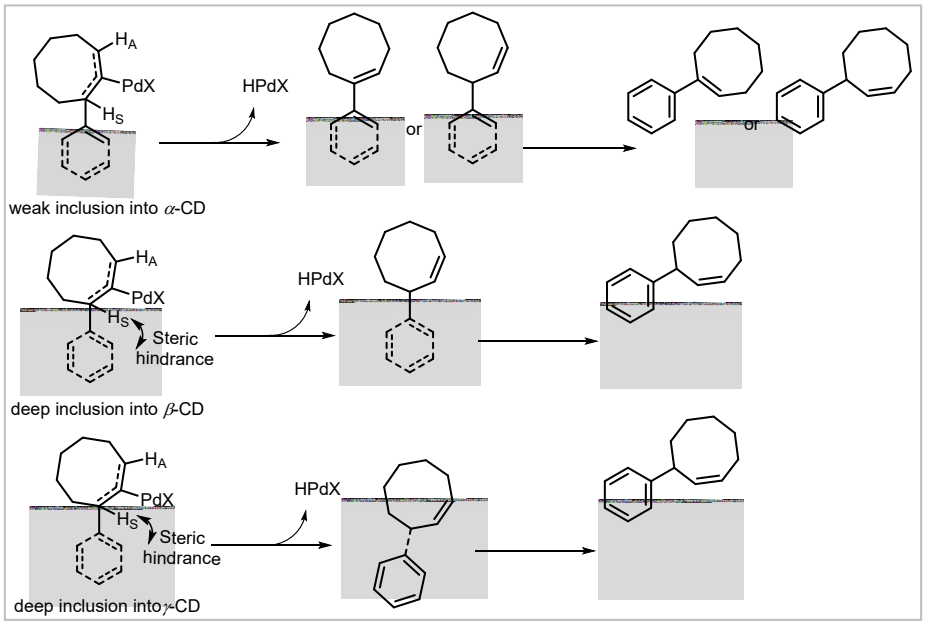

Figure S16. The plausible effect of CDs on the reaction of cyclooctene and phenylboronic acid

Cyclooctene demonstrates distinct behavior compared to cyclopentene, as it is unable to enter the α-CD cavity. When the aromatic ring of phenylboronic acid partially enters the α-CD cavity, there is minimal differentiation between H_A and H_S during the β-H elimination, resulting in a mixture of styrenyl and allylic isomers. Conversely, in the presence of β-CD, the aromatic ring can fully enter the β-CD cavity, favoring the elimination of β-H_A over β-H_S (due to steric hinderance), and thus facilitating the formation of the allylic product. Moreover, the presence of some hindrance between the eight-membrane-ring and CD within the γ-CD cavity causes the intermediate product to slightly detach, furnishing a small amount of allylic product.

4.4 The influence of CDs on the reaction of camphene and phenylboronic acid

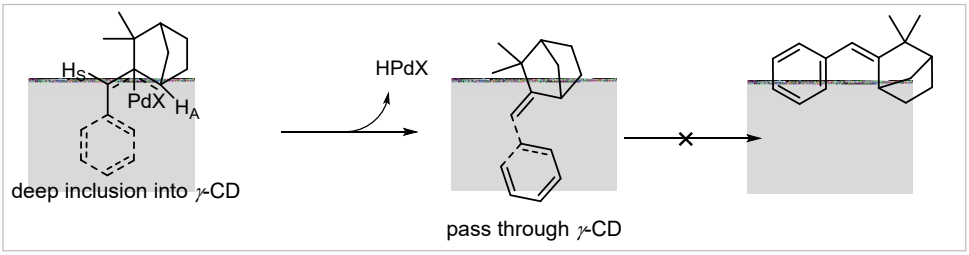

Figure S17. The plausible effect of CDs on the reaction of camphene and phenylboronic acid

Maintaining a coplanar state between the β-H and the departing PdX is essential for the β-H elimination process. However, the rotation of the C–C bond is constrained in bridged-ring compound, which limits the H_A and PdX to being in a coplanar state, leading to a selective styrenyl product. Additionally, the cavity of γ-CD also had good adaptability to the product, rendering detachment from the cavity difficult.

5. Green chemistry metrics calculations

To assess the environmental impact of our mechanochemical reaction in comparison to traditional solution-based approaches[10,11], we quantified various green chemistry metrics such as effective mass yield (EMY), atom economy (AE), atom efficiency (AEF), optimum efficiency (OE), mass productivity (MP), reaction mass efficiency (RME), process mass intensity (PMI), mass intensity (MI), solvent intensity (SI), and *E*-factor. The calculations also accounted for the potential recovery of the additives and catalysts. For simplification, the mass of catalyst and additive were considered as 1/5 (based on 5 runs in the recycling experiments), and the product yield was the average of the five experiments.

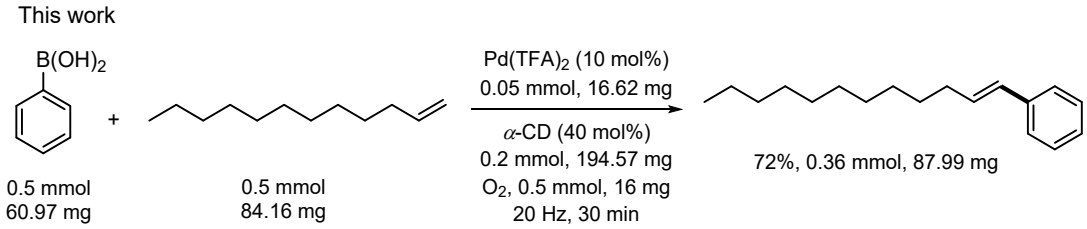

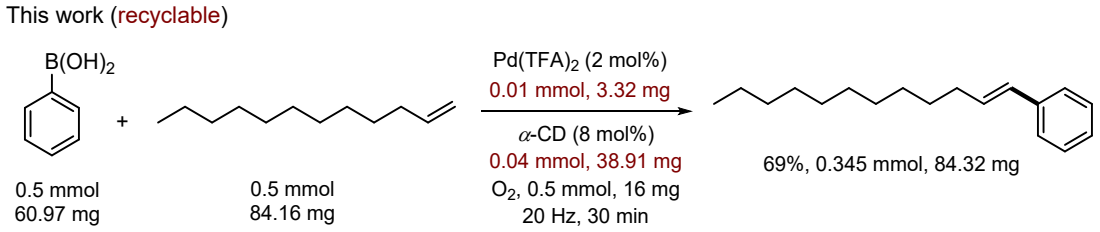

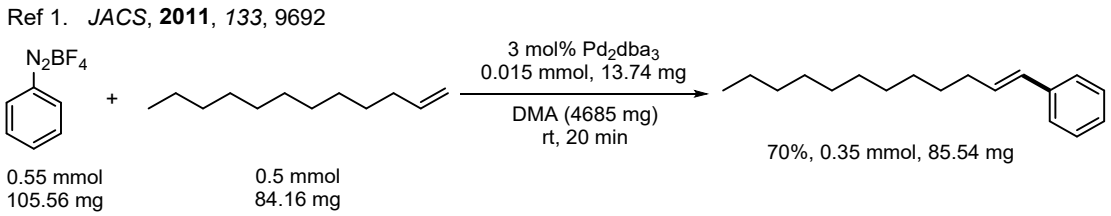

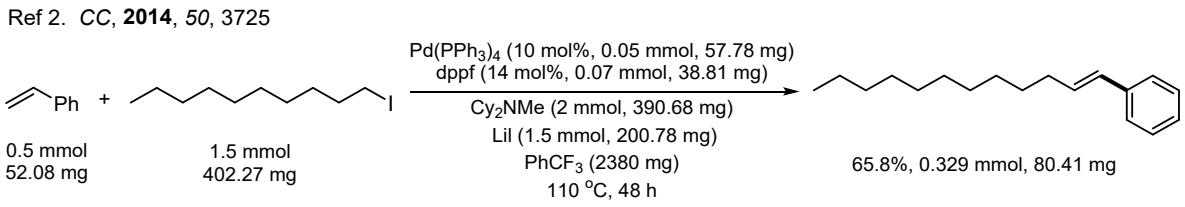

Based on the most advantageous reaction mentioned above, green chemistry metrics were calculated as follows:

$$EMY\ (\%) = \frac{Mass\ of\ product}{Mass\ of\ non-benign\ reagents} \times 100 = \frac{87.99\ mg}{60.97\ mg + 84.16\ mg + 16.62\ mg} \times 100 = 54.4\%$$

$$AE\ (\%) = \frac{Molecular\ weight\ of\ product}{Total\ molecular\ weight\ of\ reagents} \times 100 = \frac{244.41}{121.93 + 168.32 + 32} = 75.8\%$$

$$AEF\ (\%) = AE \times Yield = 75.8\% \times 72\% = 54.6\%$$

$$RME\ (\%) = \frac{Mass\ of\ isolated\ product}{Total\ mass\ of\ reagents} \times 100 = \frac{87.99\ mg}{60.97\ mg + 84.16\ mg + 194.57\ mg + 16\ mg} \times$$

$$OE\ (\%) = \frac{RME}{AE} \times 100 = \frac{23.6\%}{75.8\%} \times 100 = 31\%$$

$$PMI = \frac{Total\ mass\ of\ input\ material}{Mass\ of\ product} = \frac{60.97\ mg + 84.16\ mg + 16.62\ mg + 194.57\ mg + 16\ mg}{87.99\ mg} = 4.23$$

$$MI = \frac{Total\ mass\ of\ input\ material\ (excluding\ water)}{Mass\ of\ product} = \frac{60.97\ mg + 84.16\ mg + 16.6}{87.99}$$
$$= 4.23$$

$$E\text{–}factor = \frac{Total\ mass\ of\ waste}{Mass\ of\ products} = \frac{60.97\ mg + 84.16\ mg + 16.62\ mg + 194.57\ mg + 16\ mg}{87.99\ mg}$$
3.23

$$SI = \frac{Total\ mass\ of\ slovents}{Mass\ of\ product} = \frac{0}{87.99\ mg} = 0$$

6. Characterization data

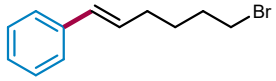

(*E*)-(6-bromohex-1-en-1-yl)benzene (**3a**)[12]

Colorless oil (75.0 mg, 63% yield), **^{1}H NMR** (600 MHz, Chloroform-*d*) δ 7.36 – 7.32 (m, 2H), 7.30 (t, *J* = 7.7 Hz, 2H), 7.22 – 7.18 (m, 1H), 6.40 (d, *J* = 15.8 Hz, 1H), 6.23 – 6.17 (m, 1H), 3.44 (t, *J* = 6.8 Hz, 2H), 2.28 – 2.23 (m, 2H), 1.95 – 1.90 (m, 2H), 1.67 – 1.61 (m, 2H). **^{13}C NMR** (150 MHz, Chloroform-*d*) δ 137.6, 130.5, 130.0, 128.5 (2C), 127.0, 126.0 (2C), 33.7, 32.2, 32.1, 27.8.

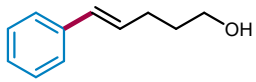

(*E*)-6-phenylhex-5-en-1-ol (**3b**)[13]

Colorless oil (24.3 mg, 30% yield), **^{1}H NMR** (600 MHz, Chloroform-*d*) δ 7.37 – 7.33 (m, 2H), 7.33 – 7.28 (m, 2H), 7.23 – 7.18 (m, 1H), 6.43 (d, *J* = 15.8 Hz, 1H), 6.24 (dt, *J* = 15.8, 7.0 Hz, 1H), 3.71 (t, *J* = 6.5 Hz, 2H), 2.34 – 2.30 (m, 2H), 1.79 – 1.74 (m, 2H), 1.67 (s, 1H). **^{13}C NMR** (150 MHz, Chloroform-*d*) δ 137.6, 130.3, 130.0, 128.5 (2C), 126.9, 125.9 (2C), 62.3, 32.2, 29.3.

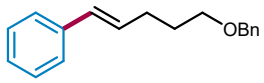

(*E*)-(6-(benzyloxy)hex-1-en-1-yl)benzene (**3c**)[13]

Colorless oil (51.7 mg, 41% yield), **^{1}H NMR** (600 MHz, Chloroform-*d*) δ 7.38 – 7.33 (m, 6H), 7.33 – 7.29 (m, 3H), 7.24 – 7.19 (m, 1H), 6.41 (d, *J* = 15.8 Hz, 1H), 6.24 (dt, *J* = 15.8, 6.9 Hz, 1H), 4.54 (s, 2H), 3.55 (t, *J* = 6.4 Hz, 2H), 2.36 – 2.32 (m, 2H), 1.85 – 1.80 (m, 2H). **^{13}C NMR** (150 MHz, Chloroform-*d*) δ 138.6, 137.7, 130.2, 130.2, 128.4 (2C), 128.3 (2C), 127.6 (2C), 127.5, 126.8, 125.9 (2C), 72.9, 69.7, 29.6, 29.4.

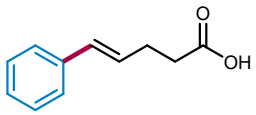

(*E*)-5-phenylpent-4-enoic acid (**3d**) [14]

White solid (54.6 mg, 62% yield), mp 91−92 °C (lit. mp 90−91 °C), **^{1}H NMR** (600 MHz, Chloroform-*d*) δ 7.34 (d, *J* = 7.3 Hz, 2H), 7.30 (t, *J* = 7.7 Hz, 2H), 7.23 – 7.19 (m, 1H), 6.45 (d, *J* = 15.8 Hz, 1H), 6.24 – 6.19 (m, 1H), 2.57 – 2.54 (m, 4H). **^{13}C NMR** (100 MHz, Chloroform-*d*) δ 178.9, 137.2, 131.2, 128.5 (2C), 128.0, 127.2, 126.1 (2C), 33.7, 27.9.

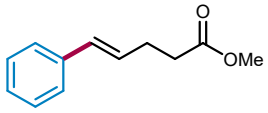

methyl (*E*)-5-phenylpent-4-enoate (**3e**)[13]

Colorless oil (67.5 mg, 71% yield), **^{1}H NMR** (600 MHz, Chloroform-*d*) δ 7.36 – 7.33 (m, 2H), 7.32 – 7.28 (m, 2H), 7.23 – 7.19 (m, 1H), 6.44 (d, *J* = 15.8 Hz, 1H), 6.21 (dt, *J* = 15.8, 6.6 Hz, 1H), 3.70 (s,

3H), 2.57 – 2.53 (m, 2H), 2.52 – 2.49 (m, 2H). **^{13}C NMR** (150 MHz, Chloroform-*d*) δ 173.3, 137.3, 131.0, 128.4 (2C), 128.4, 127.1, 126.0 (2C), 51.5, 33.8, 28.2.

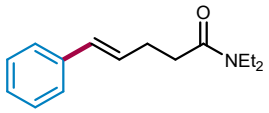

(*E*)-*N*,*N*-diethyl-5-phenylpent-4-enamide (**3f)**

Yellow oil (68.2 mg, 59% yield), **^{1}H NMR** (600 MHz, Chloroform-*d*) δ 7.33 (d, *J* = 7.4 Hz, 2H), 7.31 – 7.26 (m, 2H), 7.23 – 7.15 (m, 1H), 6.44 (d, *J* = 15.8 Hz, 1H), 6.27 (dt, *J* = 15.7, 6.9 Hz, 1H), 3.42 – 3.29 (m, 4H), 2.57 (q, *J* = 7.3 Hz, 2H), 2.49 – 2.46 (m, 2H), 1.21 – 1.09 (m, 6H). **^{13}C NMR** (150 MHz, Chloroform-*d*) δ 171.3, 137.5, 130.6, 129.5, 128.5 (2C), 127.0, 126.0 (2C), 32.8, 28.9. **HRMS (ESI)** *m/z* calcd for $C_{15}H_{22}NO$ $[M+H]^+$, 232.1696, found 232.1699.

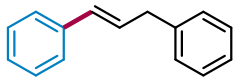

(*E*)-prop-1-ene-1,3-diyldibenzene (**3g**)[15]

Colorless oil (70.9 mg, 73% yield), **^{1}H NMR** (600 MHz, Chloroform-*d*) δ 7.38 – 7.35 (m, 2H), 7.33 – 7.28 (m, 4H), 7.26 – 7.18 (m, 4H), 6.46 (d, *J* = 15.8 Hz, 1H), 6.37 (dt, *J* = 15.7, 6.8 Hz, 1H), 3.56 (d, *J* = 6.8 Hz, 2H). **^{13}C NMR** (150 MHz, Chloroform-*d*) δ 140.2, 137.5, 131.1, 129.2, 128.7 (2C), 128.5 (2C), 128.5 (2C), 127.1, 126.2, 126.1, 39.3.

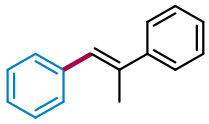

(*E*)-prop-1-ene-1,2-diyldibenzene (**3h**)[16]

White solid (63.1 mg, 65% yield), mp 81−82 °C (lit. mp 80−81 °C), **^{1}H NMR** (400 MHz, Chloroform-*d*) δ 7.57 – 7.53 (m, 2H), 7.42 – 7.37 (m, 6H), 7.33 – 7.24 (m, 2H), 6.86 (q, *J* = 1.4 Hz, 1H), 2.31 (d, *J* = 1.4 Hz, 3H). **^{13}C NMR** (100 MHz, Chloroform-*d*) δ 143.9, 138.3, 137.4, 129.1 (2C), 128.3 (2C), 128.2 (2C), 127.7, 127.2, 126.4, 126.0 (2C), 17.5.

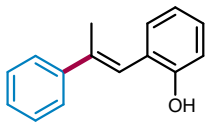

(*E*)-2-(2-phenylprop-1-en-1-yl)phenol (**3i**)

Colorless oil (57.8 mg, 55% yield), **^{1}H NMR** (400 MHz, Chloroform-*d*) δ 7.60 – 7.56 (m, 2H), 7.44 – 7.33 (m, 3H), 7.25 – 7.19 (m, 2H), 6.99 – 6.94 (m, 2H), 6.79 (s, 1H), 5.09 (s, 1H), 2.15 (d, *J* = 1.3 Hz, 3H). **^{13}C NMR** (100 MHz, Chloroform-*d*) δ 152.9, 142.2, 141.5, 129.9, 128.7, 128.4 (2C), 127.9, 125.9 (2C), 124.6, 121.0, 120.4, 115.2, 17.2. **HRMS (EI)** *m/z* calcd for $C_{15}H_{14}O$ $[M]^+$, 210.1045, found 210.1052.

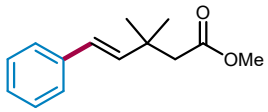

methyl (*E*)-3,3-dimethyl-5-phenylpent-4-enoate (**3j**)[17]

Colorless oil (89.4 mg, 82% yield), **^{1}H NMR** (600 MHz, Chloroform-*d*) δ 7.36 (d, *J* = 7.5 Hz, 2H), 7.30 (t, *J* = 7.7 Hz, 2H), 7.23 – 7.18 (m, 1H), 6.35 (d, *J* = 16.2 Hz, 1H), 6.30 (d, *J* = 16.2 Hz, 1H), 3.64 (s, 3H), 2.40 (s, 2H), 1.25 (s, 6H). **^{13}C NMR** (150 MHz, Chloroform-*d*) δ 172.1, 138.8, 137.7, 128.5 (2C), 127.0, 126.2, 126.2 (2C), 51.2, 47.0, 35.8, 27.4.

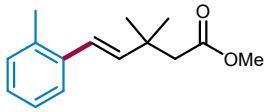

methyl (*E*)-3,3-dimethyl-5-(*o*-tolyl)pent-4-enoate (**3k**)

Colorless oil (84.7 mg, 73% yield), **^{1}H NMR** (400 MHz, Chloroform-*d*) δ 7.43 – 7.37 (m, 1H), 7.19 – 7.11 (m, 3H), 6.55 (d, *J* = 16.0 Hz, 1H), 6.14 (d, *J* = 16.0 Hz, 1H), 3.65 (s, 3H), 2.43 (s, 2H), 2.34 (s, 3H), 1.27 (s, 6H). **^{13}C NMR** (100 MHz, Chloroform-*d*) δ 172.0, 140.3, 136.9, 135.2, 130.0, 127.0, 126.0, 125.7, 124.1, 51.2, 47.0, 36.0, 27.5 (2C), 19.7. **HRMS (ESI)** *m/z* calcd for $C_{15}H_{21}O_2$ $[M+H]^+$, 233.1542, found 233.1538.

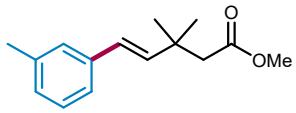

methyl (*E*)-3,3-dimethyl-5-(m-tolyl)pent-4-enoate (**3l**)

Colorless oil (82.4 mg, 71% yield), **^{1}H NMR** (400 MHz, Chloroform-*d*) δ 7.22 – 7.15 (m, 3H), 7.06 – 7.00 (m, 1H), 6.33 (d, *J* = 16.0 Hz, 1H), 6.28 (d, *J* = 16.0 Hz, 1H), 3.64 (s, 3H), 2.41 (s, 2H), 2.35 (s, 3H), 1.25 (s, 6H). **^{13}C NMR** (100 MHz, Chloroform-*d*) δ 172.1, 138.5, 138.0, 137.5, 128.4, 127.8, 126.8, 126.2, 123.3, 51.2, 47.0, 35.8, 27.4 (2C), 21.4. **HRMS (ESI)** *m/z* calcd for $C_{15}H_{21}O_2$ $[M+H]^+$, 233.1542, found 233.1537.

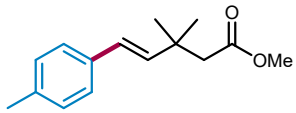

methyl (*E*)-3,3-dimethyl-5-(*p*-tolyl)pent-4-enoate (**3m**)

Colorless oil (88.2 mg, 76% yield), **^{1}H NMR** (400 MHz, Chloroform-*d*) δ 7.25 (d, *J* = 8.0 Hz, 2H), 7.09 (d, *J* = 8.0 Hz, 2H), 6.31 (d, *J* = 16.2 Hz, 1H), 6.23 (d, *J* = 16.2 Hz, 1H), 3.62 (s, 3H), 2.38 (s, 2H), 2.31 (s, 3H), 1.23 (s, 6H). **^{13}C NMR** (100 MHz, Chloroform-*d*) δ 172.1, 137.6, 136.7, 134.8, 129.1 (2C), 126.2 (2C), 125.9, 51.2, 47.0, 35.7, 27.3 (2C), 21.1. **HRMS (ESI)** *m/z* calcd for $C_{15}H_{21}O_2$ $[M+H]^+$, 233.1542, found 233.1536.

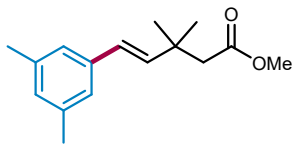

methyl (*E*)-5-(3,5-dimethylphenyl)-3,3-dimethylpent-4-enoate (**3n**)

Colorless oil (83.7 mg, 68% yield), **^{1}H NMR** (400 MHz, Chloroform-*d*) δ 6.99 (s, 2H), 6.86 (s, 1H), 6.30 (d, *J* = 16.5 Hz, 1H), 6.26 (d, *J* = 16.5 Hz, 1H), 3.64 (s, 3H), 2.40 (s, 2H), 2.30 (s, 6H), 1.24 (s, 6H). **^{13}C NMR** (100 MHz, Chloroform-*d*) δ 172.1, 138.3 (2C), 137.9, 137.5, 128.8, 126.2, 124.0 (2C), 51.2, 47.0, 35.8, 27.4 (2C), 21.2 (2C). **HRMS (ESI)** *m/z* calcd for $C_{16}H_{23}O_2$ $[M+H]^+$, 247.1693, found 247.1684.

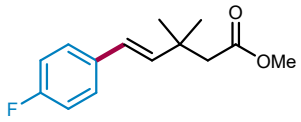

methyl (*E*)-5-(4-fluorophenyl)-3,3-dimethylpent-4-enoate (**3o**)

Colorless oil (63.8 mg, 54% yield), **^{1}H NMR** (400 MHz, Chloroform-*d*) δ 7.34 – 7.28 (m, 2H), 7.02 – 6.95 (m, 2H), 6.31 (d, *J* = 16.2 Hz, 1H), 6.18 (d, *J* = 16.2 Hz, 1H), 3.63 (s, 3H), 2.40 (s, 2H), 1.24 (s, 6H). **^{13}C NMR** (100 MHz, Chloroform-*d*) δ 172.0, 162.0 (d, J_1 = 244.3 Hz), 138.4, 133.7 (d, J_4 = 3.3 Hz), 127.6 (d, J_3 = 7.8 Hz, 2C), 125.1, 115.3 (d, J_2 = 21.4 Hz, 2C), 51.2, 47.0, 35.7, 27.4 (2C). **HRMS (ESI)** *m/z* calcd for $C_{14}H_{18}FO_2$ $[M+H]^+$, 237.1285, found 237.1280.

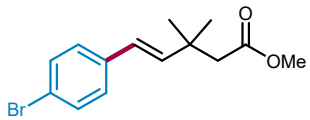

methyl (*E*)-5-(4-bromophenyl)-3,3-dimethylpent-4-enoate (**3p**)

Colorless oil (77.0 mg, 52% yield), **^{1}H NMR** (600 MHz, Chloroform-*d*) δ 7.41 (d, *J* = 8.2 Hz, 2H), 7.22 (d, *J* = 8.2 Hz, 2H), 6.30 (d, *J* = 16.2 Hz, 1H), 6.27 (d, *J* = 16.2 Hz, 1H), 3.63 (s, 3H), 2.39 (s, 2H), 1.24 (s, 6H). **^{13}C NMR** (150 MHz, Chloroform-*d*) δ 172.1, 139.7, 136.8, 131.7 (2C), 127.9 (2C), 125.3, 120.9, 51.4, 47.1, 36.0, 27.5 (2C). **HRMS (ESI)** *m/z* calcd for $C_{14}H_{18}{}^{79}BrO_2$ $[M+H]^+$, 297.0485, found 297.0491.

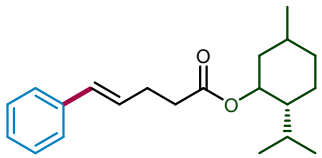

2-isopropyl-5-methylcyclohexyl (*E*)-5-phenylpent-4-enoate (**3q**)

Colorless oil (70.7 mg, 45% yield), **^{1}H NMR** (400 MHz, Chloroform-*d*) δ 7.36 – 7.27 (m, 4H), 7.24 – 7.17 (m, 1H), 6.44 (d, *J* = 15.8 Hz, 1H), 6.21 (dt, *J* = 15.8, 6.6 Hz, 1H), 4.72 (td, *J* = 10.9, 4.4 Hz, 1H), 2.59 – 2.52 (m, 2H), 2.50 – 2.45 (m, 2H), 2.02 – 1.96 (m, 1H), 1.92 – 1.83 (m, 1H), 1.72 – 1.64 (m, 2H), 1.53 – 1.43 (m, 1H), 1.42 – 1.34 (m, 1H), 1.12 – 0.95 (m, 2H), 0.88 (dd, *J* = 9.2, 6.8 Hz, 7H), 0.74 (d, *J* = 7.0 Hz, 3H). **^{13}C NMR** (100 MHz, Chloroform-*d*) δ 172.5, 137.3, 130.9, 128.4 (2C), 128.4, 127.0, 126.0 (2C), 74.1, 46.9, 41.0, 34.4, 34.2, 31.3, 28.5, 26.2, 23.3, 22.0, 20.7, 16.2 (2C). **HRMS (ESI)** *m/z* calcd for $C_{21}H_{30}NaO_2$ $[M+Na]^+$, 337.2138, found 337.2130.

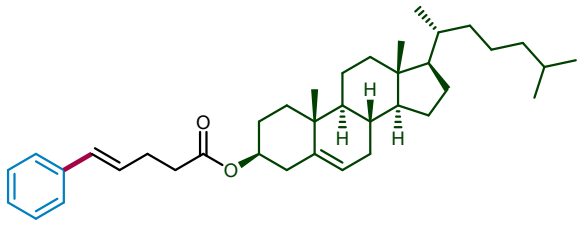

(3S,10R,13R)-10,13-dimethyl-17-(6-methylheptan-2-yl)-2,3,4,7,8,9,10,11,12,13,14,15,16,17-tetradecahydro-1H-cyclopenta[a]phenanthren-3-yl (*E*)-5-phenylpent-4-enoate (**3r**)

White solid (98.1 mg, 36% yield); mp 127–129 °C; **^{1}H NMR** (600 MHz, Chloroform-*d*) δ 7.35 – 7.32 (m, 2H), 7.29 (dd, *J* = 8.5, 6.9 Hz, 2H), 7.23 – 7.18 (m, 1H), 6.43 (d, *J* = 15.8 Hz, 1H), 6.21 (dt, *J* = 15.8, 6.7 Hz, 1H), 5.38 – 5.35 (m, 1H), 4.68 – 4.59 (m, 1H), 2.56 – 2.52 (m, 2H), 2.48 – 2.45 (m, 2H), 2.35 – 2.29 (m, 2H), 2.03 – 1.94 (m, 2H), 1.88 – 1.80 (m, 3H), 1.62 – 1.06 (m, 19H), 1.02 (s, 5H), 0.92 (d, *J* = 6.5 Hz, 3H), 0.87 (dd, *J* = 6.6, 2.7 Hz, 6H), 0.68 (s, 3H). **^{13}C NMR** (150 MHz, Chloroform-*d*) δ 130.9, 128.5, 128.5 (2C), 127.1, 126.0 (2C), 74.0, 56.7, 56.1, 50.0, 42.3, 39.7, 39.5, 38.2, 37.0, 36.6, 36.2, 35.8, 34.4, 31.9, 31.9, 28.4, 28.2, 28.0, 27.8, 24.3, 23.8, 22.8, 22.6 (2C), 21.0, 19.3, 18.7, 11.8. **HRMS (ESI)** *m/z* calcd for $C_{38}H_{56}NaO_2$ $[M+Na]^+$, 567.4172, found 567.4151.

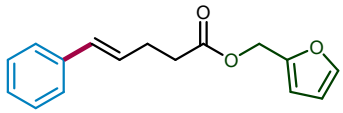

furan-2-ylmethyl (*E*)-5-phenylpent-4-enoate (**3s**)

Colorless oil (51.3 mg, 40% yield), **^{1}H NMR** (600 MHz, Chloroform-*d*) δ 7.43 – 7.39 (m, 1H), 7.33 – 7.27 (m, 4H), 7.23 – 7.18 (m, 1H), 6.44 – 6.38 (m, 2H), 6.35 – 6.34 (m, 1H), 6.18 (dt, *J* = 15.8, 6.5 Hz, 1H), 5.09 (s, 2H), 2.56 – 2.50 (m, 4H). **^{13}C NMR** (150 MHz, Chloroform-*d*) δ 172.6, 149.5, 143.2, 137.3, 131.1, 128.5 (2C), 128.2, 127.1, 126.1 (2C), 110.6, 110.5, 58.2, 33.9, 28.2. **HRMS (ESI)** *m/z* calcd for $C_{16}H_{16}NaO_3$ $[M+Na]^+$, 279.0991, found 279.0986.

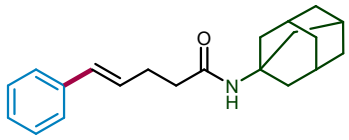

(*E*)-*N*-(adamantan-1-yl)-5-phenylpent-4-enamide (**3t**)

White solid (89.7 mg, 58% yield); mp 115–117 °C; **^{1}H NMR** (600 MHz, Chloroform-*d*) δ 7.33 – 7.27 (m, 4H), 7.21 – 7.18 (m, 1H), 6.43 (d, *J* = 15.8 Hz, 1H), 6.20 (dt, *J* = 15.9, 6.9 Hz, 1H), 5.22 (s, 1H), 2.55 – 2.48 (m, 2H), 2.28 – 2.23 (m, 2H), 2.08 – 2.03 (m, 3H), 1.99 (d, *J* = 3.5 Hz, 6H), 1.66 (t, *J* = 3.2 Hz, 6H). **^{13}C NMR** (150 MHz, Chloroform-*d*) δ 171.3, 137.4, 130.9, 129.0, 128.5 (2C), 127.0, 126.0, 51.9, 41.7 (3C), 37.3, 36.3 (3C), 29.4 (3C), 29.1. **HRMS (ESI)** *m/z* calcd for $C_{21}H_{27}NNaO$ $[M+Na]^+$, 332.1985, found 332.1978.

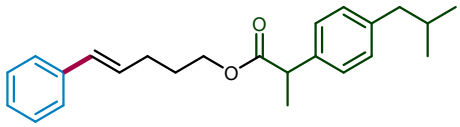

(*E*)-5-phenylpent-4-en-1-yl 2-(4-isobutylphenyl)propanoate (**3u**)

Colorless oil (65.5 mg, 37% yield), **^{1}H NMR** (600 MHz, Chloroform-*d*) δ 7.37 – 7.27 (m, 4H), 7.26 – 7.19 (m, 3H), 7.13 (d, *J* = 7.9 Hz, 2H), 6.33 (d, *J* = 16.0 Hz, 1H), 6.15 (dt, *J* = 15.6, 6.9 Hz, 1H), 4.16 – 4.11 (m, 2H), 3.73 (q, *J* = 7.2 Hz, 1H), 2.48 (d, *J* = 7.2 Hz, 2H), 2.19 (q, *J* = 7.2 Hz, 2H), 1.91 – 1.84 (m, 1H), 1.80 – 1.75 (m, 2H), 1.52 (d, *J* = 7.2 Hz, 3H), 0.92 (d, *J* = 6.7 Hz, 6H). **^{13}C NMR** (150 MHz, Chloroform-*d*) δ 174.7 (2C), 140.5, 137.9, 137.5, 130.7, 129.3 (2C), 129.2, 128.4 (2C), 127.1 (2C), 126.9, 125.9 (2C), 63.9, 45.2, 45.0, 30.1, 29.2, 28.2, 22.3 (2C), 18.4. **HRMS (ESI)** *m/z* calcd for $C_{24}H_{30}NNaO_2$ $[M+Na]^+$, 373.2138, found 373.2136.

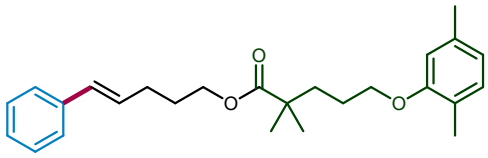

(*E*)-5-phenylpent-4-en-1-yl 5-(2,5-dimethylphenoxy)-2,2-dimethylpentanoate (**3v**)

White solid (69.8 mg, 35% yield); mp 221–223 °C; **^{1}H NMR** (400 MHz, Chloroform-*d*) δ 7.35 – 7.26 (m, 4H), 7.23 – 7.16 (m, 1H), 7.00 (d, *J* = 7.5 Hz, 1H), 6.66 (d, *J* = 7.5 Hz, 1H), 6.61 (s, 1H), 6.40 (d, *J* = 15.8 Hz, 1H), 6.20 (dt, *J* = 15.8, 6.9 Hz, 1H), 4.12 (t, *J* = 6.5 Hz, 2H), 3.92 (t, *J* = 5.4 Hz, 2H), 2.34 – 2.26 (m, 5H), 2.18 (s, 3H), 1.85 – 1.79 (m, 2H), 1.74 (d, *J* = 3.1 Hz, 4H), 1.23 (s, 6H). **^{13}C NMR** (150 MHz, Chloroform-*d*) δ 156.9, 136.4, 130.7, 130.3, 129.3, 128.5 (2C), 127.0, 126.0 (2C), 123.6, 120.7, 112.0, 67.9, 63.8, 42.1, 37.1, 29.4, 28.4, 25.2, 25.2 (2C), 21.4, 15.8. **HRMS (ESI)** *m/z* calcd for $C_{26}H_{35}O_3$ $[M+H]^+$, 395.2581, found 395.2572.

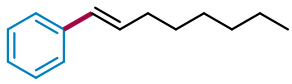

(*E*)-oct-1-en-1-ylbenzene (**5a**)[18]

Colorless oil (64.9 mg, 69% yield); **^{1}H NMR** (600 MHz, Chloroform-*d*) δ 7.39 – 7.27 (m, 4H), 7.22 – 7.19 (m, 1H), 6.40 (d, *J* = 15.8 Hz, 1H), 6.25 (dt, *J* = 15.8, 6.9 Hz, 1H), 2.27 – 2.20 (m, 2H), 1.53 – 1.45 (m, 2H), 1.39 – 1.30 (m, 6H), 0.92 (t, *J* = 6.8 Hz, 3H). **^{13}C NMR** (100 MHz, Chloroform-*d*) δ 137.9, 131.2, 129.7, 128.4 (2C), 126.7, 125.9 (2C), 33.1, 31.8, 29.4, 28.9, 22.6, 14.1.

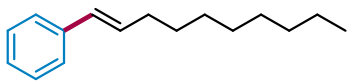

(*E*)-dec-1-en-1-ylbenzene (**5b**)[19]

Pale yellow oil (75.7 mg, 70% yield); **^{1}H NMR** (600 MHz, Chloroform-*d*) δ 7.38 – 7.32 (m, 2H), 7.29 (t, *J* = 7.7 Hz, 2H), 7.21 – 7.16 (m, 1H), 6.38 (d, *J* = 15.8 Hz, 1H), 6.23 (dt, *J* = 15.8, 6.9 Hz, 1H), 2.25 – 2.17 (m, 2H), 1.50 – 1.44 (m, 2H), 1.36 – 1.25 (m, 10H), 0.89 (t, *J* = 6.9 Hz, 3H). **^{13}C NMR** (150 MHz, Chloroform-*d*) δ 138.0, 131.3 129.7, 128.4 (2C), 126.7, 125.9 (2C), 33.1, 31.9, 29.5, 29.4, 29.3, 29.2, 22.7, 14.1.

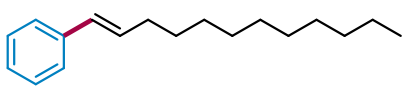

(*E*)-dodec-1-en-1-ylbenzene (**5c**)[10]

Pale yellow oil (87.9 mg, 72% yield); **^{1}H NMR** (400 MHz, Chloroform-*d*) δ 7.38 – 7.26 (m, 4H), 7.22 – 7.14 (m, 1H), 6.38 (d, *J* = 15.8 Hz, 1H), 6.23 (dt, *J* = 15.8, 6.8 Hz, 1H), 2.25 – 2.15 (m, 2H), 1.52 – 1.43 (m, 2H), 1.34 – 1.23 (m, 14H), 0.91 – 0.87 (m, 3H). **^{13}C NMR** (100 MHz, Chloroform-*d*) δ 138.0, 131.3, 129.7, 128.4 (2C), 126.7, 125.9 (2C), 33.0, 31.9, 29.6 (2C), 29.5, 29.4, 29.3, 29.2, 22.7, 14.1.

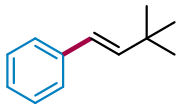

(*E*)-(3,3-dimethylbut-1-en-1-yl)benzene (**5d**)[17]

Colorless oil (68.1 mg, 85% yield); **^{1}H NMR** (400 MHz, Chloroform-*d*) δ 7.40 – 7.34 (m, 2H), 7.33 – 7.27 (m, 2H), 7.22 – 7.16 (m, 1H), 6.32 (d, *J* = 16.2 Hz, 1H), 6.26 (d, *J* = 16.2 Hz, 1H), 1.13 (s, 9H). **^{13}C NMR** (100 MHz, Chloroform-*d*) δ 141.8, 138.0, 128.5 (2C), 126.7, 126.0 (2C), 124.5, 33.3, 29.6 (3C).

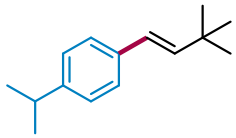

(*E*)-1-(3,3-dimethylbut-1-en-1-yl)-4-isopropylbenzene (**5e**)

Colorless oil (76.8 mg, 76% yield); **^{1}H NMR** (600 MHz, Chloroform-*d*) δ 7.32 – 7.28 (m, 2H), 7.18 – 7.15 (m, 2H), 6.29 (d, *J* = 16.2 Hz, 1H), 6.22 (d, *J* = 16.2 Hz, 1H), 2.89 (hept, *J* = 6.9 Hz, 1H), 1.25 (d, *J* = 6.9 Hz, 6H), 1.12 (s, 9H). **^{13}C NMR** (100 MHz, Chloroform-*d*) δ 147.5, 141.0, 135.6, 126.5 (2C), 125.9 (2C), 124.3, 33.8, 33.3, 29.6 (3C), 24.0 (2C). **HRMS (EI)** *m/z* calcd for $C_{15}H_{22}$ $[M]^+$, 202.1722, found 202.1732.

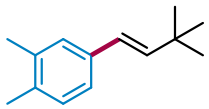

(*E*)-4-(3,3-dimethylbut-1-en-1-yl)-1,2-dimethylbenzene (**5f**)[20]

Colorless oil (64.9 mg, 69% yield); **^{1}H NMR** (600 MHz, Chloroform-*d*) δ 7.15 (s, 1H), 7.09 (dd, *J* = 7.7, 1.9 Hz, 1H), 7.05 (d, *J* = 7.7 Hz, 1H), 6.25 (d, *J* = 16.2 Hz, 1H), 6.19 (d, *J* = 16.2 Hz, 1H), 2.24 (d, *J* = 8.9 Hz, 6H), 1.11 (s, 9H). **^{13}C NMR** (100 MHz, Chloroform-*d*) δ 140.7, 136.5, 135.7, 135.1, 129.7, 127.2, 124.3, 123.5, 33.3, 29.6 (3C), 19.8, 19.4.

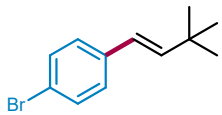

methyl (*E*)-5-(4-bromophenyl)-3,3-dimethylpent-4-enoate (**5g**)

Colorless oil (90.6 mg, 61% yield), **^{1}H NMR** (600 MHz, Chloroform-*d*) δ 7.41 (d, *J* = 8.2 Hz, 2H), 7.22 (d, *J* = 8.2 Hz, 2H), 6.26 (d, *J* = 16.3 Hz, 1H), 6.22 (d, *J* = 16.5 Hz, 1H), 3.63 (s, 3H), 2.39 (s, 2H), 1.24 (s, 6H). **^{13}C NMR** (100 MHz, Chloroform-*d*) δ 142.7, 137.0, 131.5 (2C), 127.6 (2C), 123.5, 120.3, 33.4, 29.5 (3C). **HRMS (ESI)** *m/z* calcd for $C_{14}H_{18}{}^{79}BrO_2$ $[M+H]^+$, 297.0485, found 297.0491.

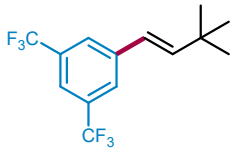

(*E*)-1-(3,3-dimethylbut-1-en-1-yl)-3,5-bis(trifluoromethyl)benzene (**5h**)

Colorless oil (84.4 mg, 57% yield); **^{1}H NMR** (600 MHz, Chloroform-*d*) δ 7.76 (s, 2H), 7.68 (s, 1H), 6.42 (d, *J* = 16.2 Hz, 1H), 6.37 (d, *J* = 16.2 Hz, 1H), 1.16 (s, 9H). **^{13}C NMR** (150 MHz, Chloroform-*d*) δ 146.0, 140.2, 131.8 (2C, q, *J* = 32.8 Hz), 125.9 (2C, d, *J* = 2.9 Hz), 123.5 (2C, q, *J* = 270.9 Hz), 122.5, 120.2 − 120.1 (m), 33.7, 29.3 (3C). **^{19}F NMR** (565 MHz, Chloroform-*d*) δ -63.06. **HRMS (EI)** *m/z* calcd for $C_{13}H_{14}F_6$ $[M]^+$, 296.1000, found 296.1014.

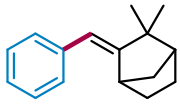

(*E*)-3-benzylidene-2,2-dimethylbicyclo[2.2.1]heptane (**5i**)

Colorless oil (54.1 mg, 51% yield); **^{1}H NMR** (400 MHz, Chloroform-*d*) δ 7.38 – 7.29 (m, 4H), 7.22 – 7.16 (m, 1H), 6.07 (s, 1H), 3.34 – 3.29 (m, 1H), 2.04 – 1.99 (m, 1H), 1.91 – 1.75 (m, 3H), 1.59 – 1.46 (m, 2H), 1.34 – 1.29 (m, 1H), 1.19 (s, 6H). **^{13}C NMR** (100 MHz, Chloroform-*d*) δ 159.2, 138.9, 128.1 (2C), 127.9 (2C), 125.5, 116.3, 47.5, 43.3, 42.5, 38.0, 29.1, 27.8, 26.3, 23.8. **HRMS (ESI)** *m/z* $[M+Na]^+$ calcd for $C_{16}H_{20}Na$ 235.1463, found 235.1466.

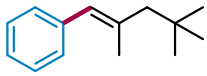

(*E*)-(2,4,4-trimethylpent-1-en-1-yl)benzene (**5j**)[17]

Colorless oil (51.8 mg, 55% yield); **^{1}H NMR** (400 MHz, Chloroform-*d*) δ 7.35 – 7.30 (m, 2H), 7.28 – 7.25 (m, 2H) ($CDCl_3$ included), 7.21 – 7.16 (m, 1H), 6.23 (s, 1H), 2.10 (s, 2H), 1.94 (s, 3H), 0.98 (s, 9H). **^{13}C NMR** (100 MHz, Chloroform-*d*) δ 138.8, 137.3, 128.9 (2C), 128.5, 128.0 (2C), 125.8, 54.9, 32.2 (3C), 30.2, 20.9.

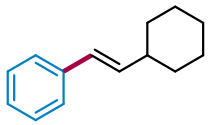

(*E*)-(2-cyclohexylvinyl)benzene (**5k**)[18]

Colorless oil (66.1 mg, 71% yield); **^{1}H NMR** (600 MHz, Chloroform-*d*) δ 7.37 – 7.33 (m, 2H), 7.31 – 7.27 (m, 2H), 7.20 – 7.17 (m, 1H), 6.35 (d, *J* = 16.0 Hz, 1H), 6.18 (dd, *J* = 16.0, 7.0 Hz, 1H), 2.18 – 2.10 (m, 1H), 1.84 – 1.75 (m, 4H), 1.71 – 1.67 (m, 1H), 1.37 – 1.29 (m, 2H), 1.25 – 1.16 (m, 3H). **^{13}C NMR** (150 MHz, Chloroform-*d*) δ 138.1, 136.9, 128.4 (2C), 127.2, 126.7, 125.9 (2C), 41.1, 33.0 (2C), 26.2, 26.0 (2C).

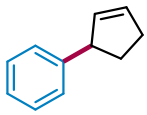

3-Phenylcyclopentene (**5l**)[21]

Colorless oil (50.5 mg, 70% yield); **^{1}H NMR** (600 MHz, Chloroform-*d*) δ 7.32 – 7.27 (m, 2H), 7.22 – 7.17 (m, 3H), 5.97 – 5.93 (m, 1H), 5.80 – 5.77 (m, 1H), 3.93 – 3.87 (m, 1H), 2.55 – 2.47 (m, 1H), 2.45 – 2.38 (m, 2H), 1.77 – 1.71 (m, 1H). **^{13}C NMR** (150 MHz, Chloroform-*d*) δ 146.5, 134.3, 131.9, 128.4 (2C), 127.2 (2C), 126.0, 51.3, 33.8, 32.5.

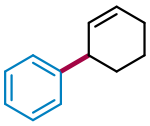

3-phenylcyclohexene (**5m**) [22]

Colorless oil (53.8 mg, 68% yield); **^{1}H NMR** (600 MHz, Chloroform-*d*) δ 7.33 – 7.29 (m, 2H), 7.26 – 7.18 (m, 3H), 5.93 – 5.88 (m, 1H), 5.73 (dd, *J* = 10.1, 2.5 Hz, 1H), 3.44 – 3.39 (m, 1H), 2.13 – 2.07 (m, 2H), 2.06 – 2.01 (m, 1H), 1.79 – 1.73 (m, 1H), 1.67 – 1.55 (m, 2H). **^{13}C NMR** (150 MHz, Chloroform-*d*) δ 146.7, 130.2, 128.3, 128.3 (2C), 127.7 (2C), 125.9, 41.9, 32.6, 25.0, 21.2.

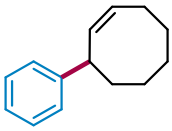

3-Phenyl-1-cyclooctene (**5n**)[22]

Colorless oil (68.9 mg, 74% yield); **^{1}H NMR** (400 MHz, Chloroform-*d*) δ 7.34 – 7.26 (m, 4H), 7.22 – 7.16 (m, 1H), 5.75 – 5.66 (m, 1H), 5.65 – 5.57 (m, 1H), 3.81 – 3.70 (m, 1H), 2.45 – 2.33 (m, 1H), 2.20 – 2.09 (m, 1H), 1.90 – 1.63 (m, 6H), 1.52 – 1.37 (m, 2H). **^{13}C NMR** (100 MHz, Chloroform-*d*) δ 146.5, 134.2, 129.0, 128.4, 127.2, 125.8, 42.3, 37.5, 29.6, 26.7, 26.5, 26.1.

7. NMR spectra

(*E*)-(6-bromohex-1-en-1-yl)benzene (**3a**)

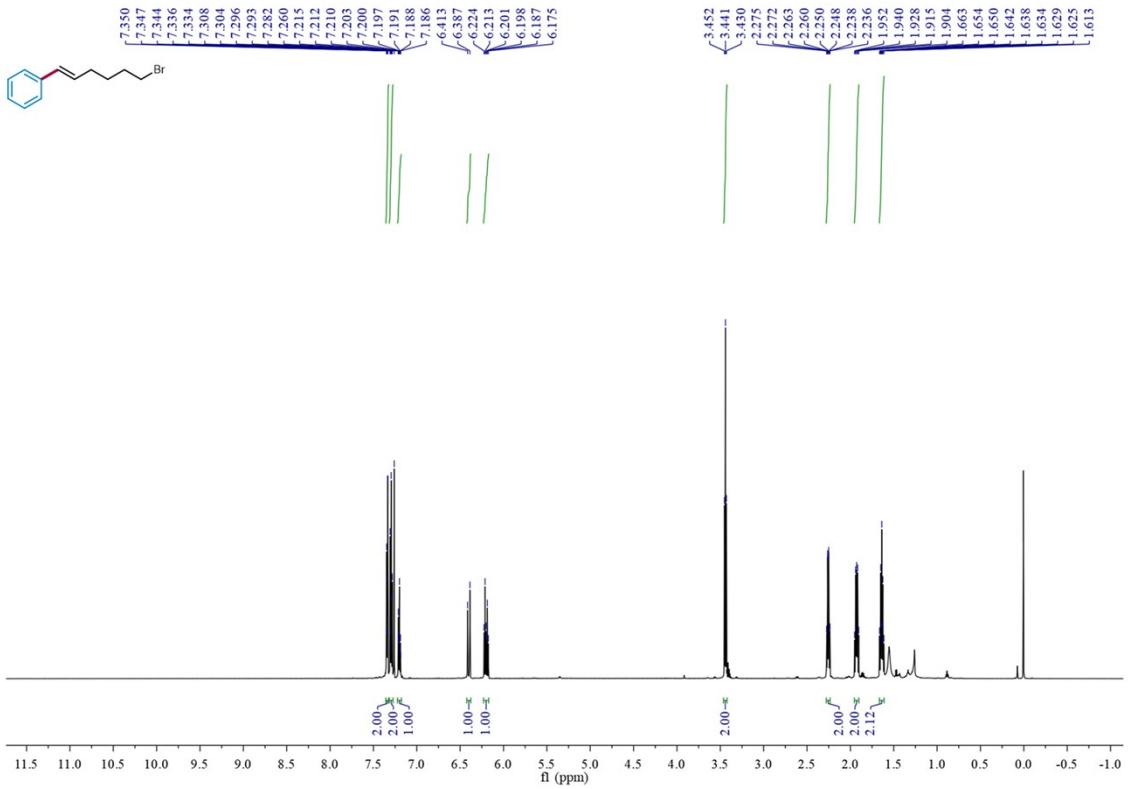

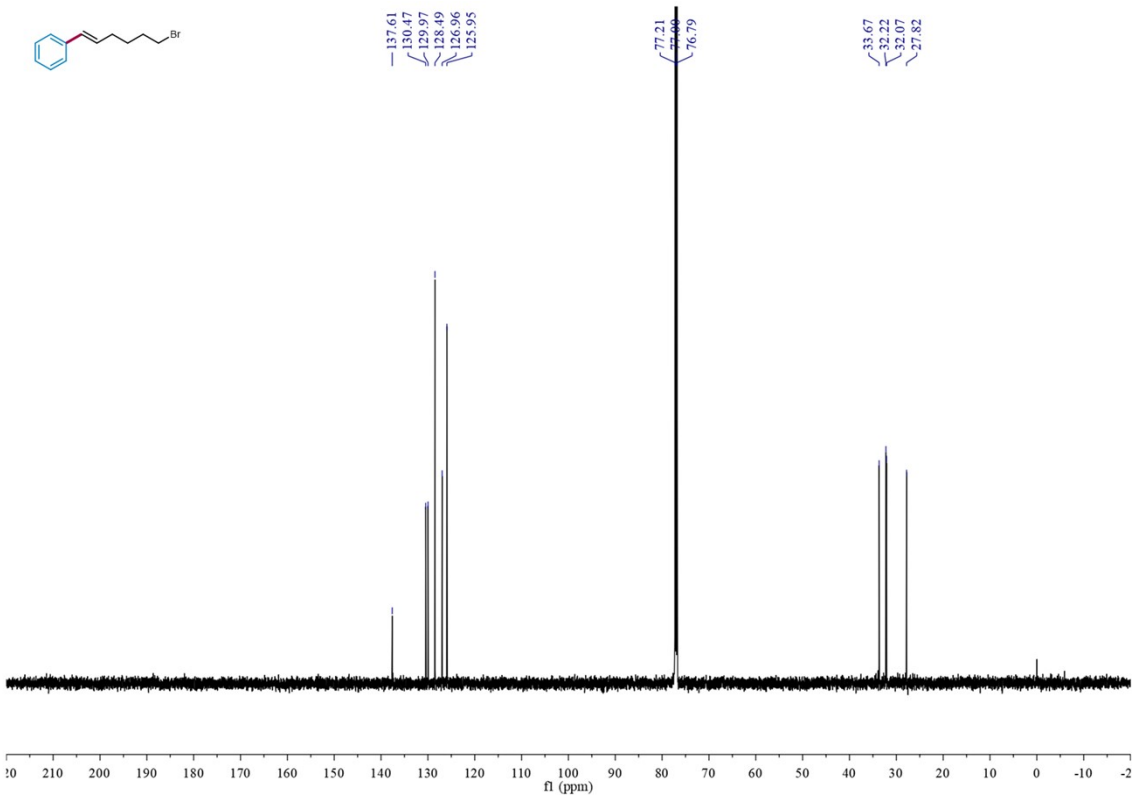

(*E*)-6-phenylhex-5-en-1-ol (**3b**)

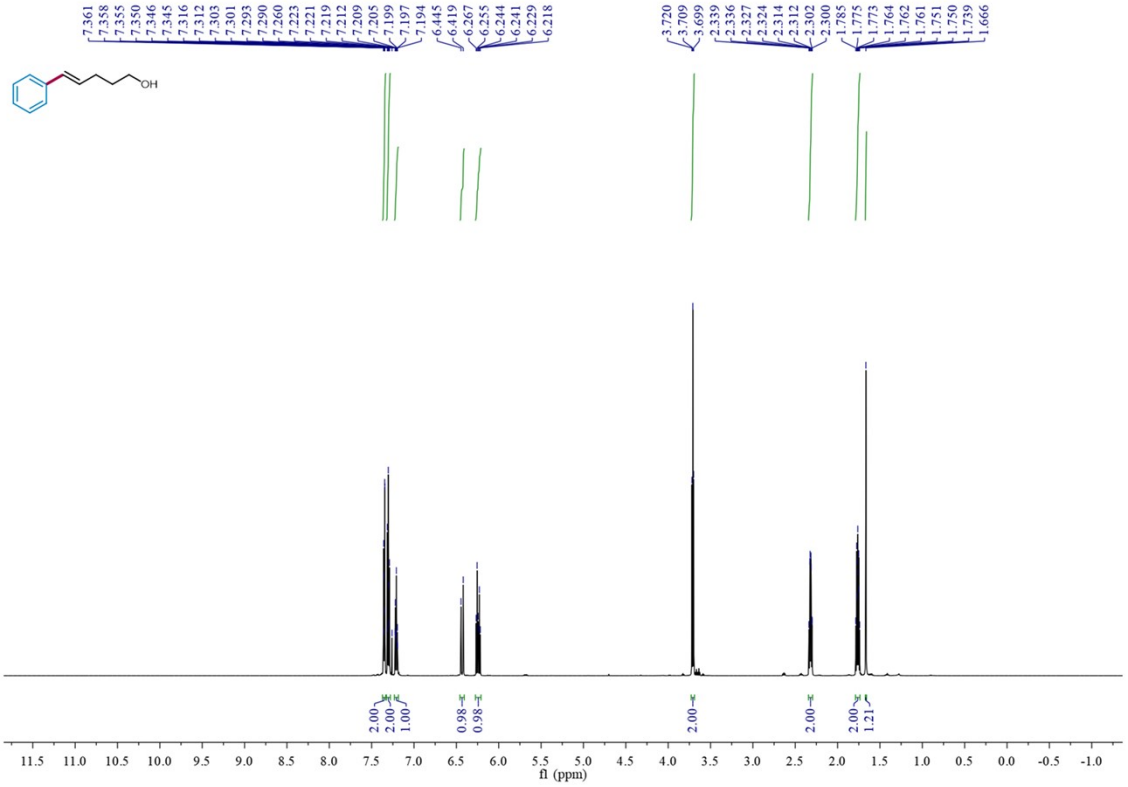

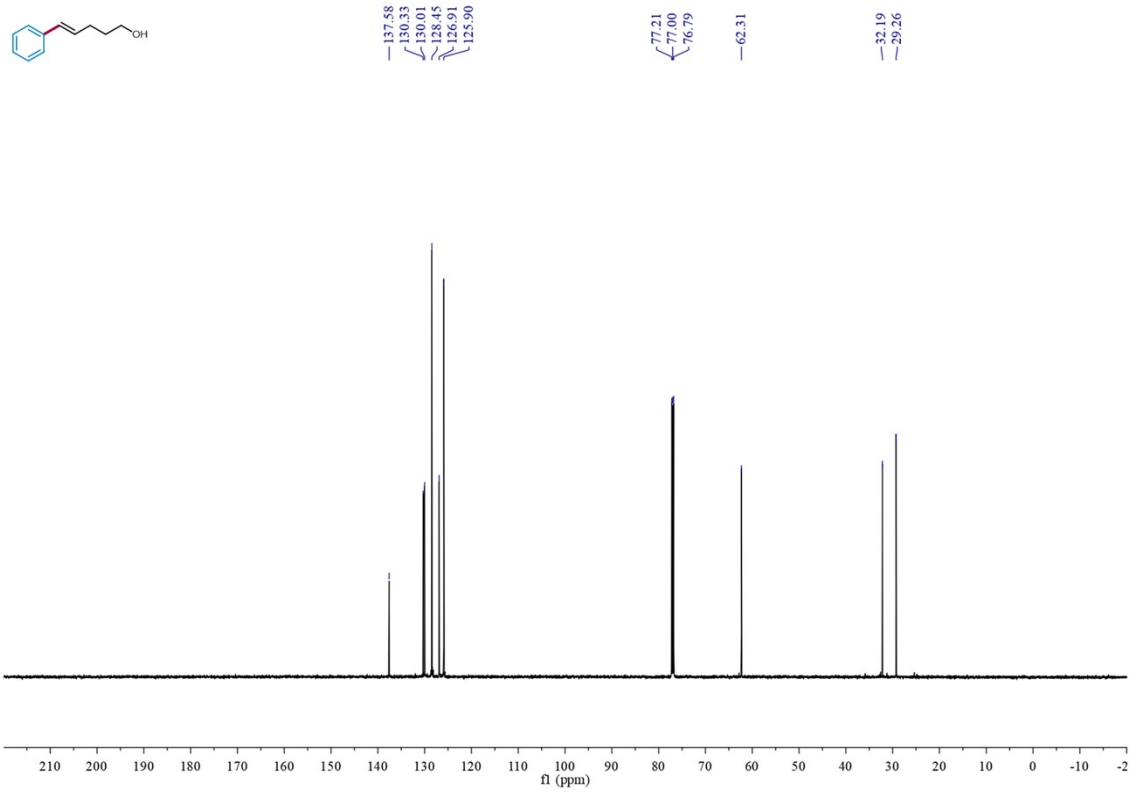

(*E*)-(6-(benzyloxy)hex-1-en-1-yl)benzene (**3c**)

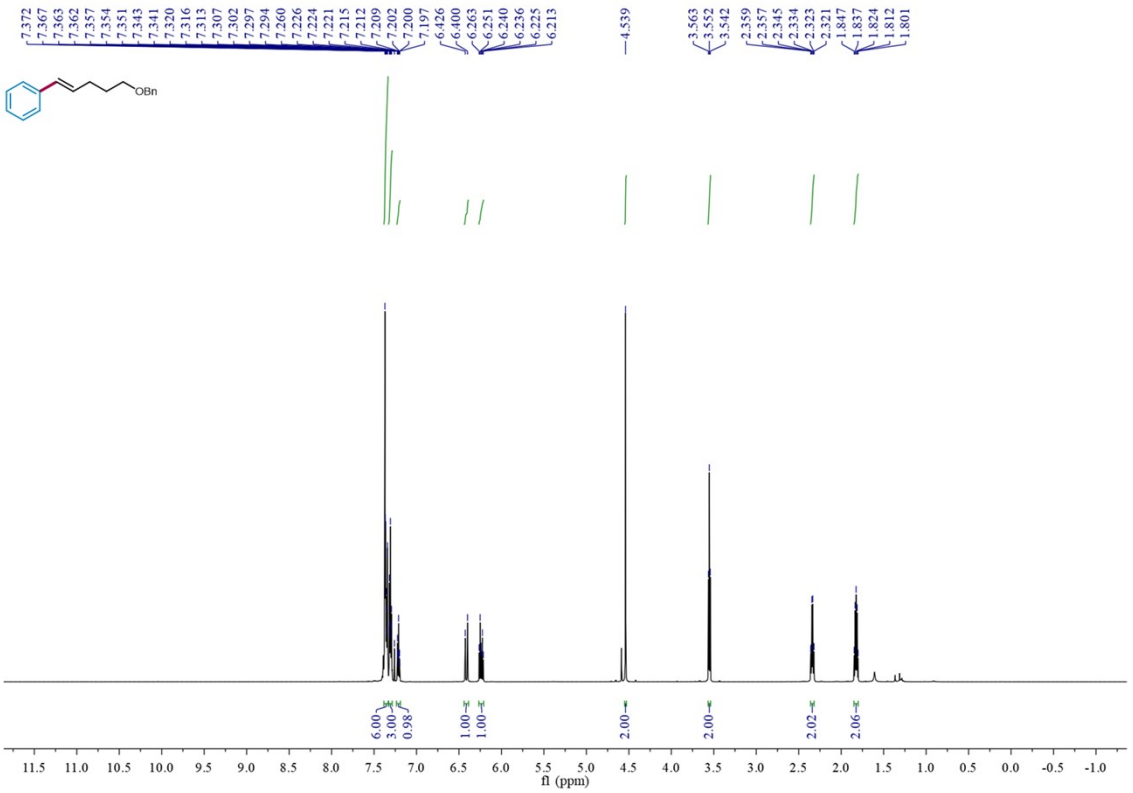

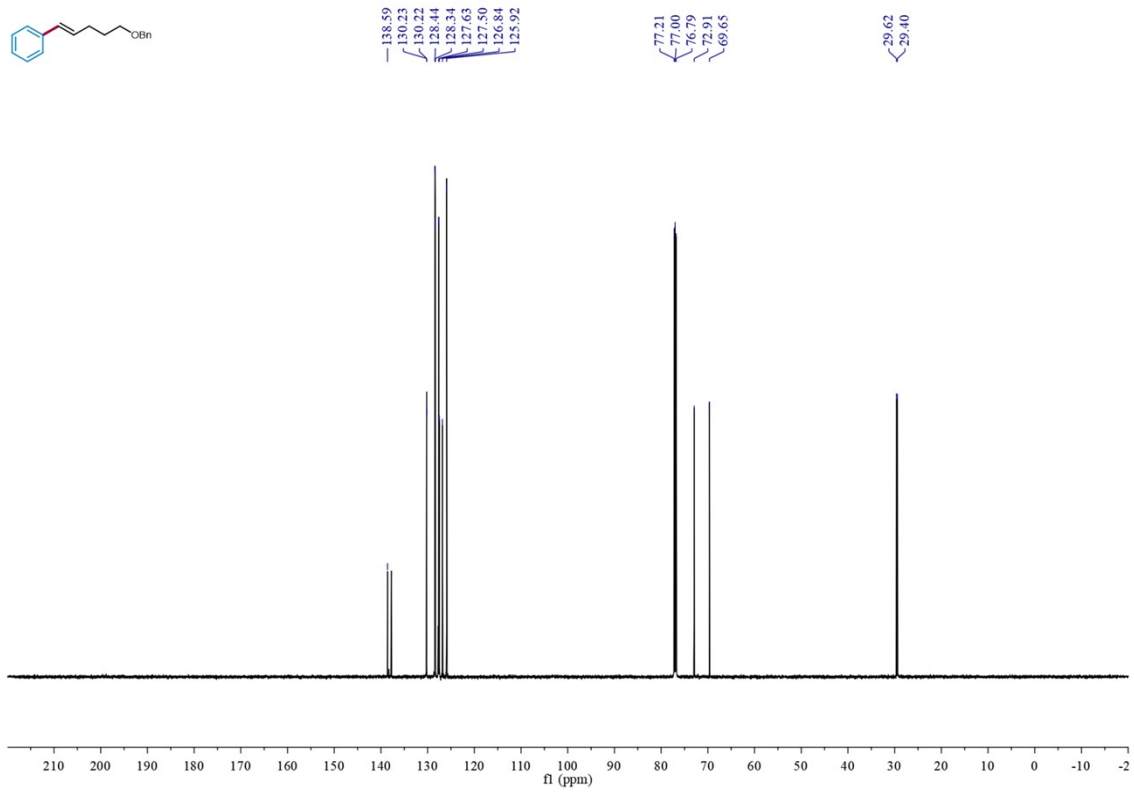

(*E*)-5-phenylpent-4-enoic acid (**3d**)

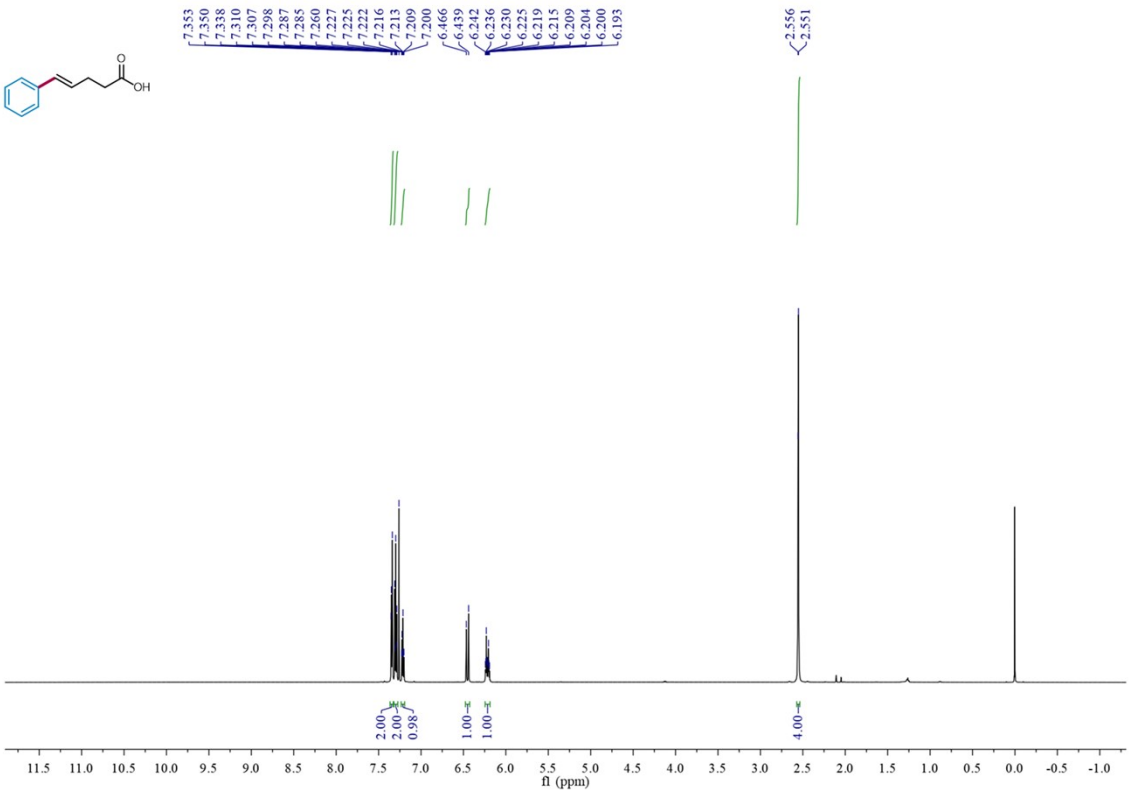

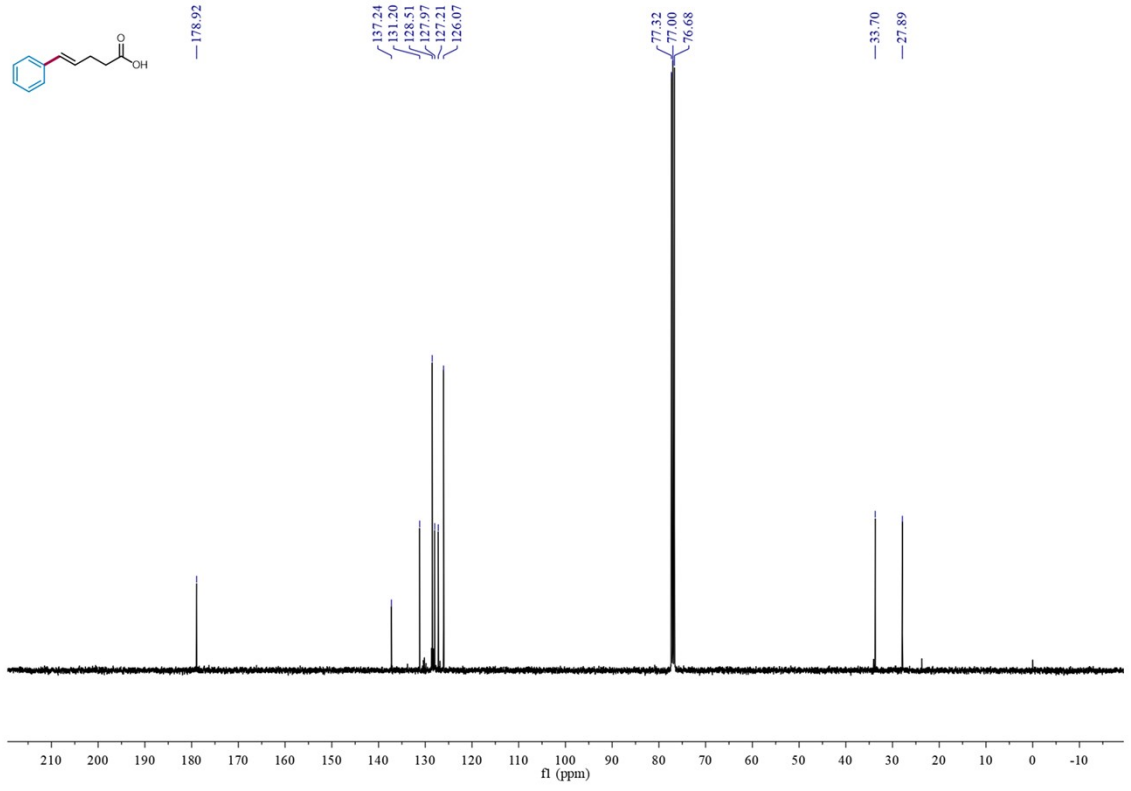

methyl (*E*)-5-phenylpent-4-enoate (**3e**)

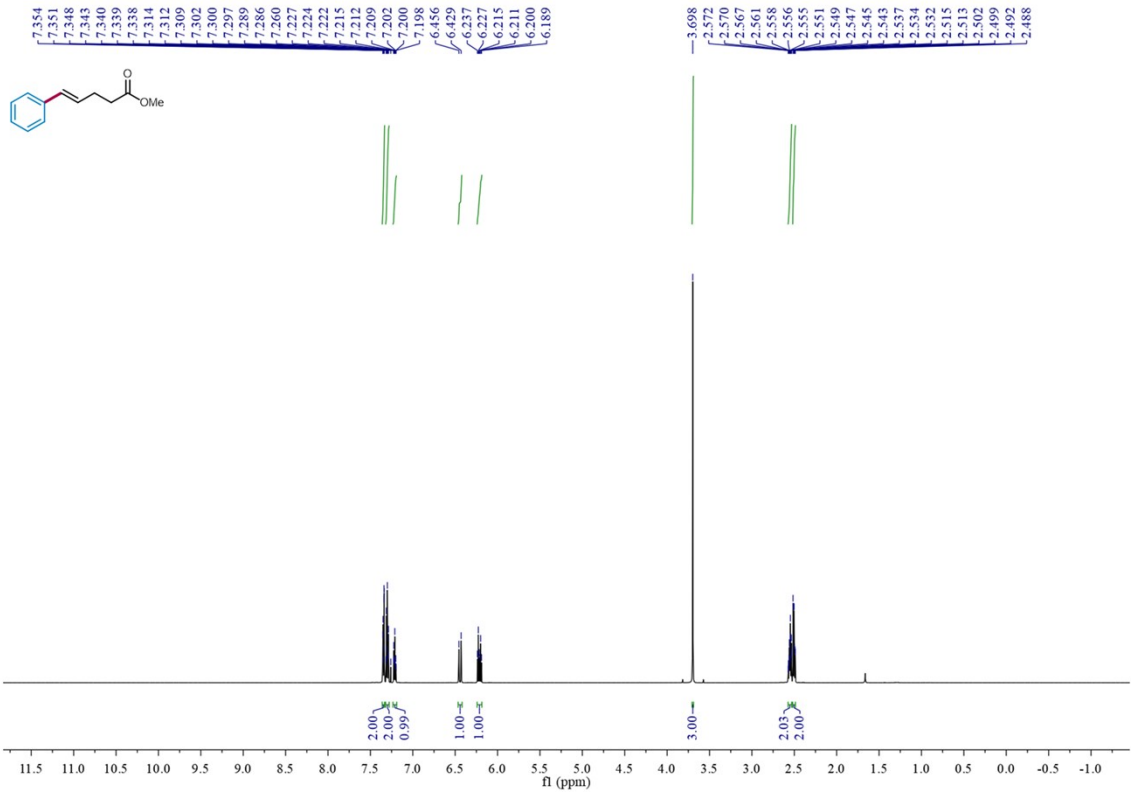

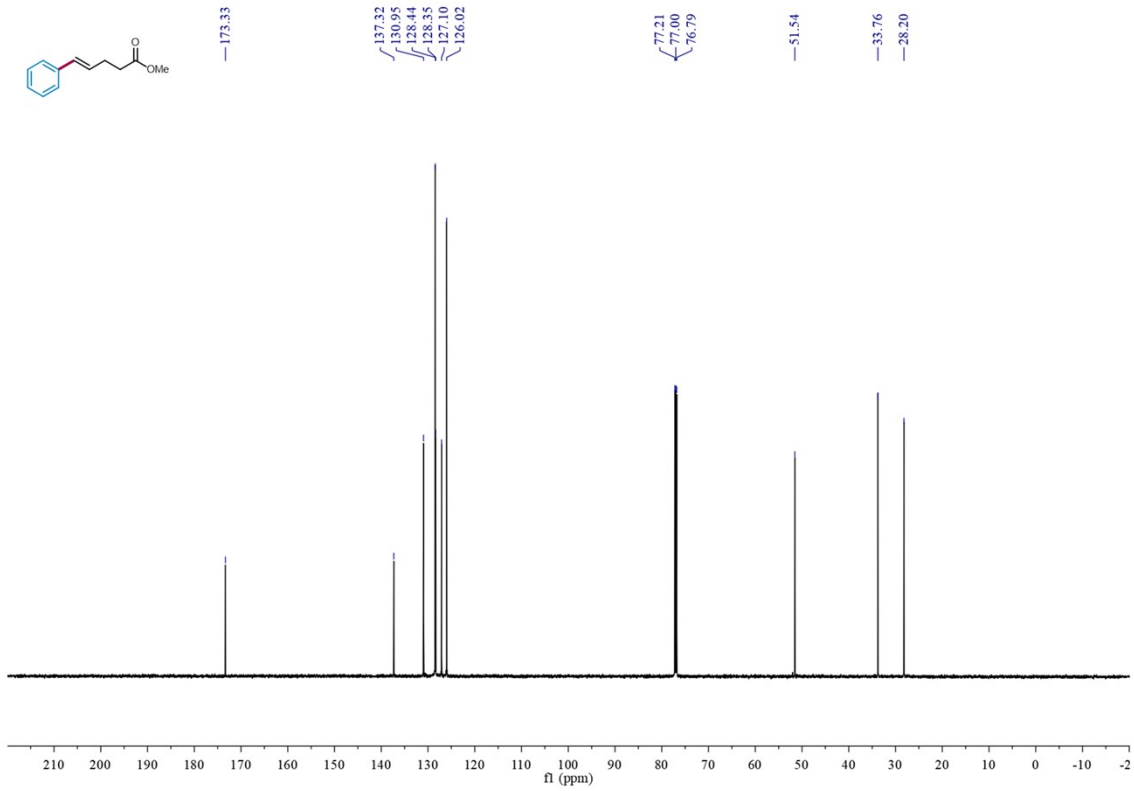

(*E*)-*N*,*N*-diethyl-5-phenylpent-4-enamide (**3f**)

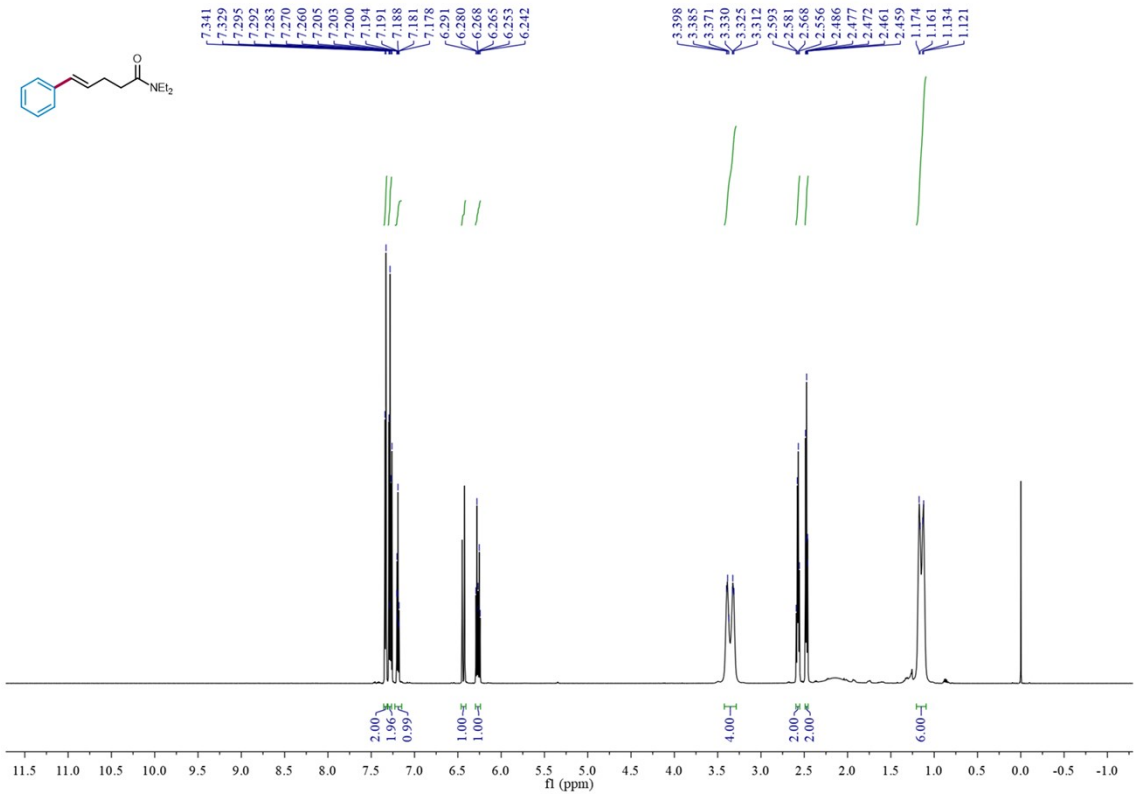

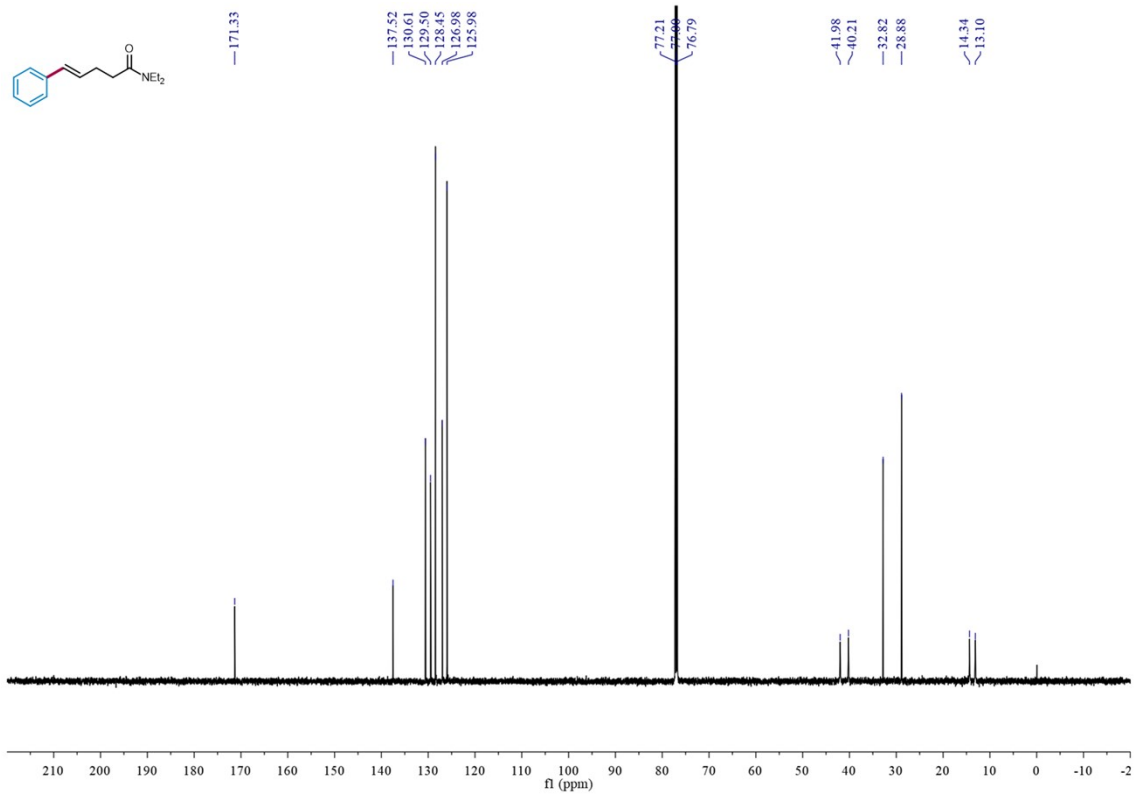

(*E*)-prop-1-ene-1,3-diyldibenzene (**3g**)

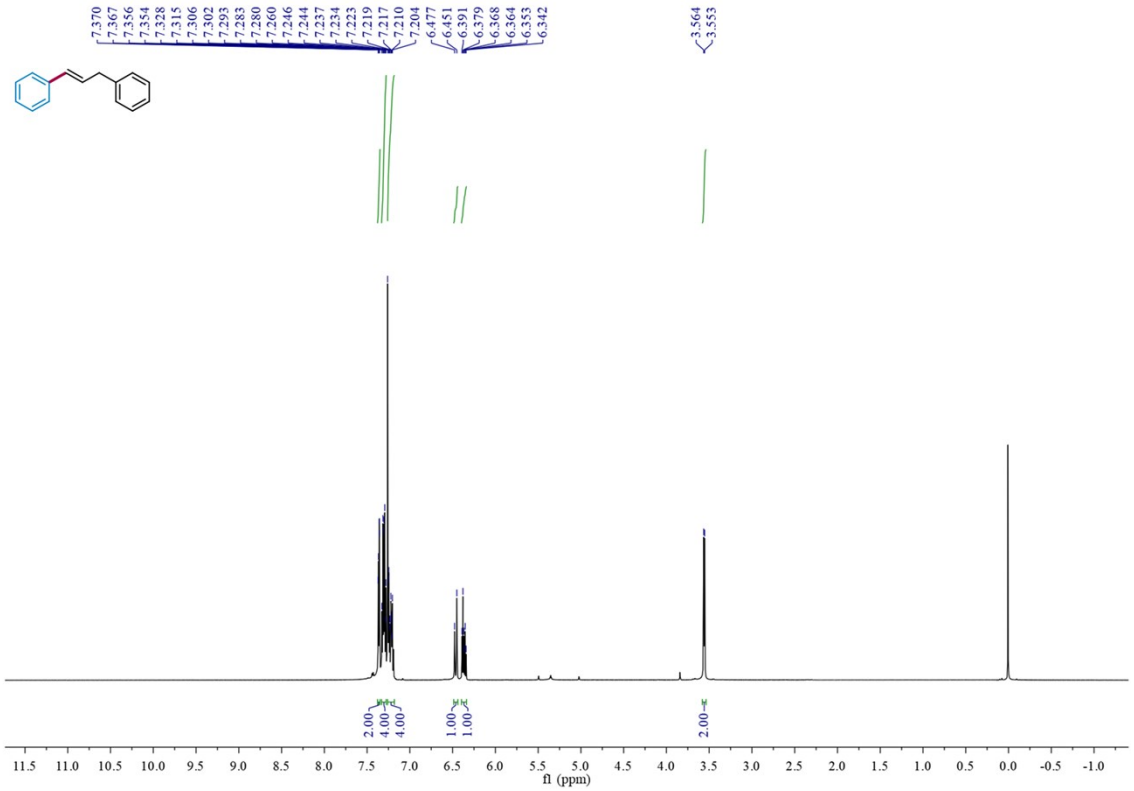

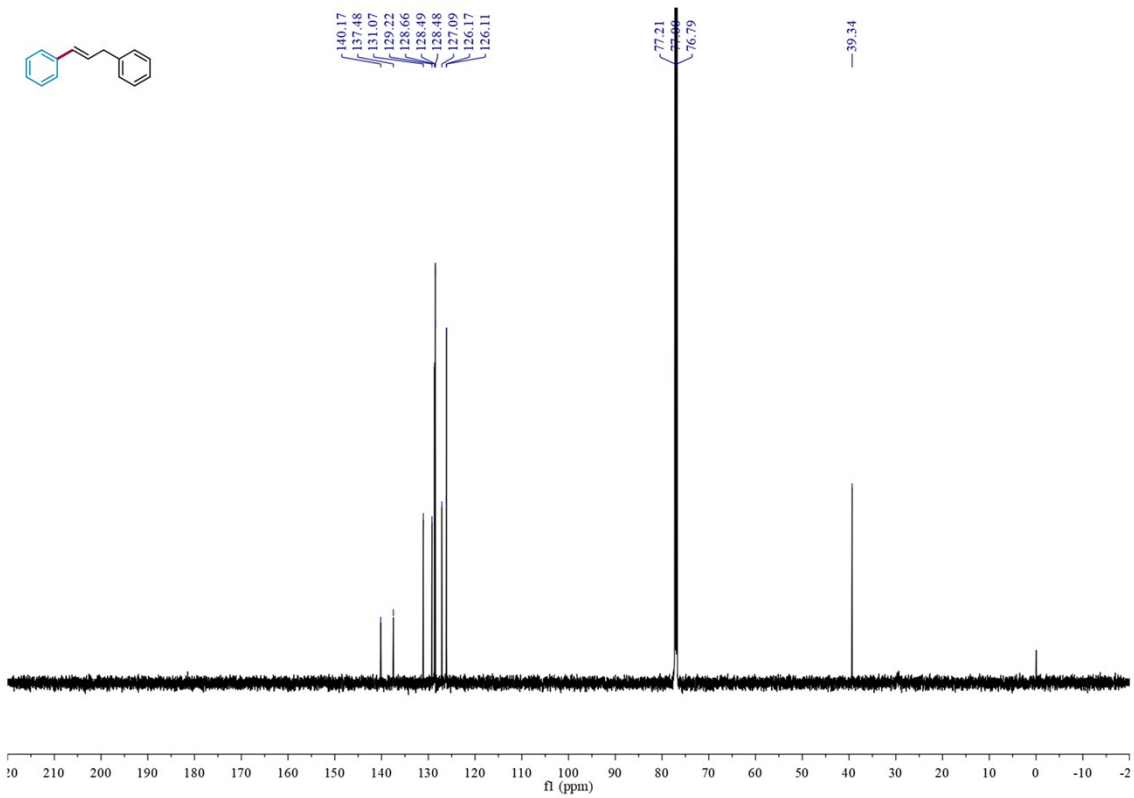

(*E*)-prop-1-ene-1,2-diyldibenzene (**3h**)

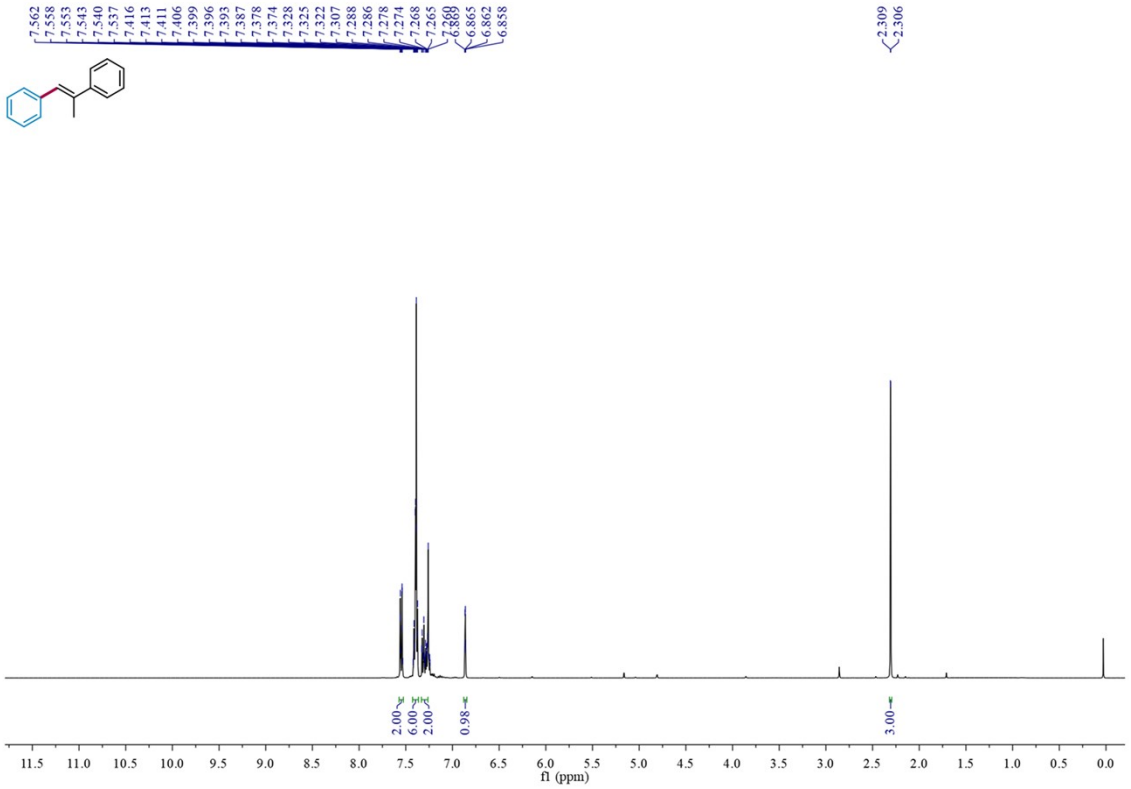

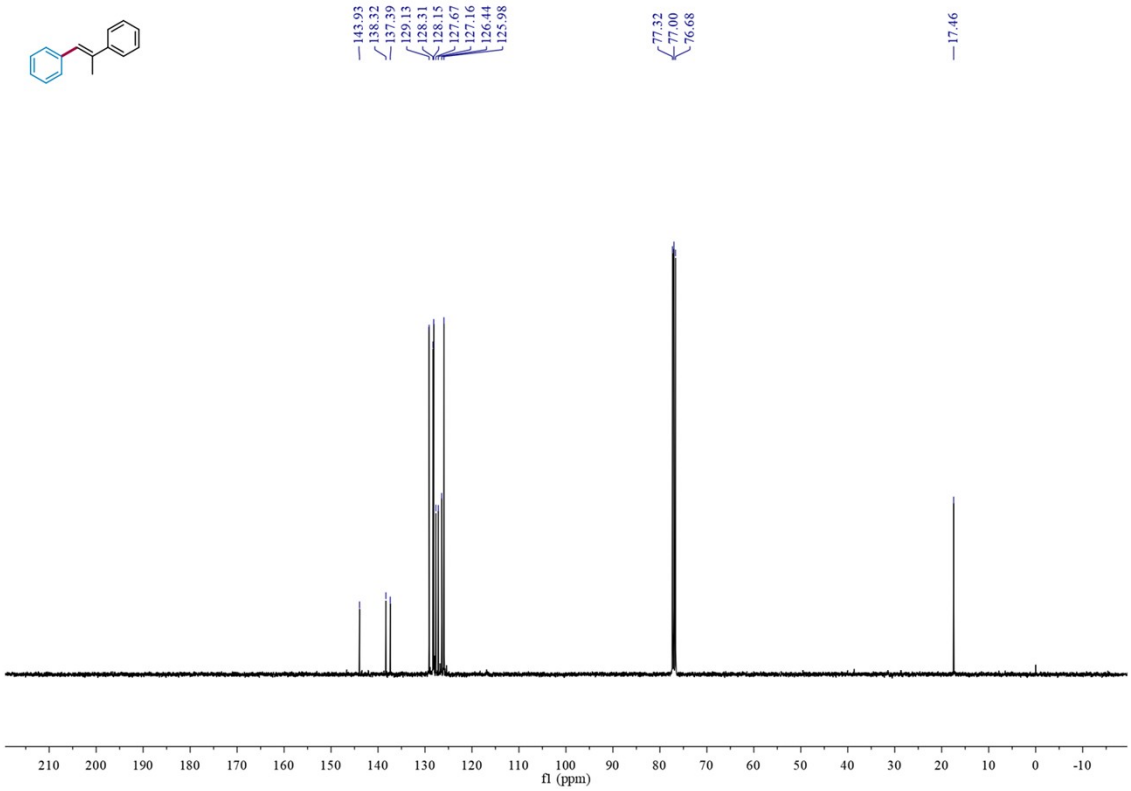

(*E*)-2-(2-phenylprop-1-en-1-yl)phenol (**3i**)

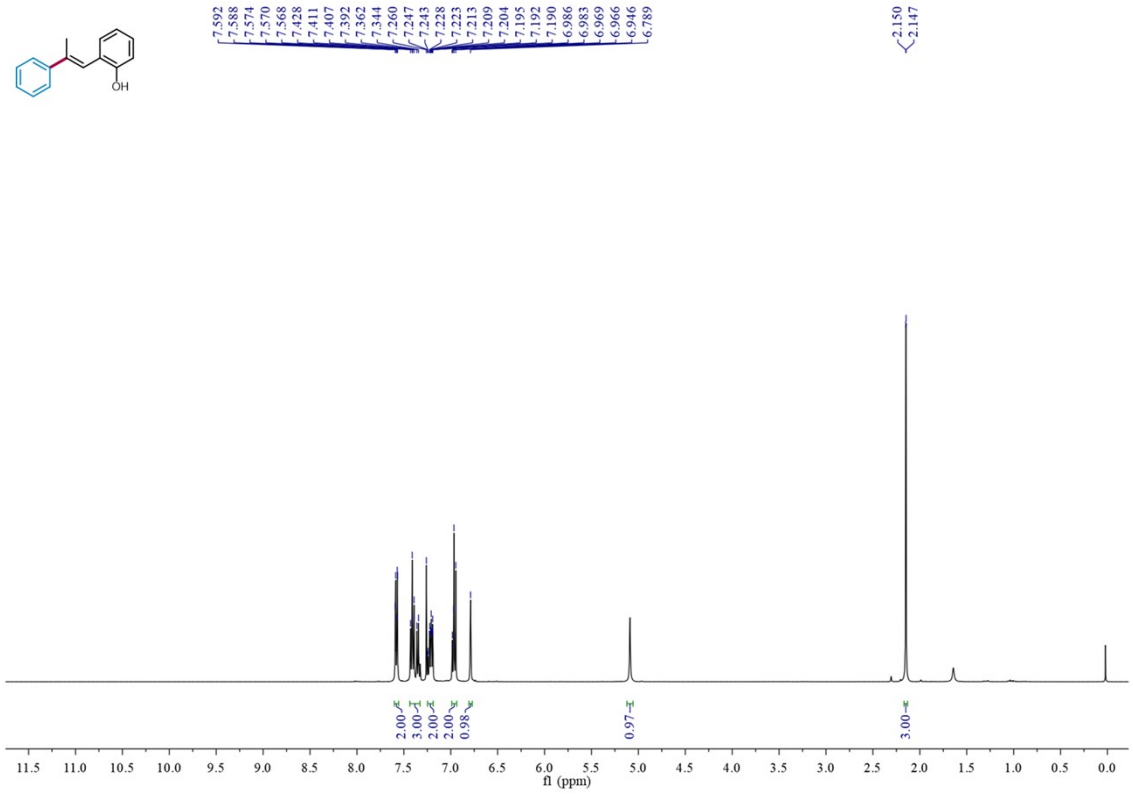

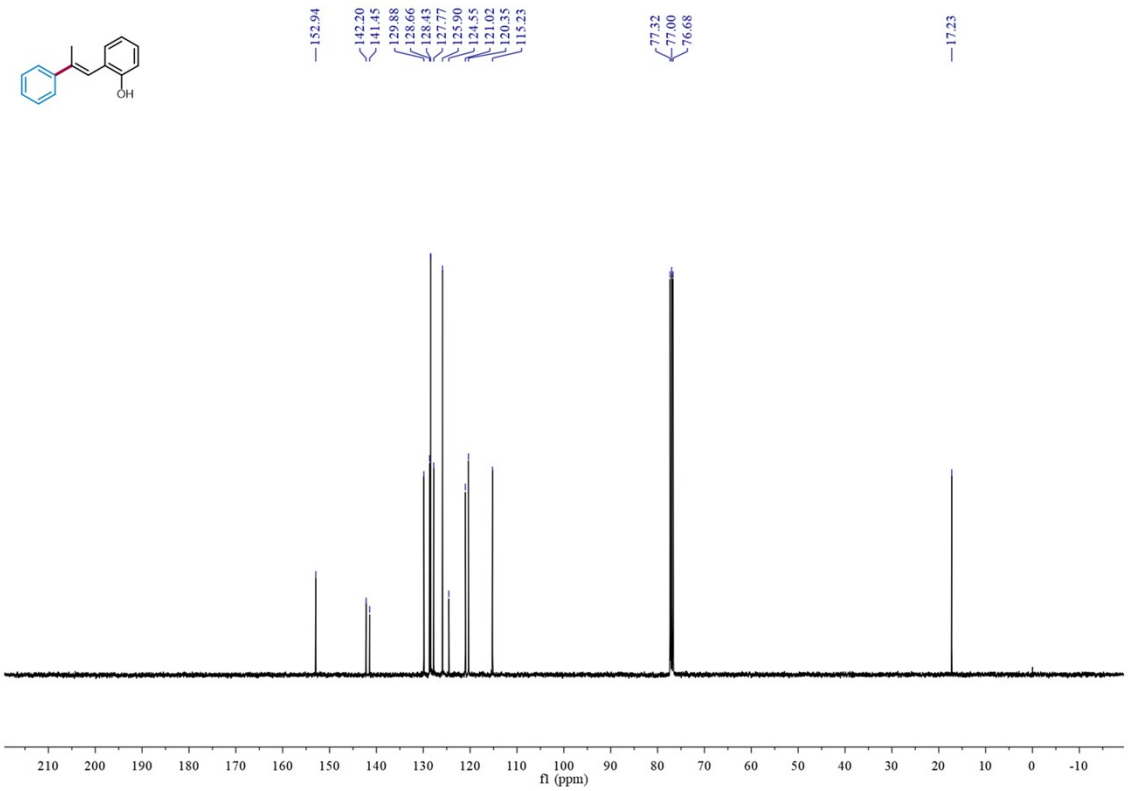

methyl (*E*)-3,3-dimethyl-5-phenylpent-4-enoate (**3j**)

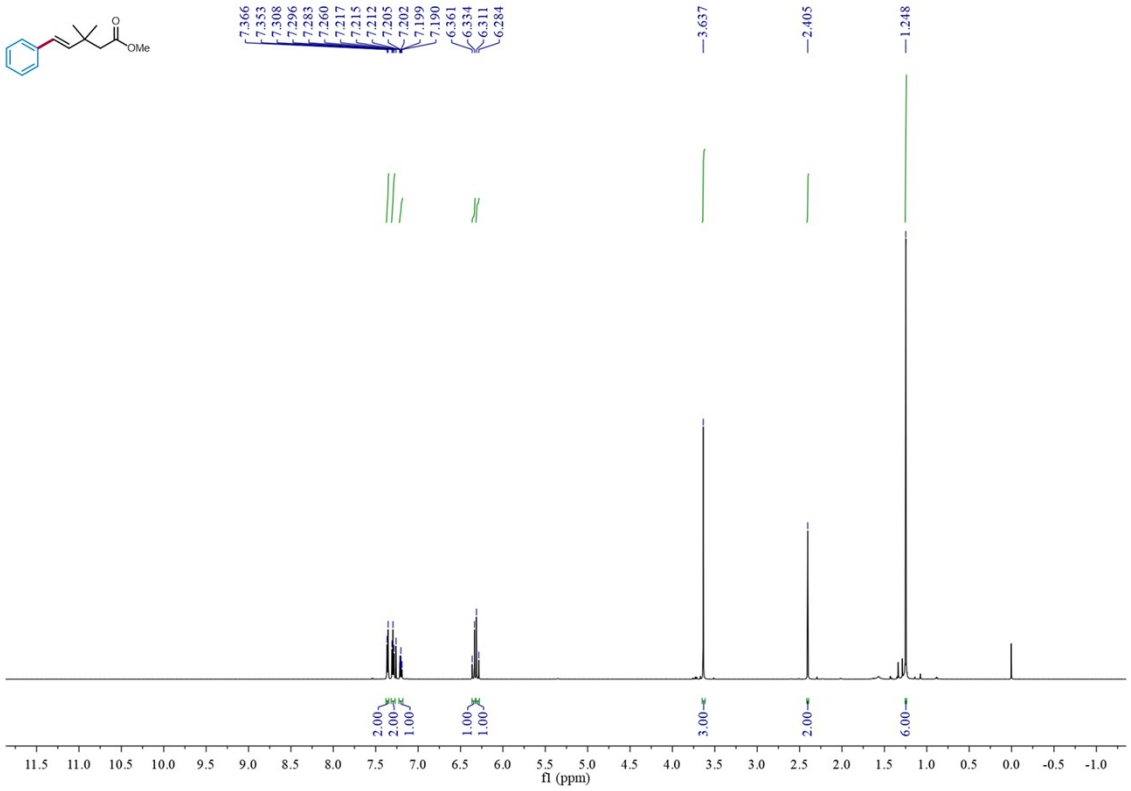

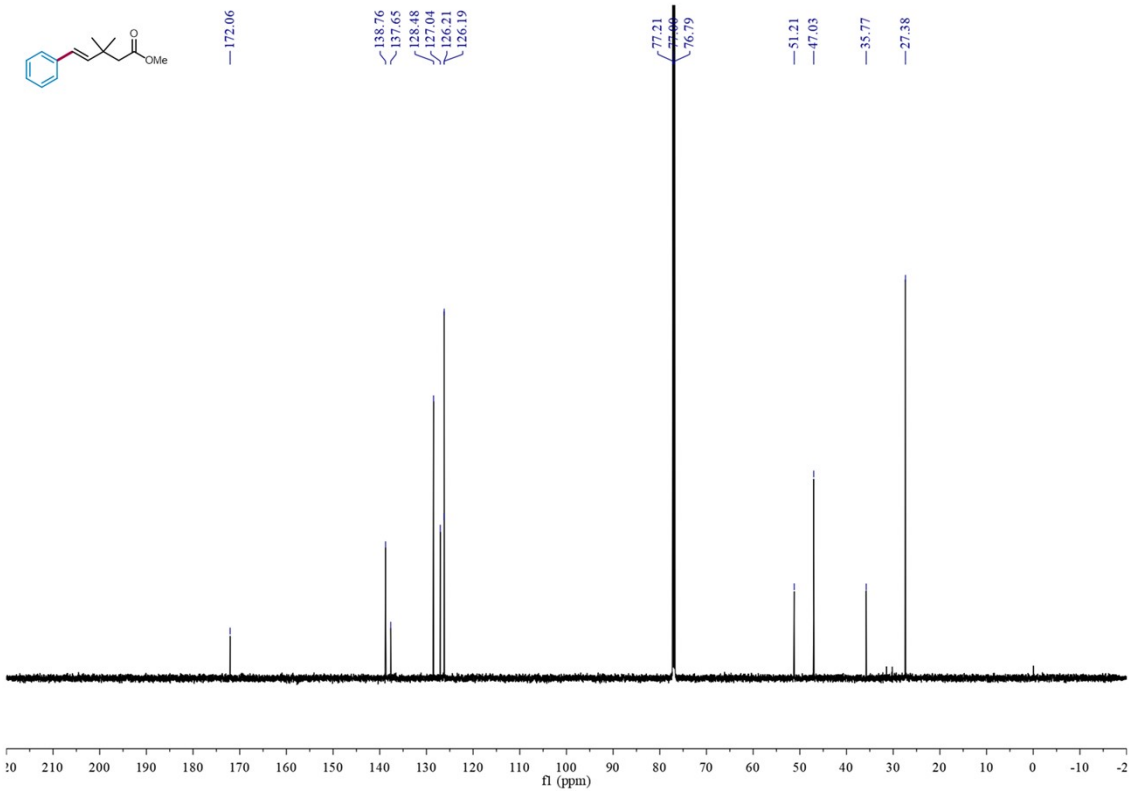

methyl (*E*)-3,3-dimethyl-5-(*o*-tolyl)pent-4-enoate (**3k**)

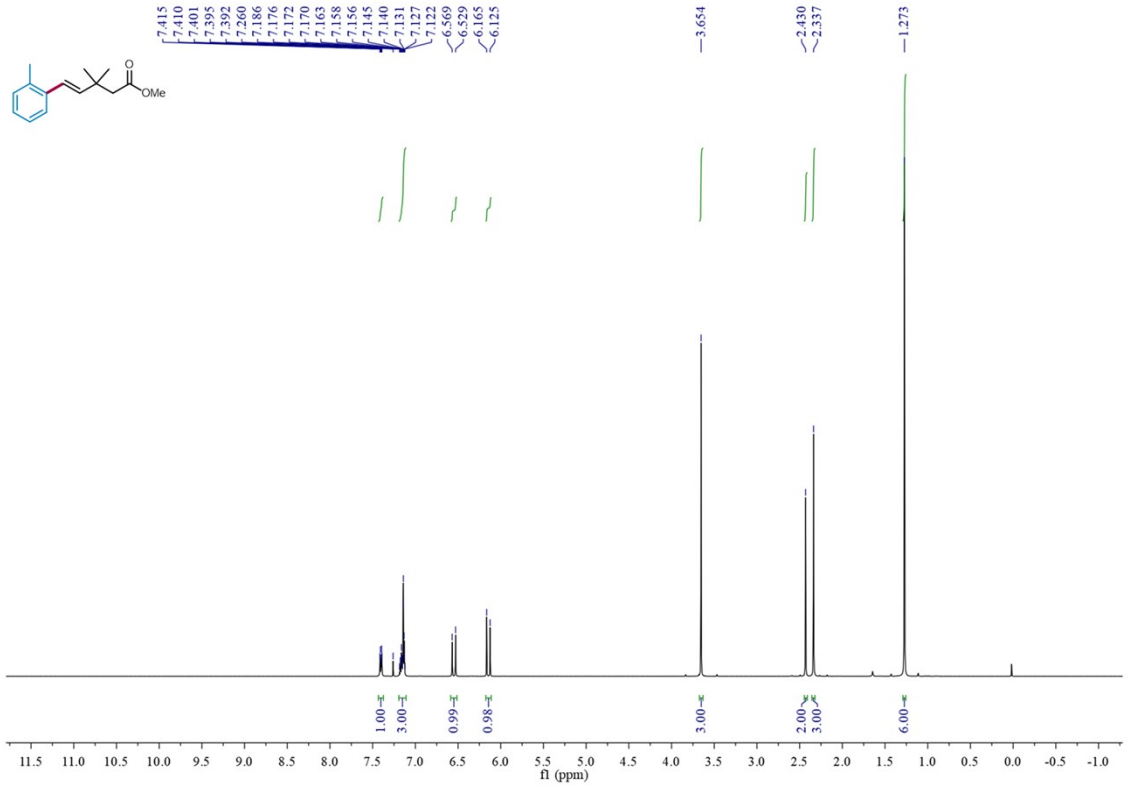

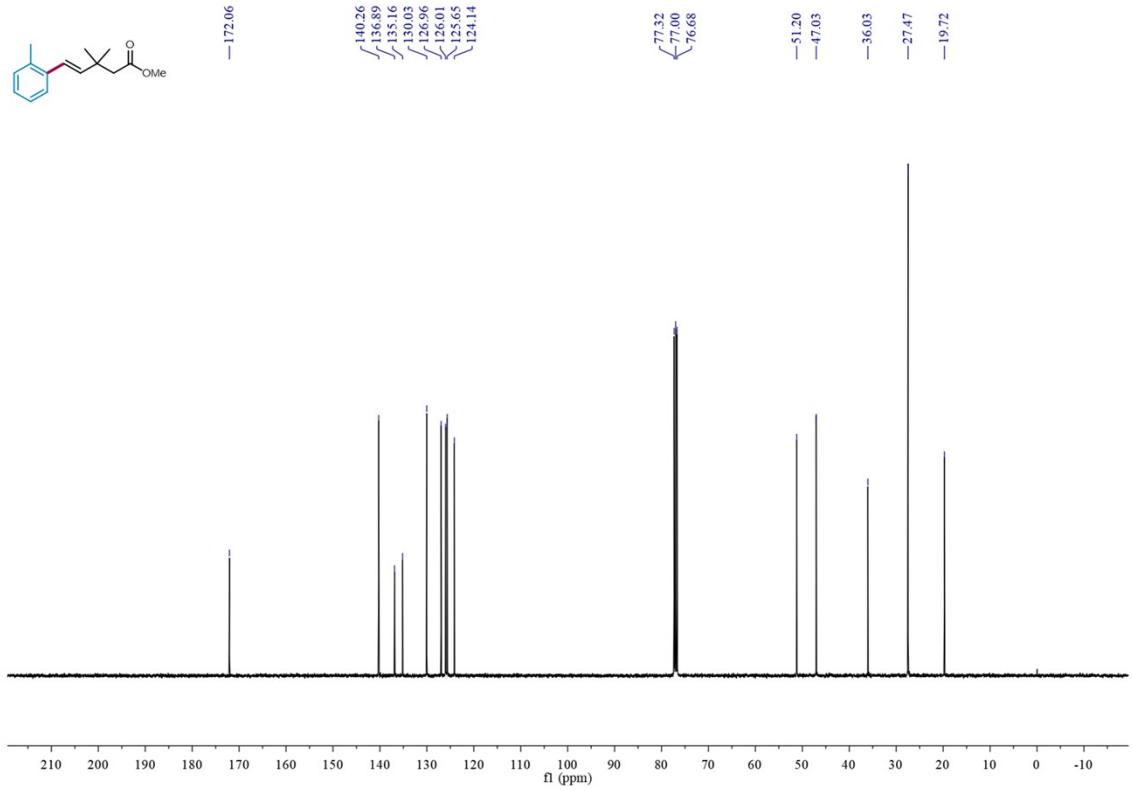

methyl (*E*)-3,3-dimethyl-5-(m-tolyl)pent-4-enoate (**3l**)

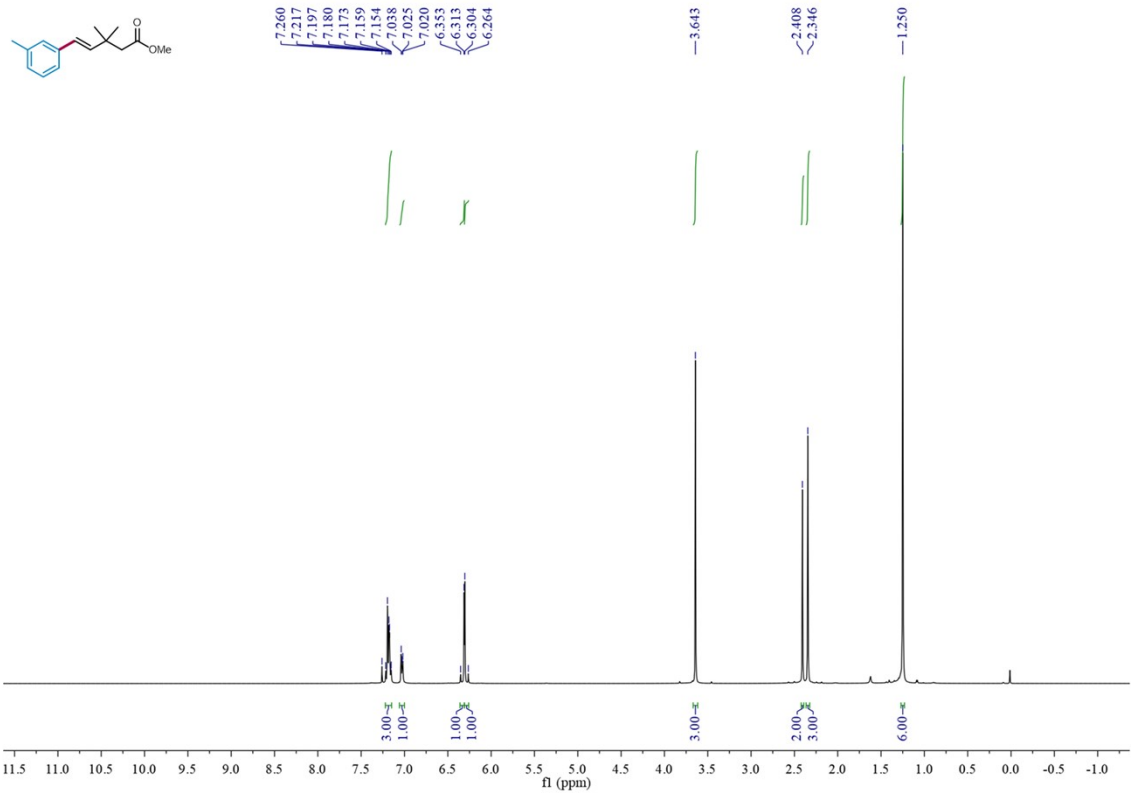

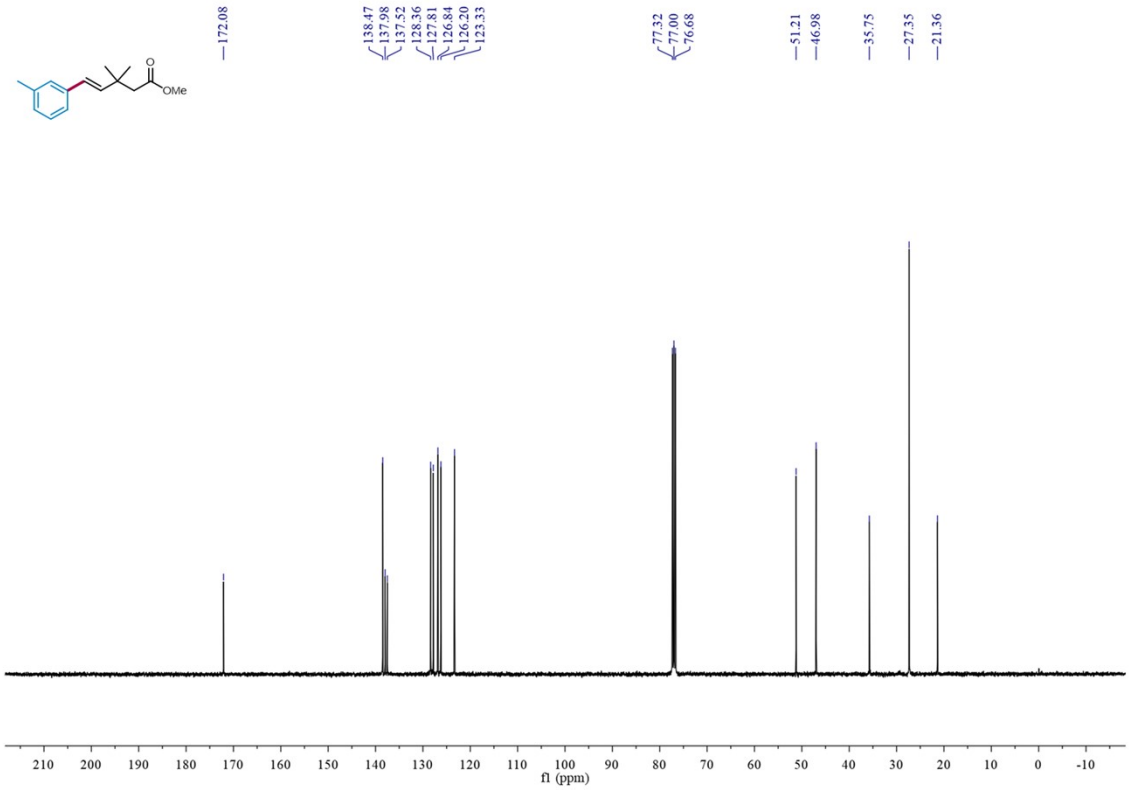

methyl (*E*)-3,3-dimethyl-5-(*p*-tolyl)pent-4-enoate (**3m**)

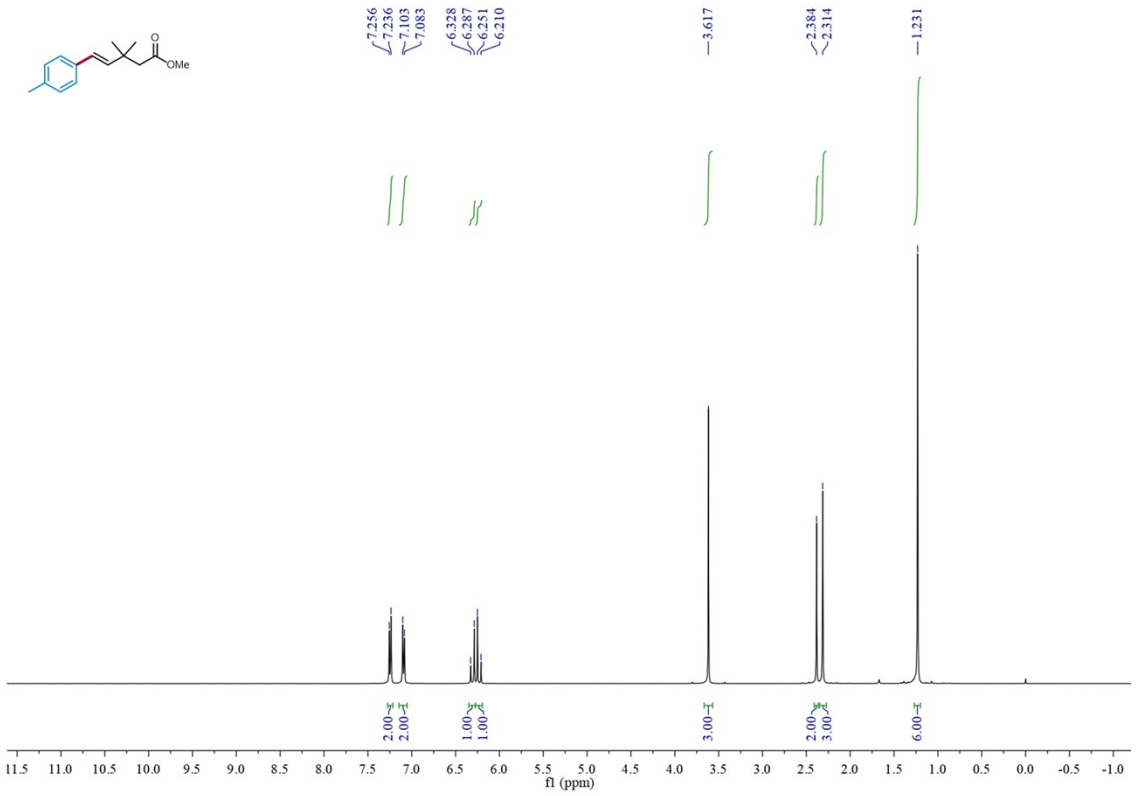

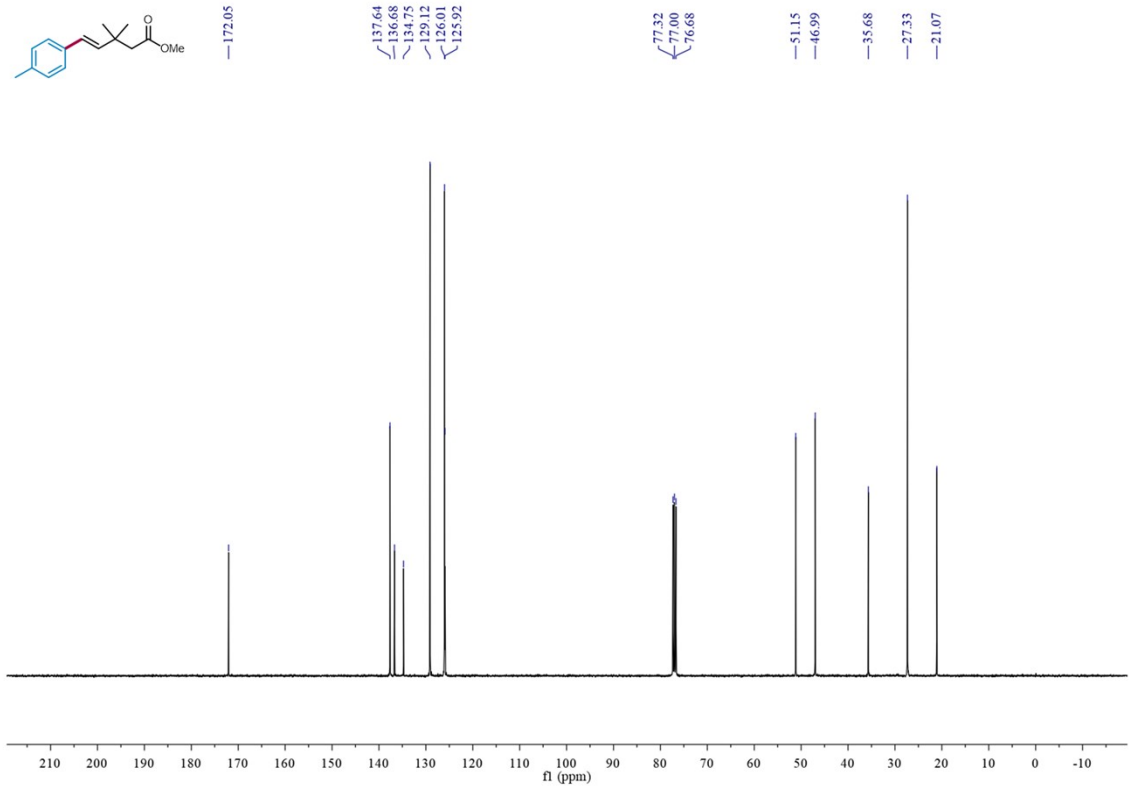

methyl (*E*)-5-(3,5-dimethylphenyl)-3,3-dimethylpent-4-enoate (**3n**)

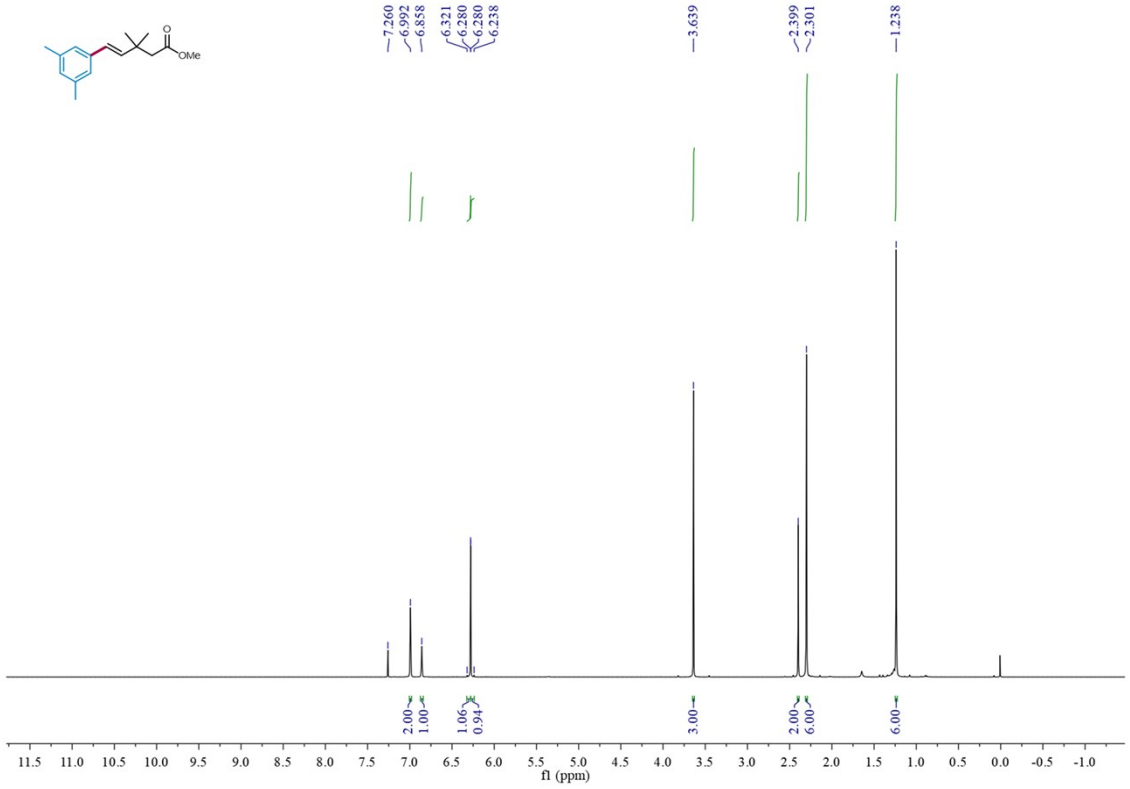

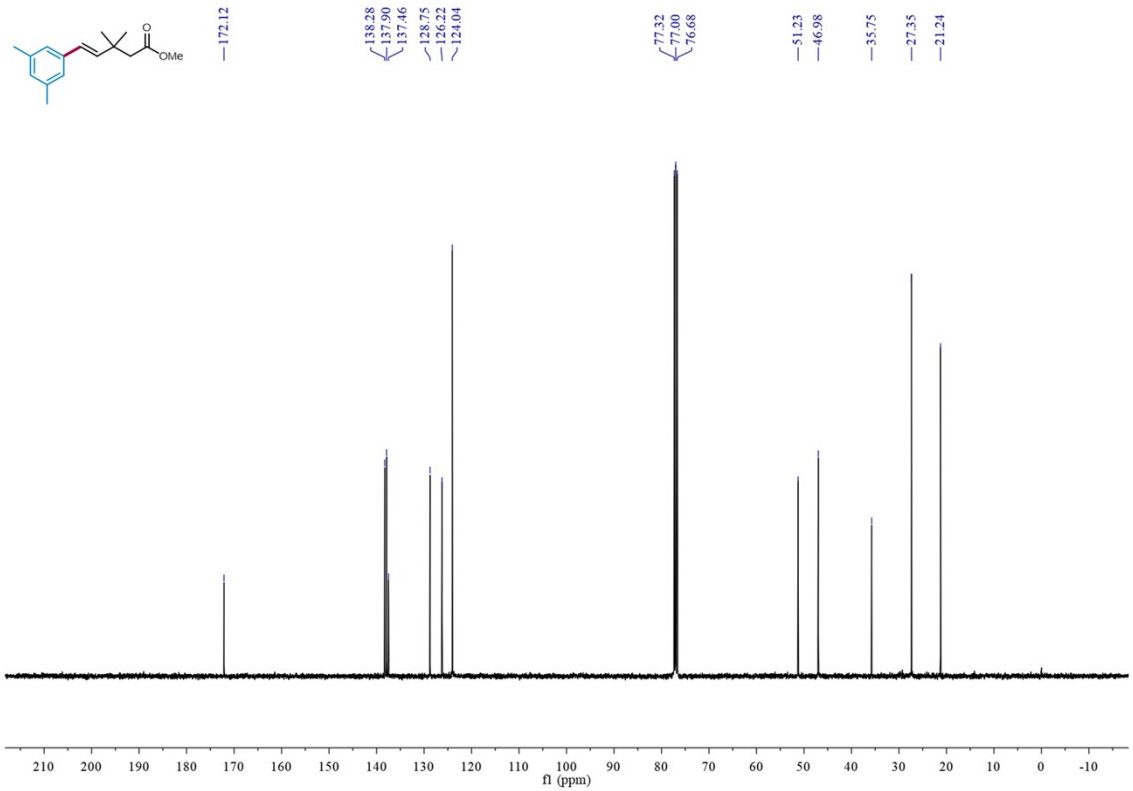

methyl (*E*)-5-(4-fluorophenyl)-3,3-dimethylpent-4-enoate (**3o**)

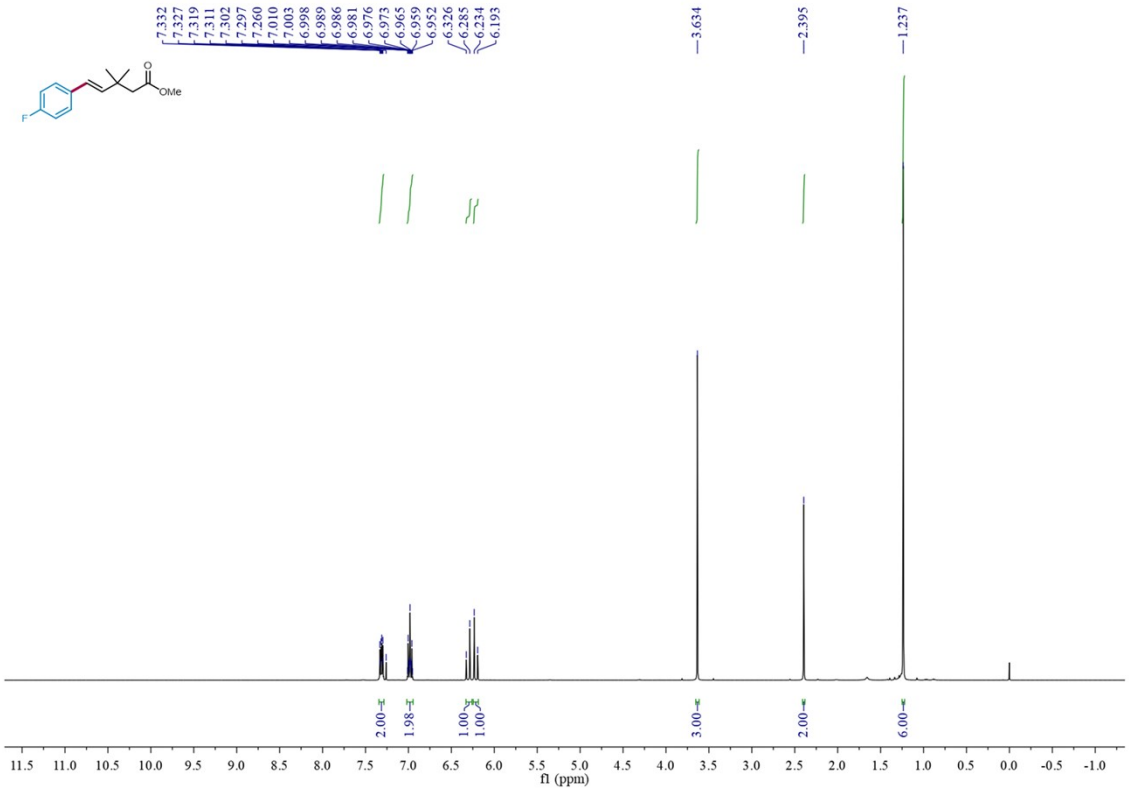

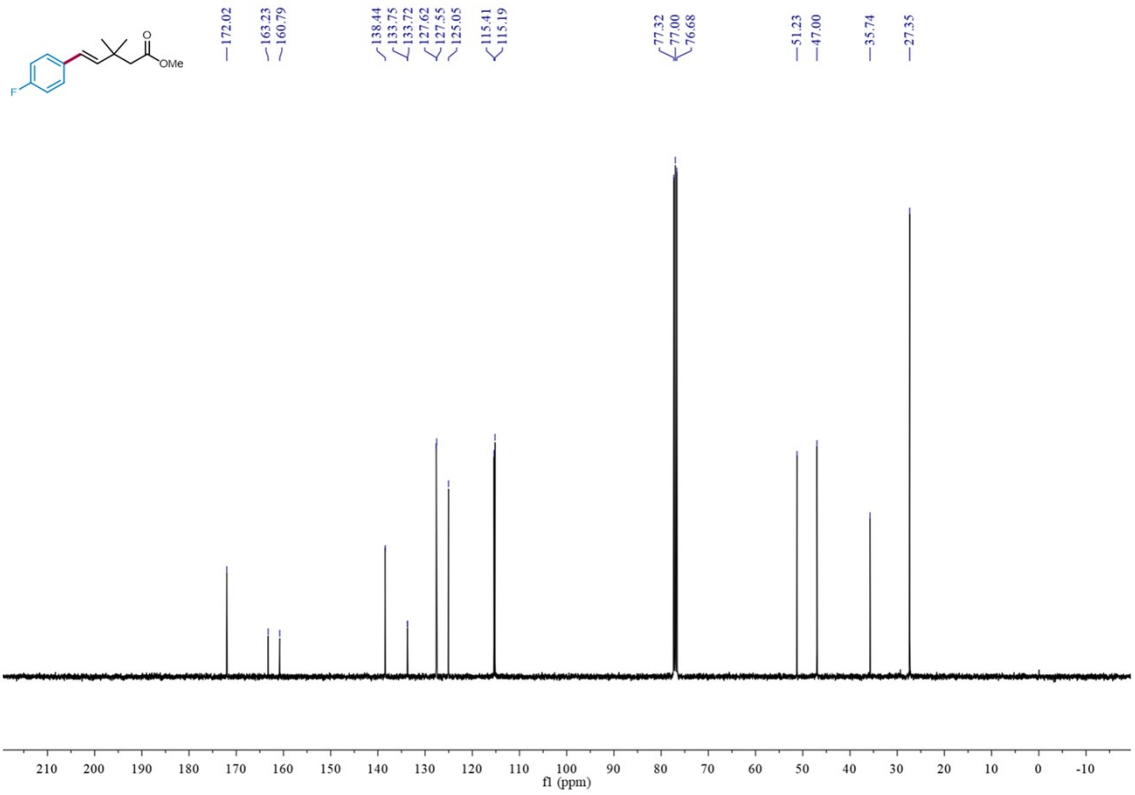

methyl (*E*)-5-(4-bromophenyl)-3,3-dimethylpent-4-enoate (**3p**)

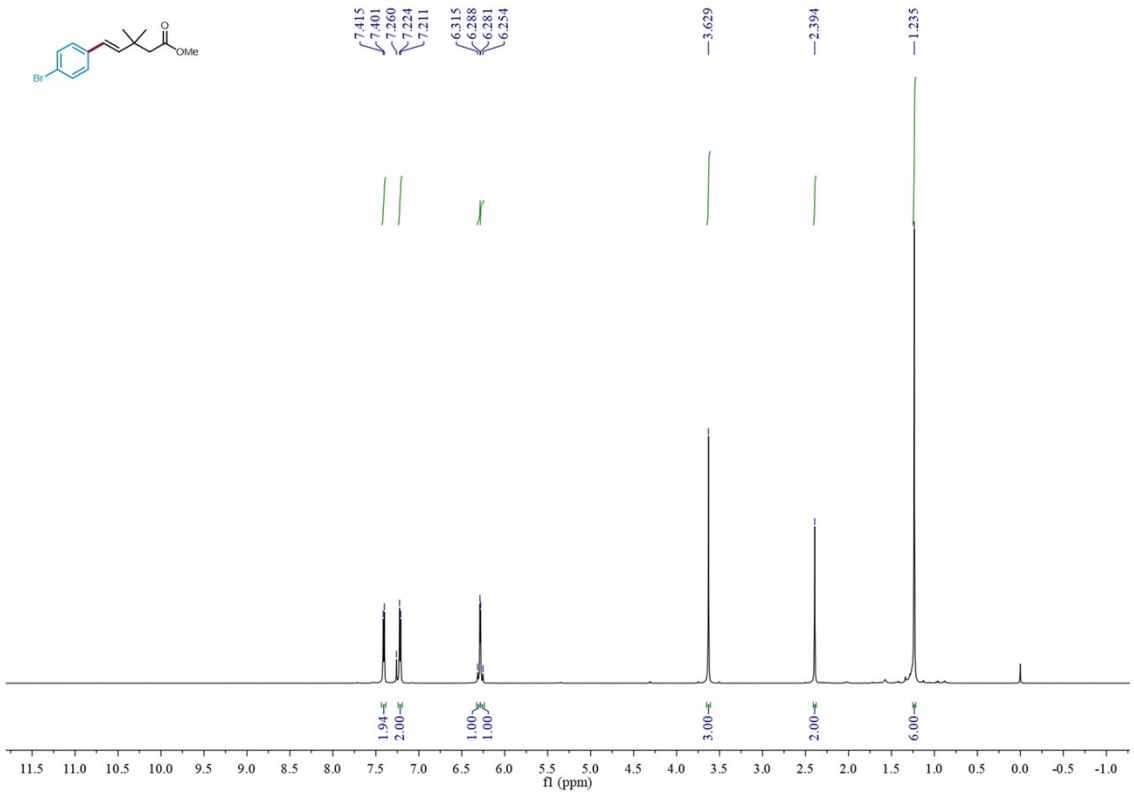

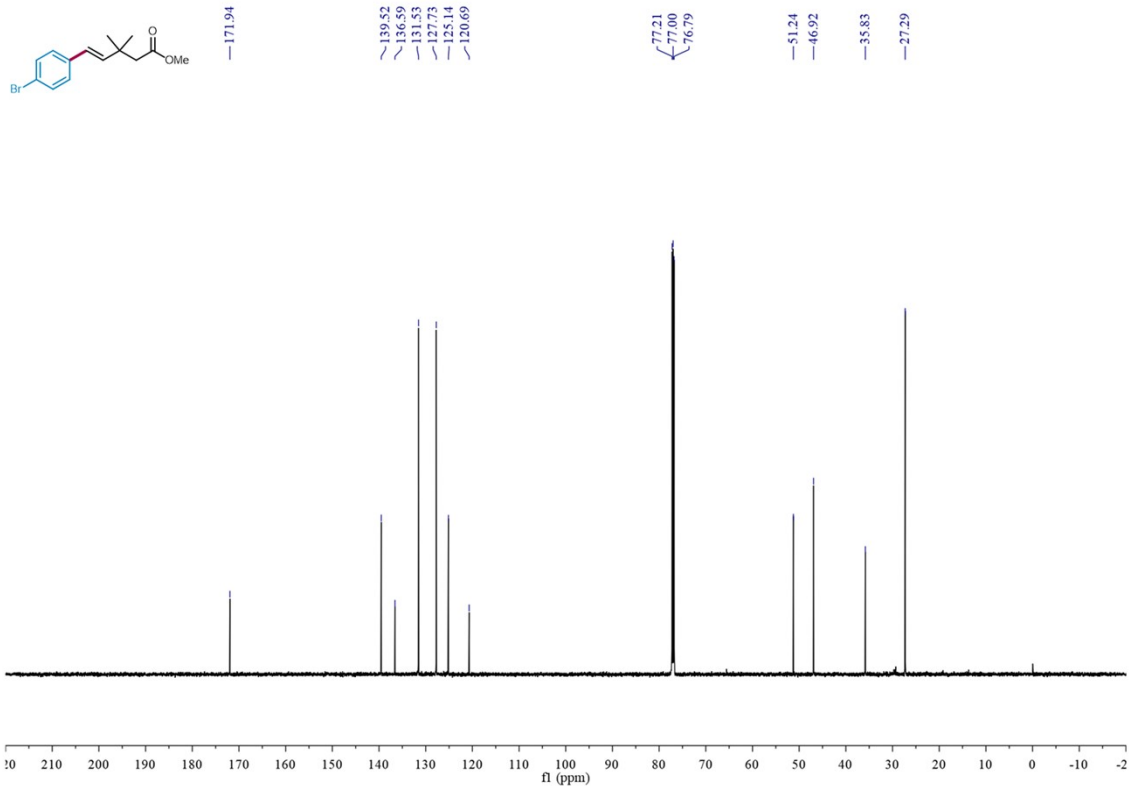

2-isopropyl-5-methylcyclohexyl (*E*)-5-phenylpent-4-enoate (**3q**)

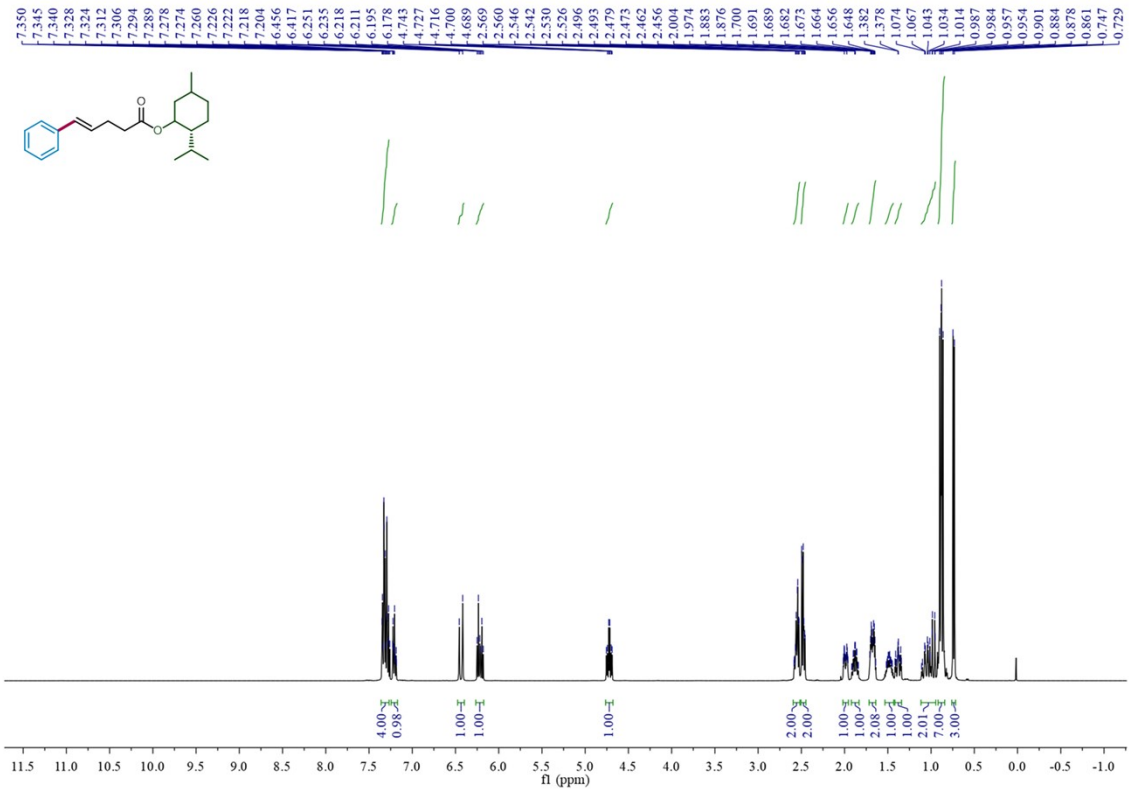

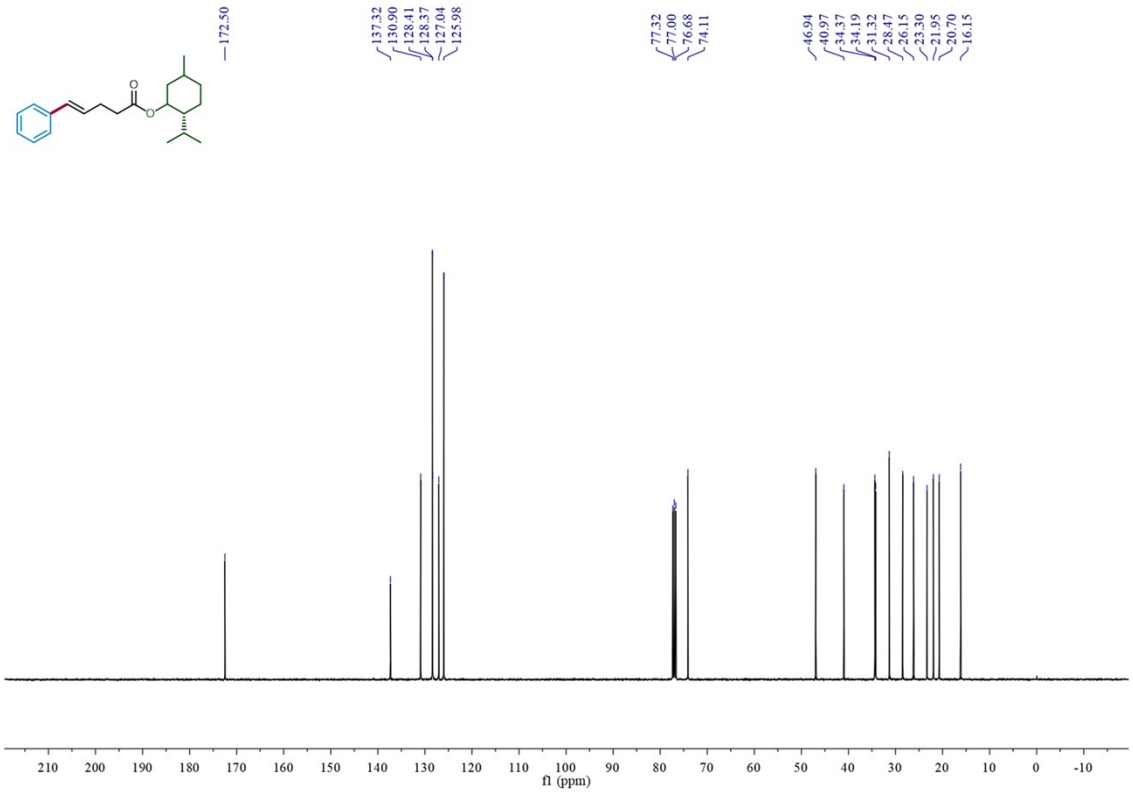

(3S,10R,13R)-10,13-dimethyl-17-(6-methylheptan-2-yl)-2,3,4,7,8,9,10,11,12,13,14,15,16,17-tetradecahydro-1H-cyclopenta[a]phenanthren-3-yl (*E*)-5-phenylpent-4-enoate (**3r**)

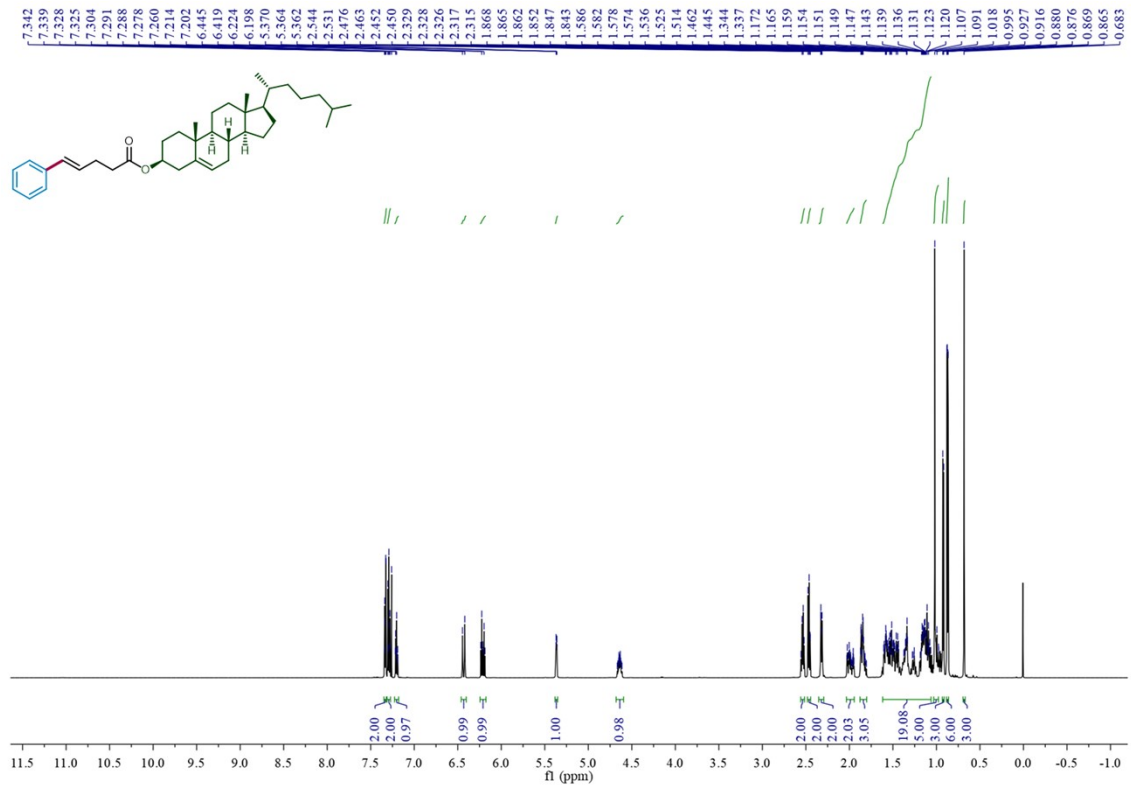

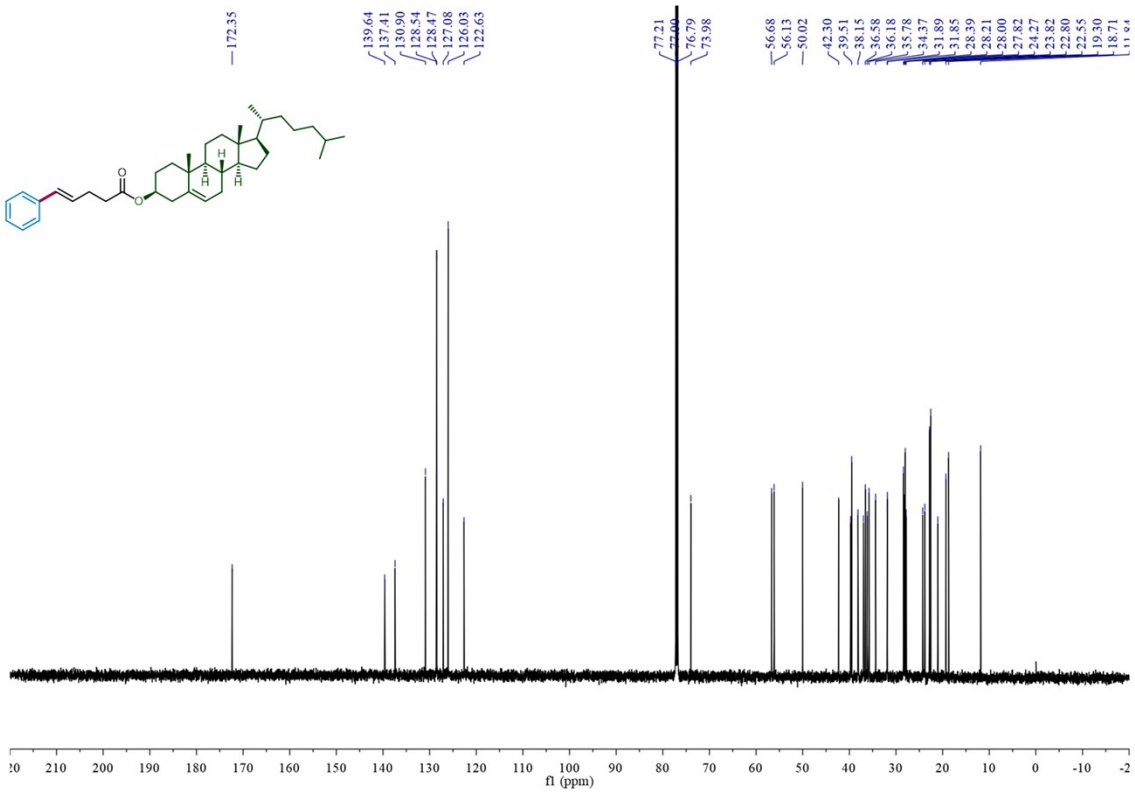

furan-2-ylmethyl (*E*)-5-phenylpent-4-enoate (**3s**)

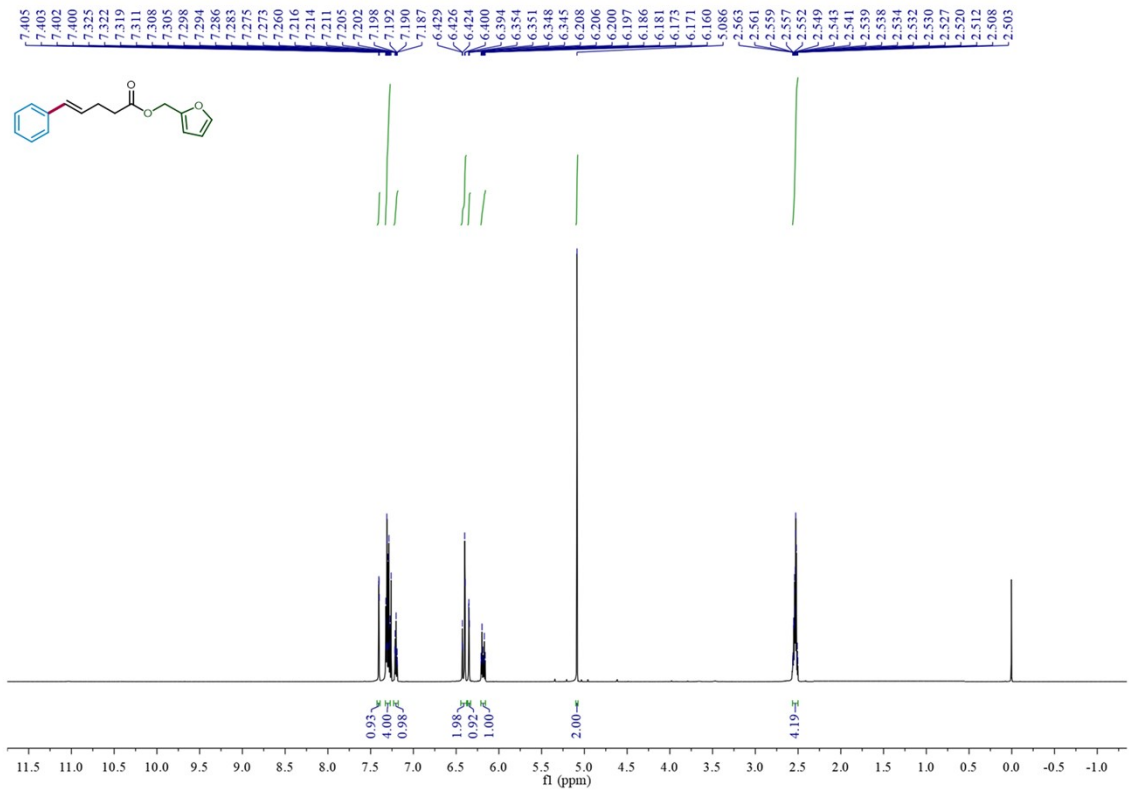

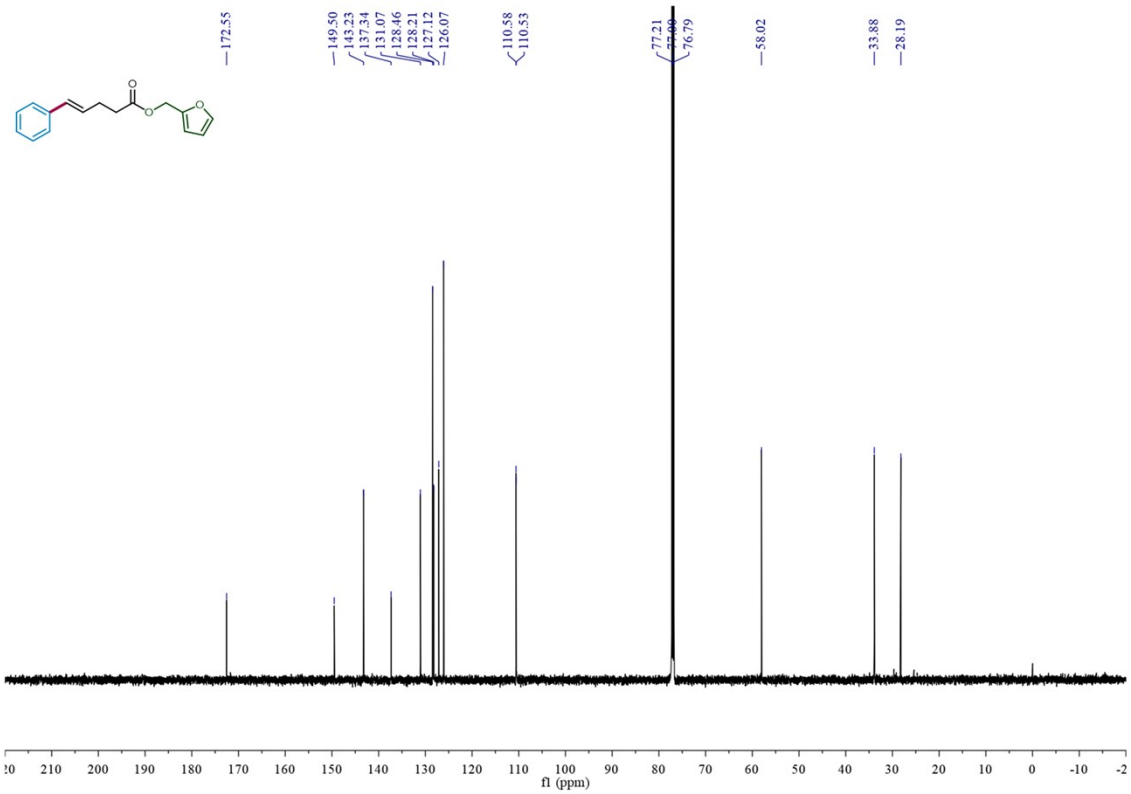

(*E*)-*N*-(adamantan-1-yl)-5-phenylpent-4-enamide (**3t**)

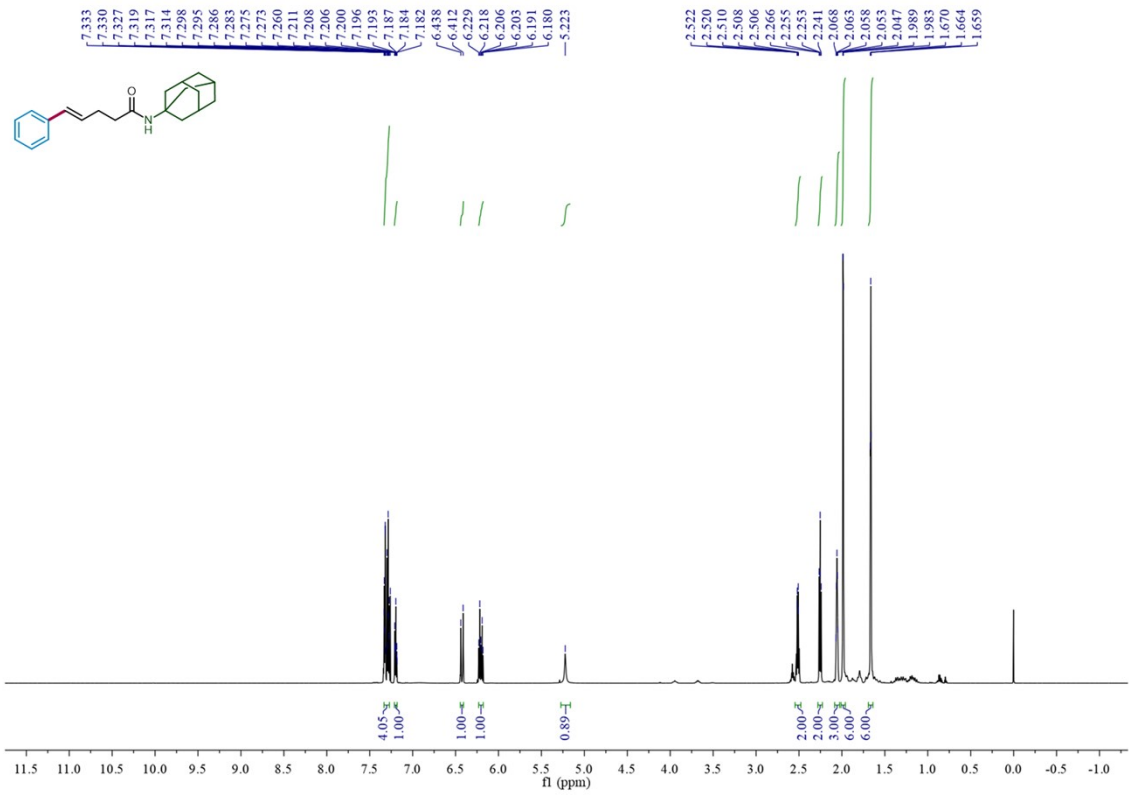

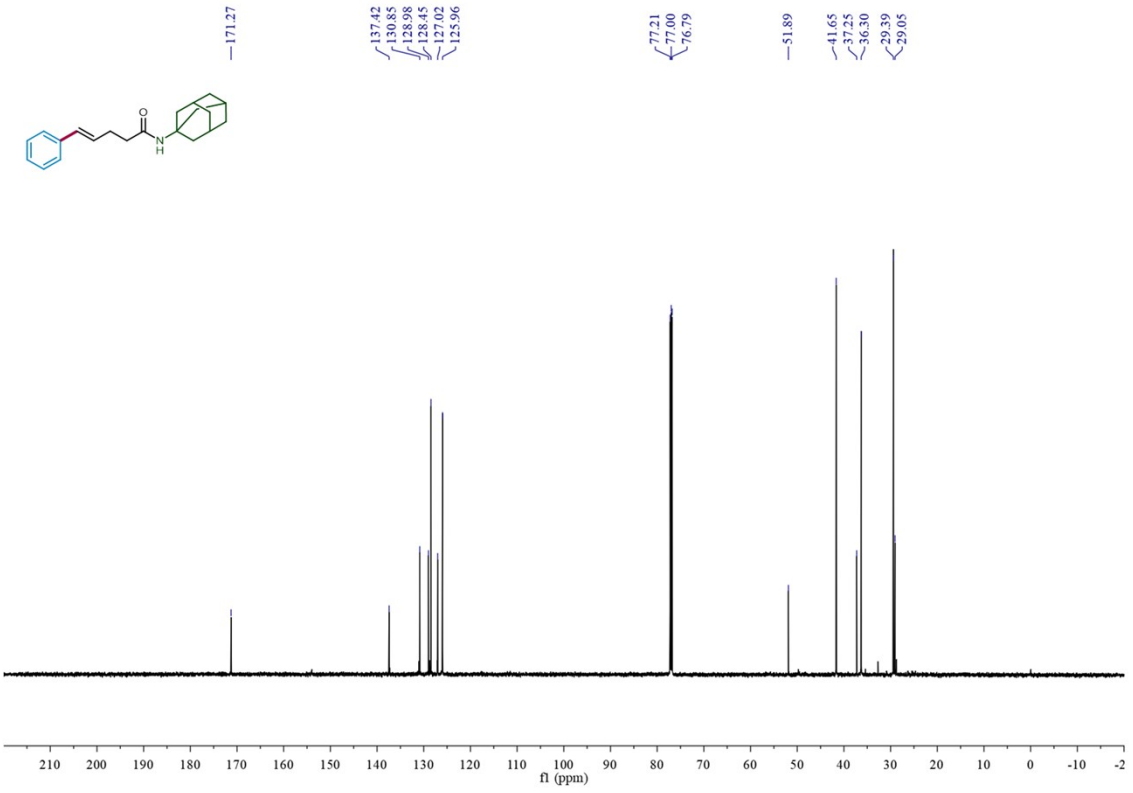

(*E*)-5-phenylpent-4-en-1-yl 5-(2,5-dimethylphenoxy)-2,2-dimethylpentanoate (**3u**)

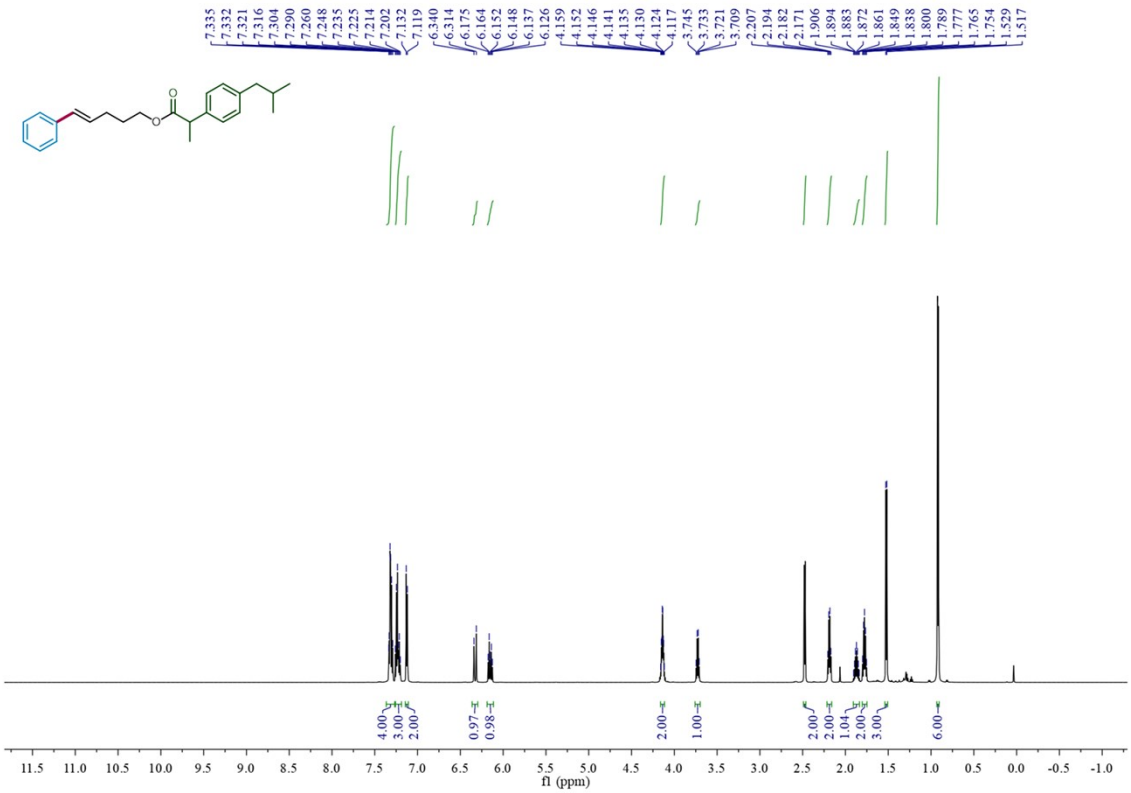

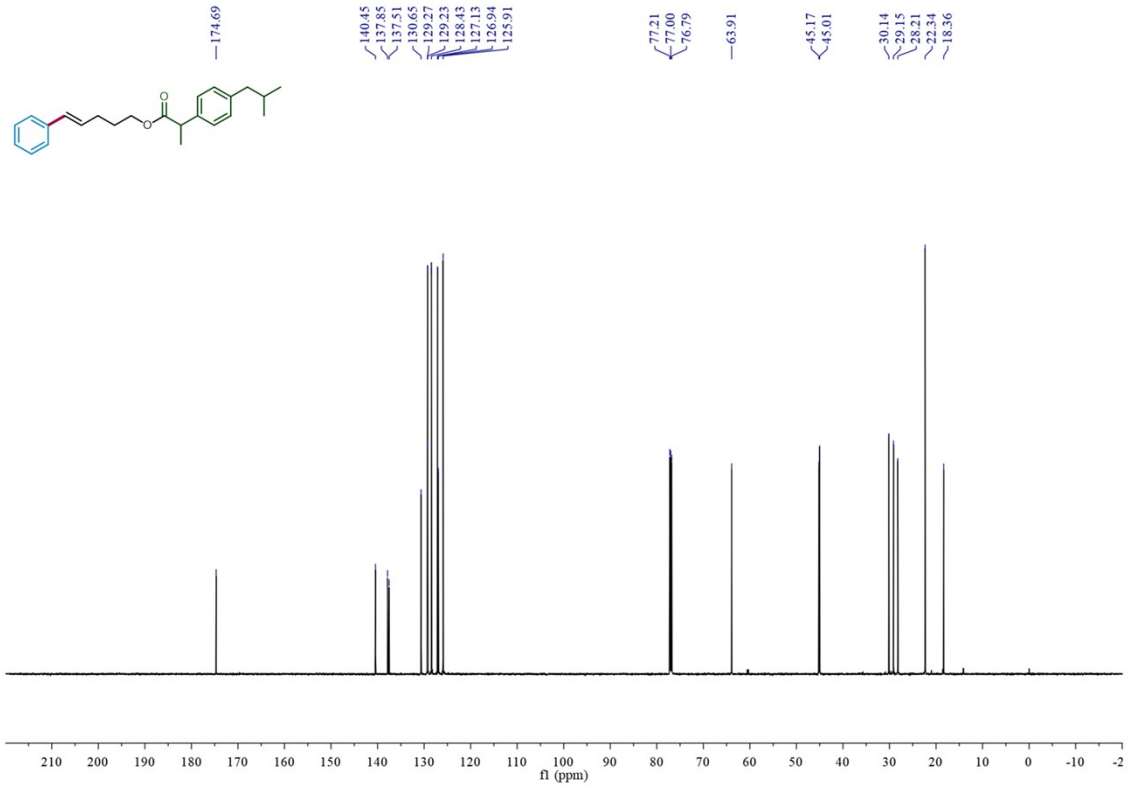

(*E*)-oct-1-en-1-ylbenzene (**5a**)

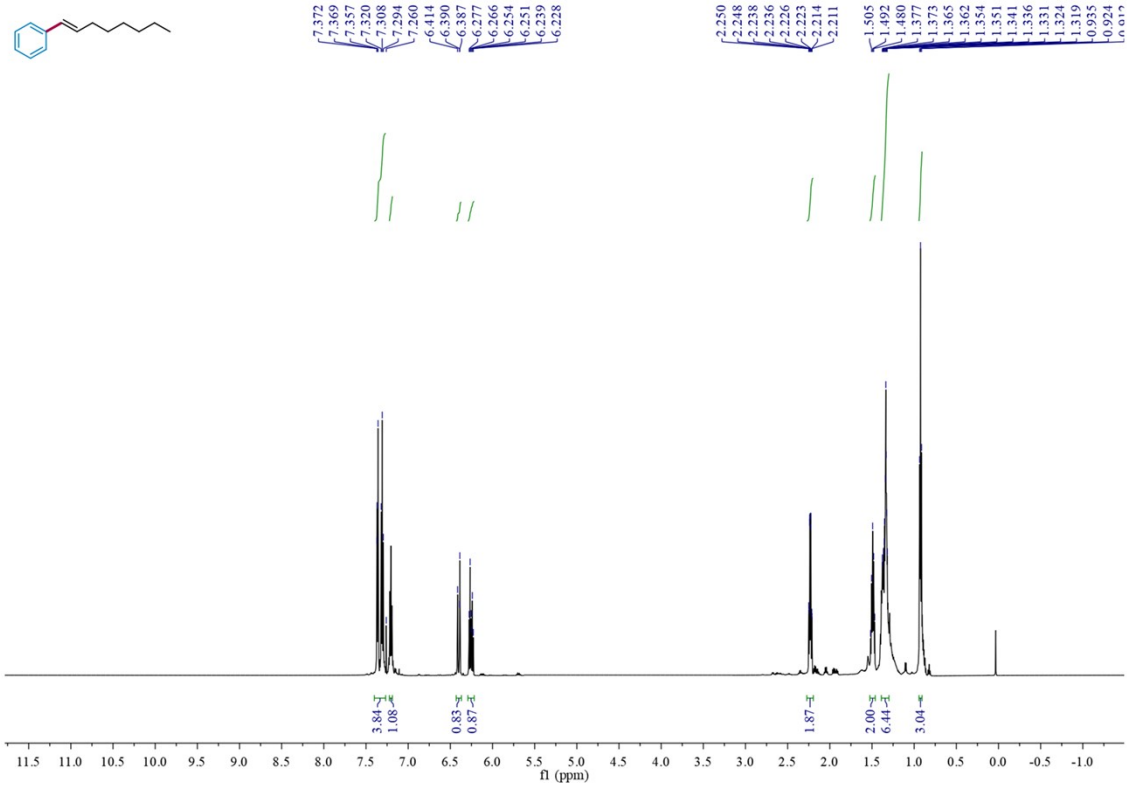

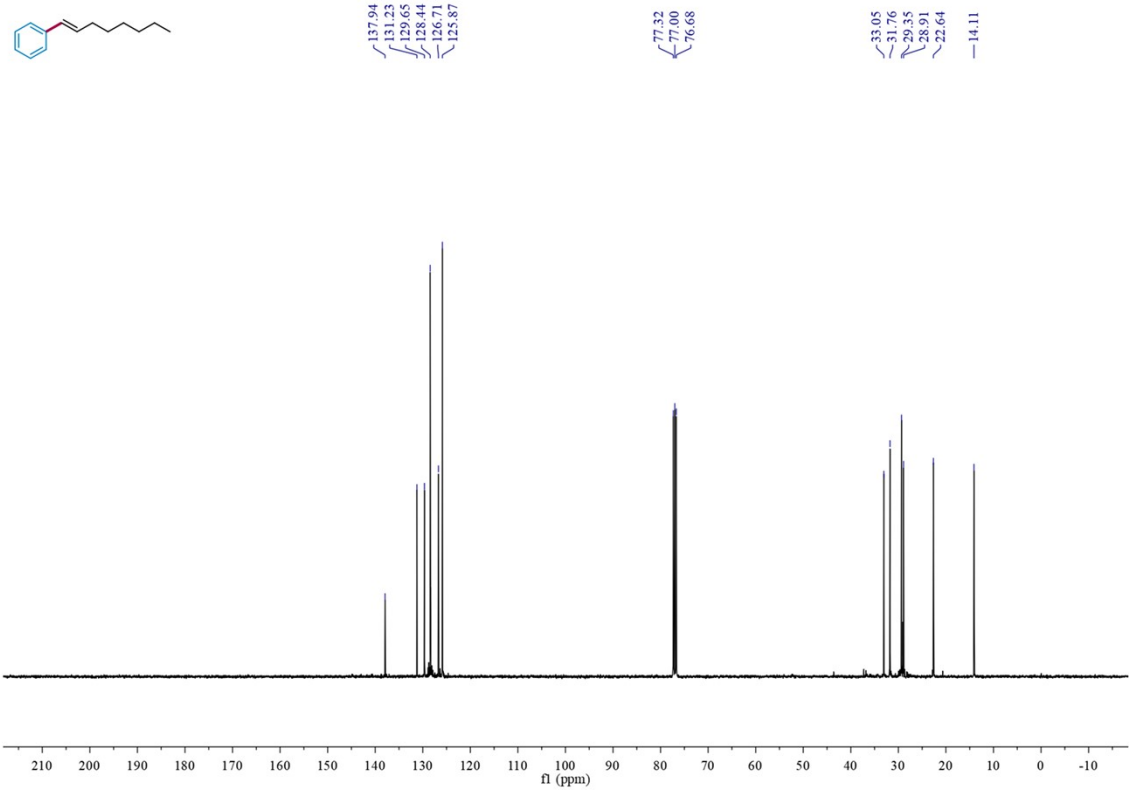

(*E*)-dec-1-en-1-ylbenzene (**5b**)

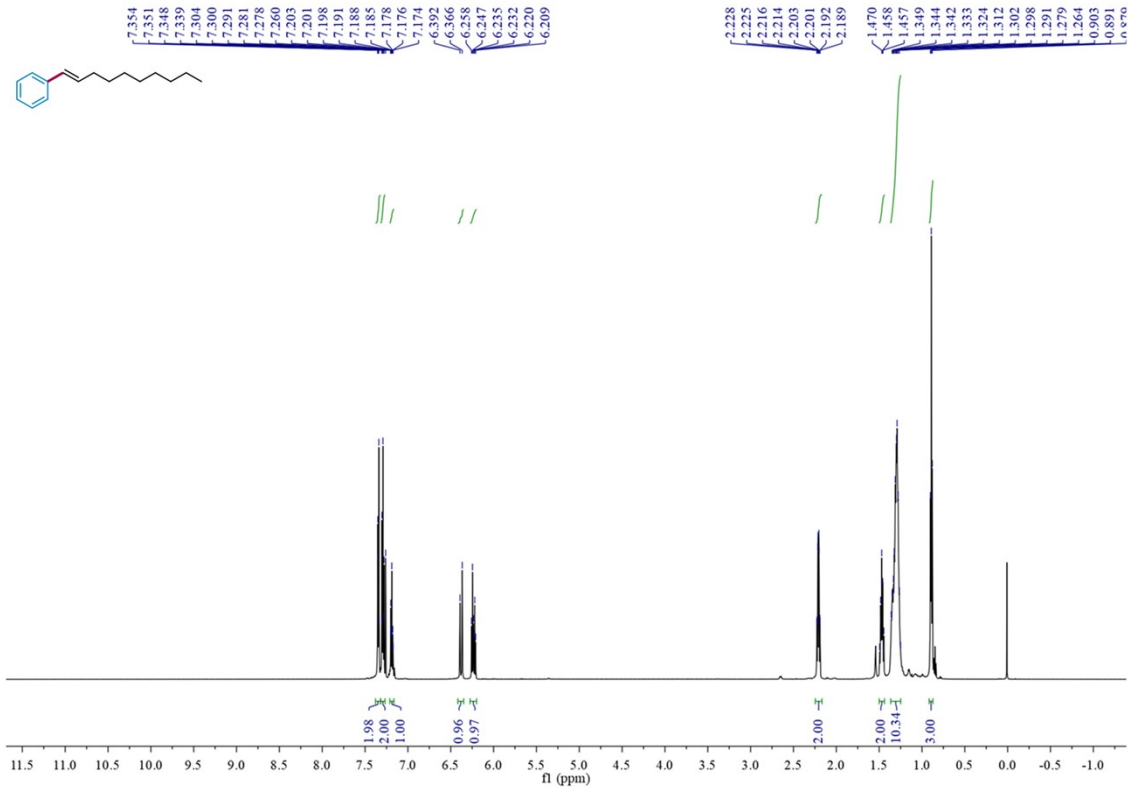

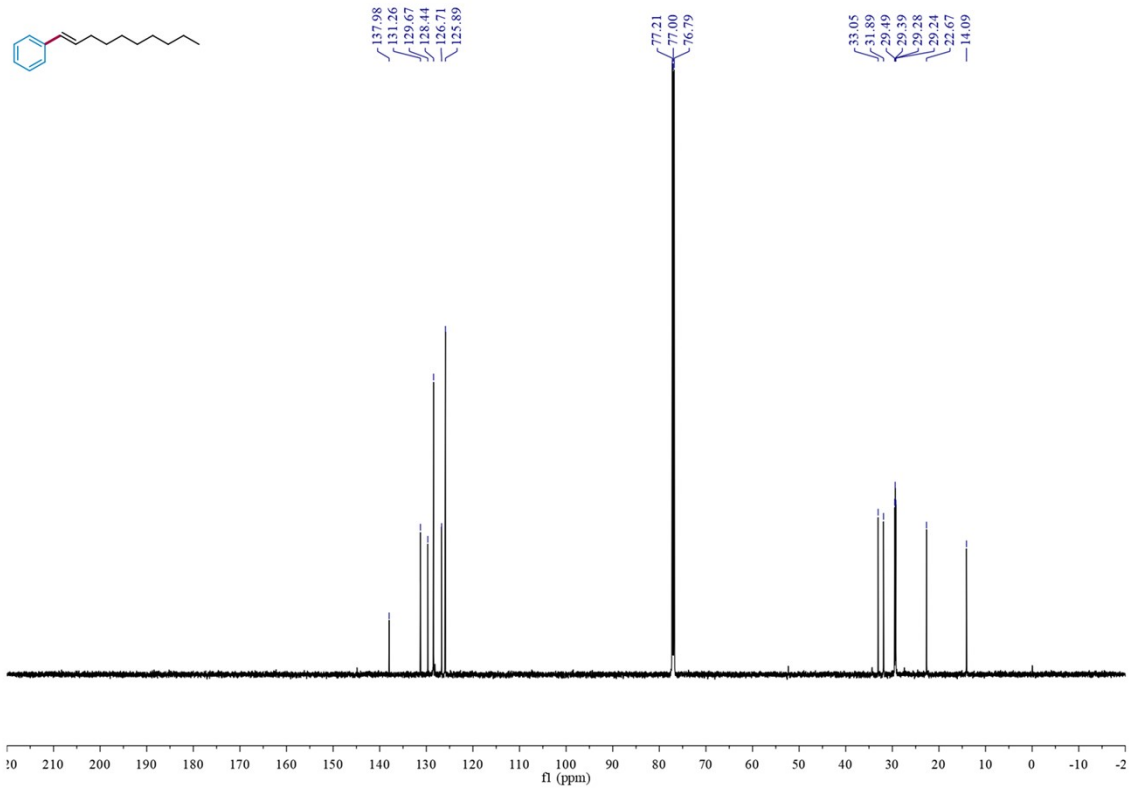

(*E*)-dodec-1-en-1-ylbenzene (**5c**)

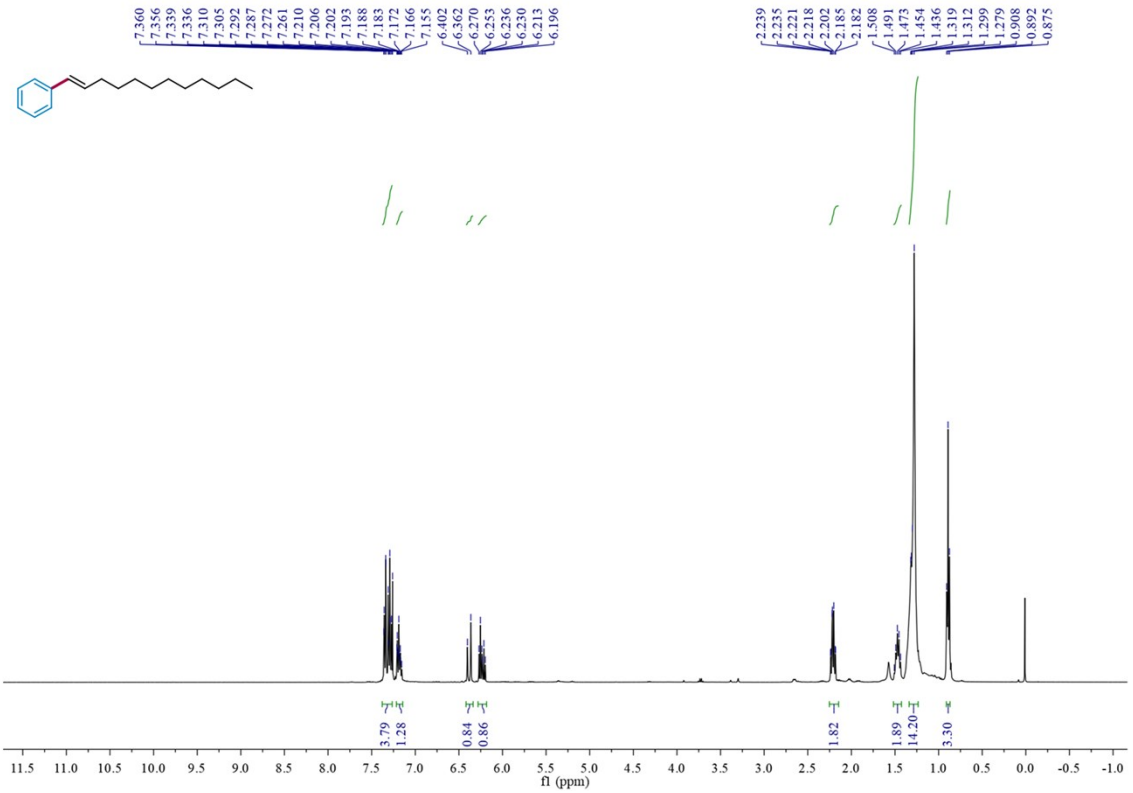

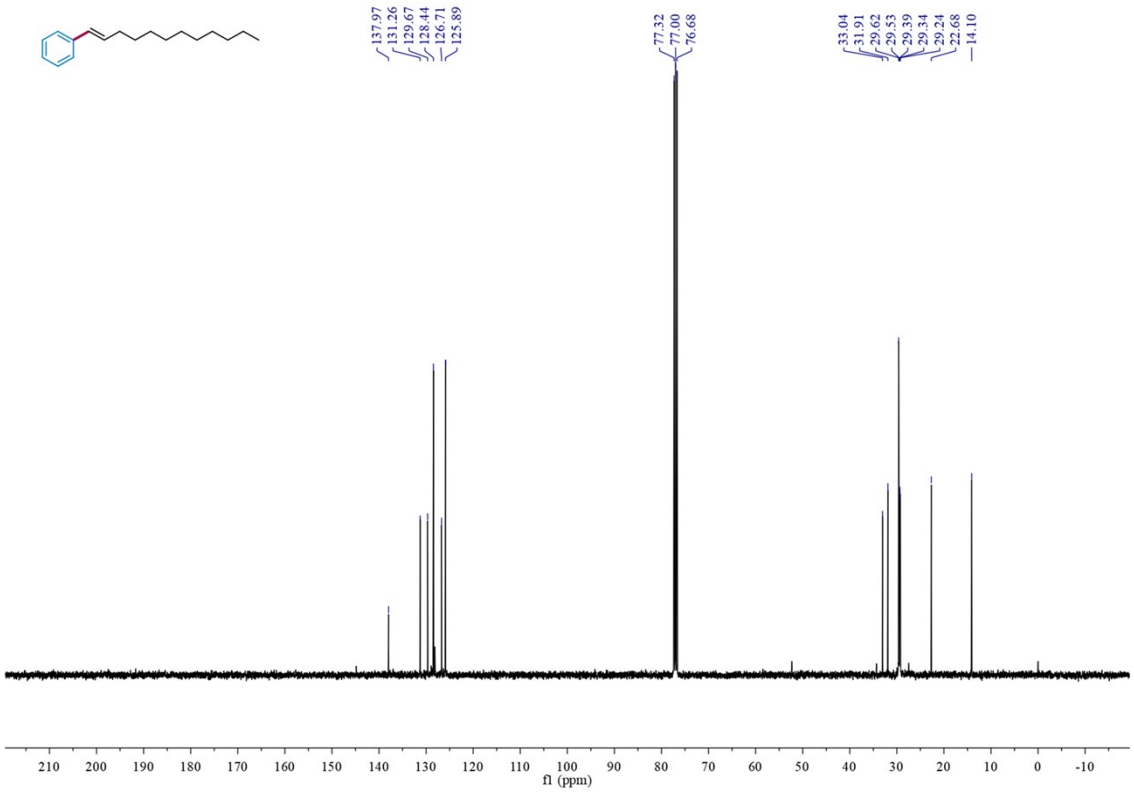

(*E*)-(3,3-dimethylbut-1-en-1-yl)benzene (**5d**)

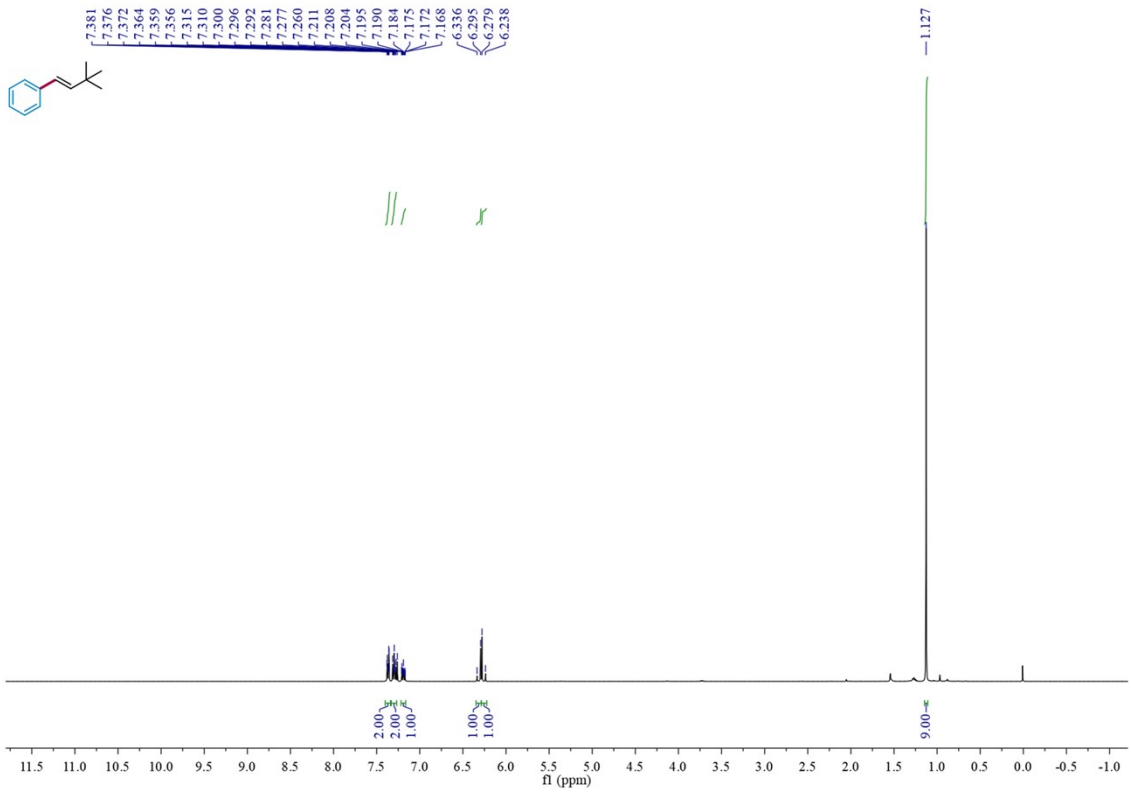

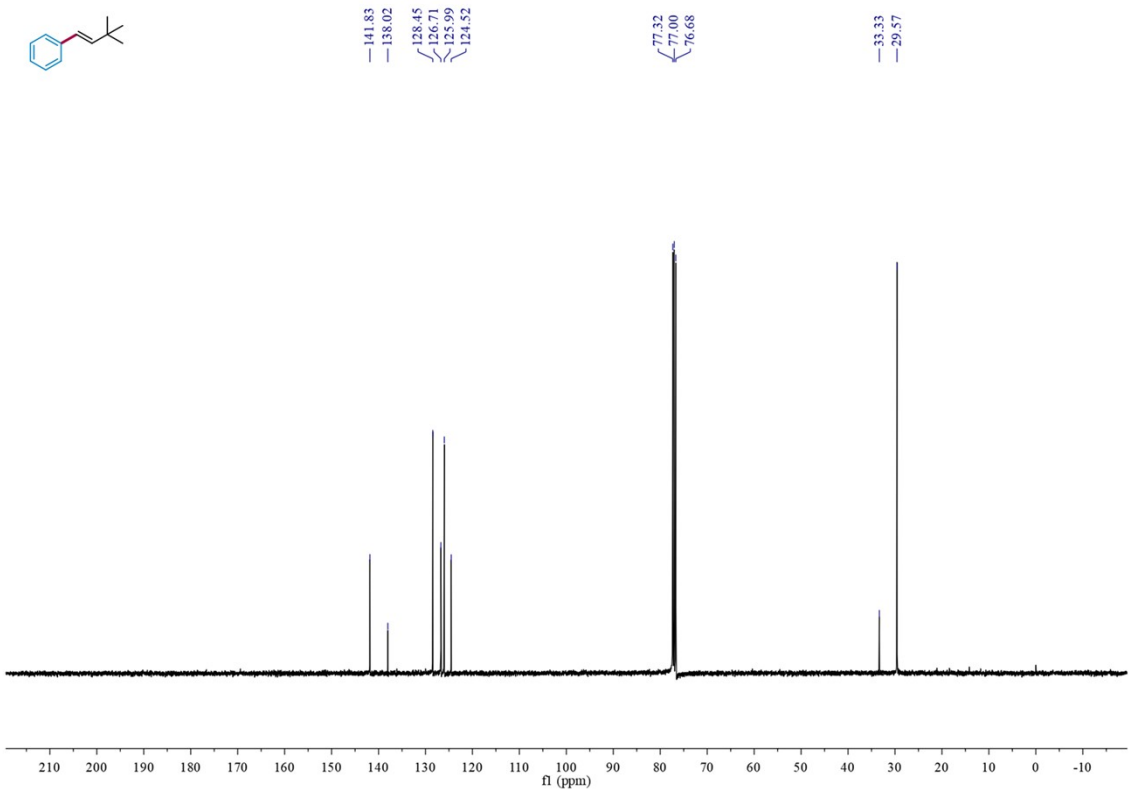

(*E*)-1-(3,3-dimethylbut-1-en-1-yl)-4-isopropylbenzene (**5e**)

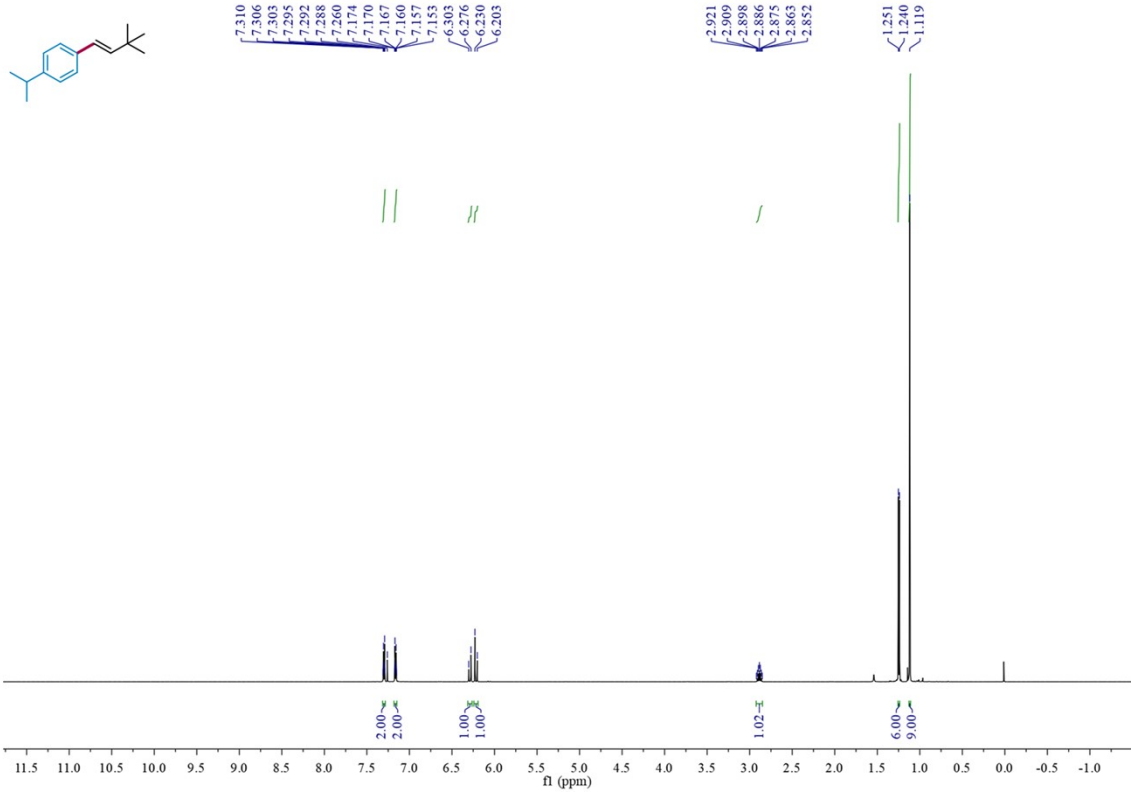

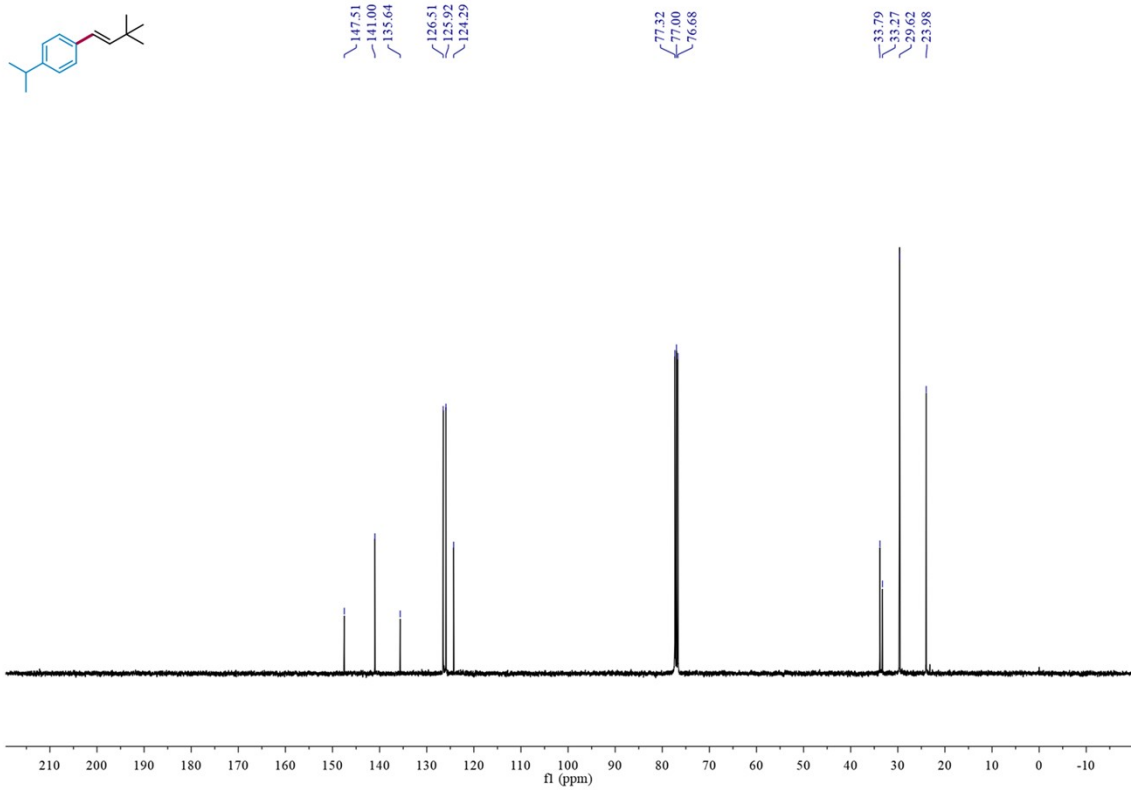

(*E*)-4-(3,3-dimethylbut-1-en-1-yl)-1,2-dimethylbenzene (**5f**)

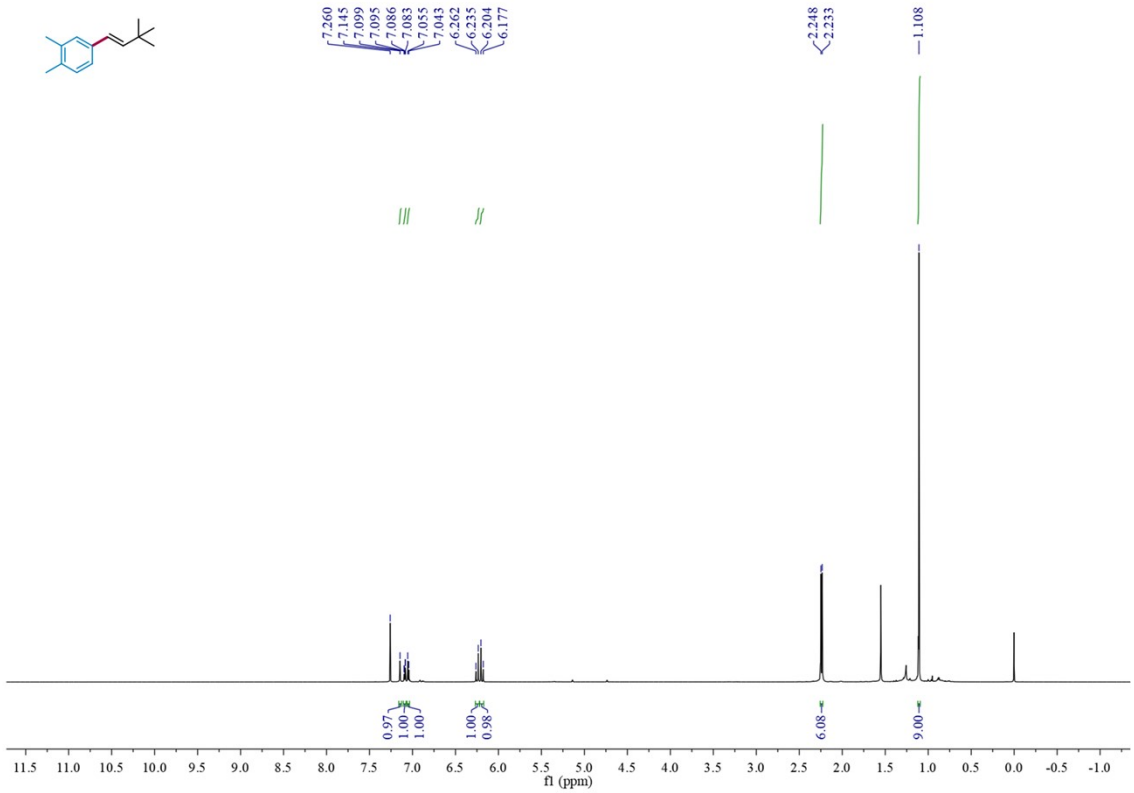

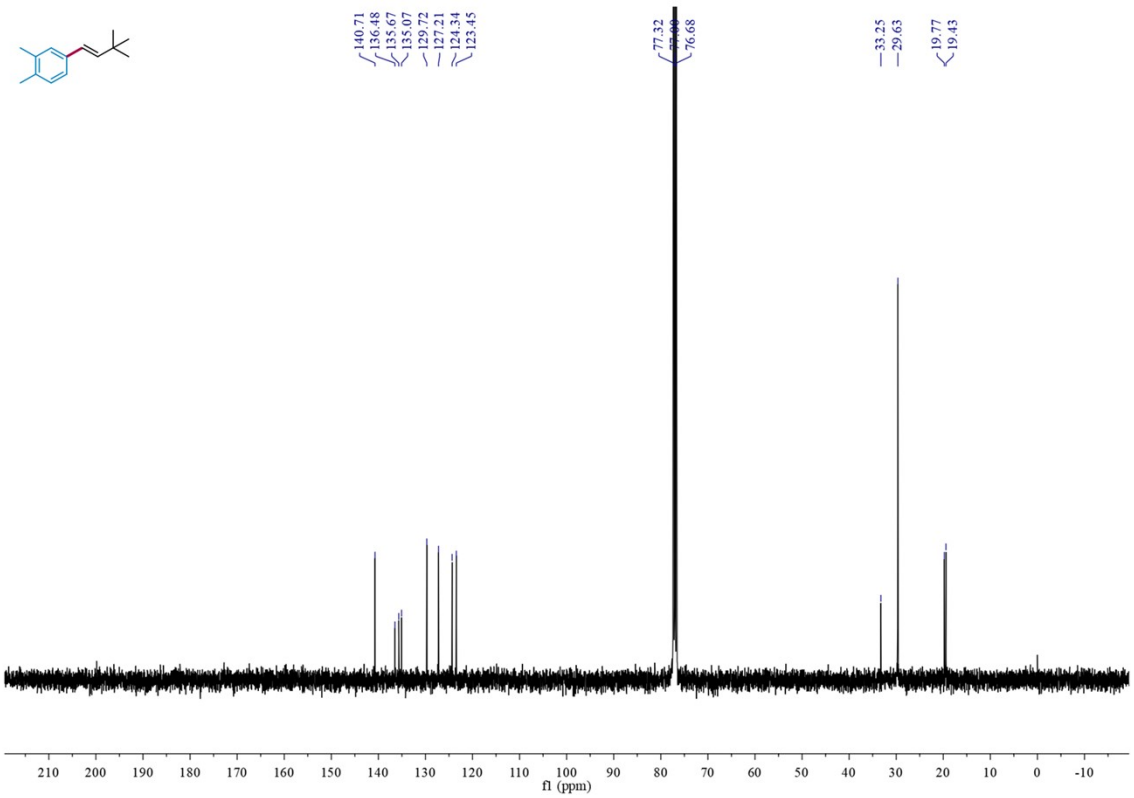

methyl (*E*)-5-(4-bromophenyl)-3,3-dimethylpent-4-enoate (**5g**)

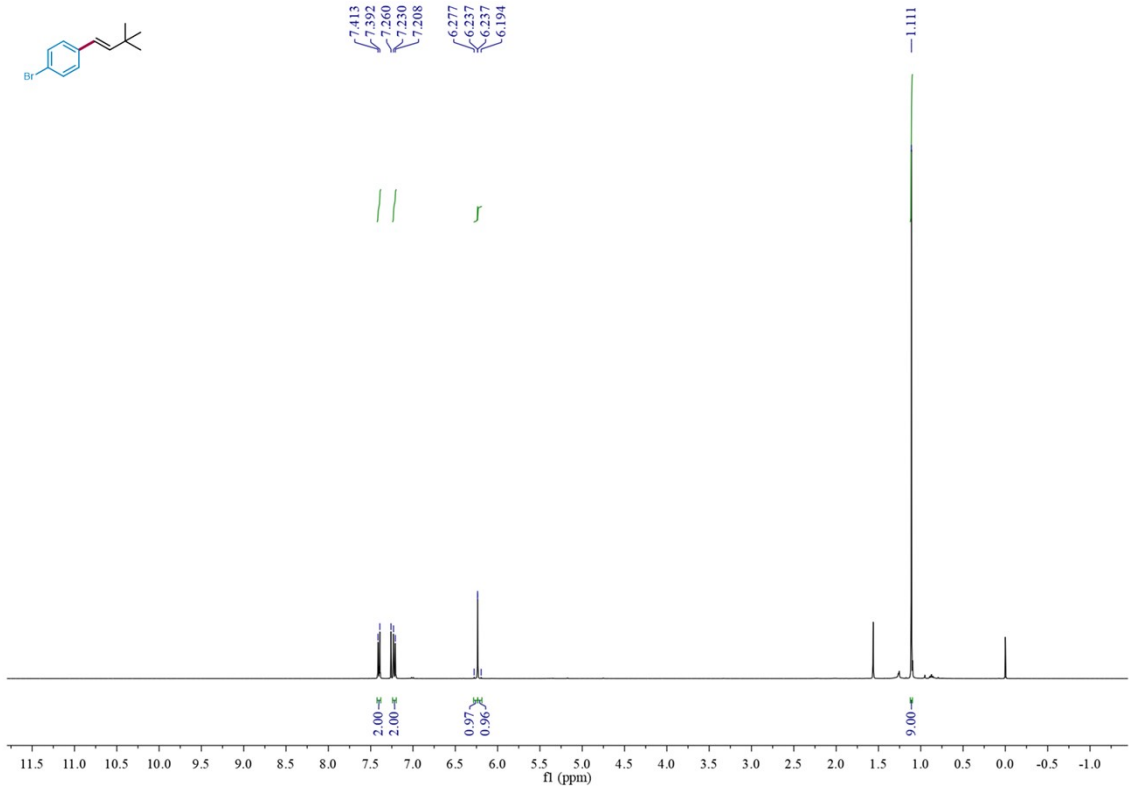

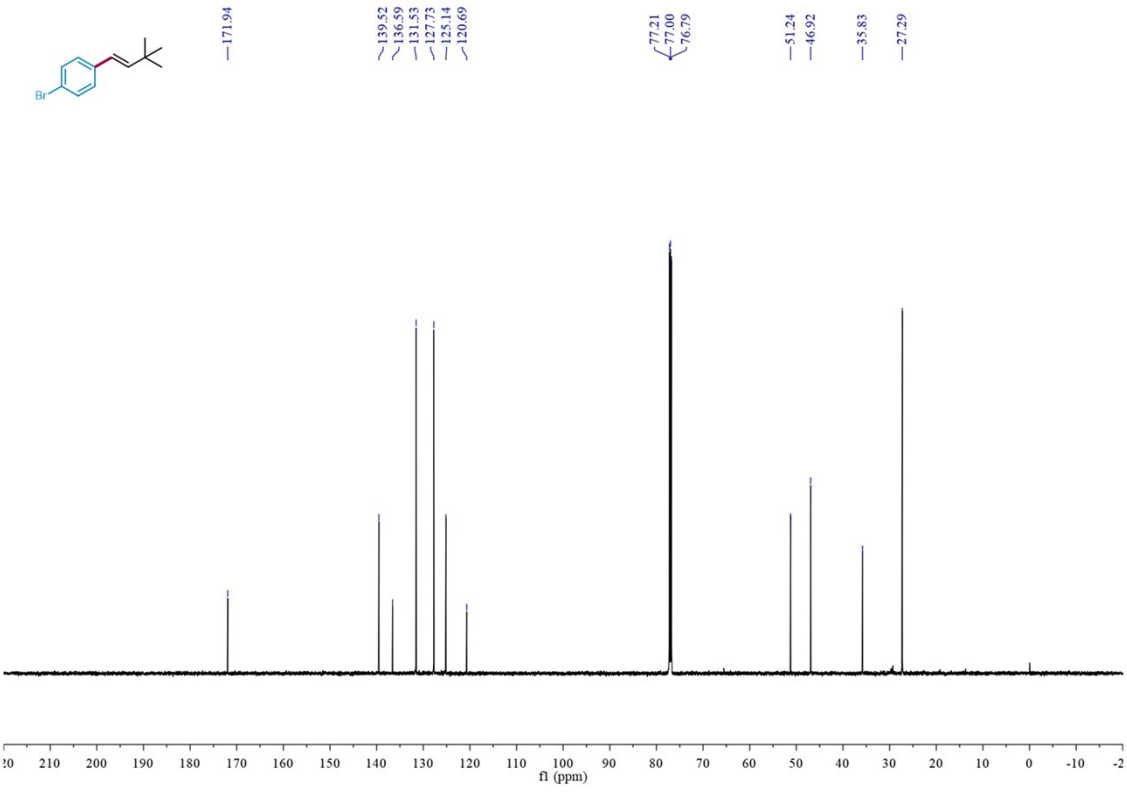

(*E*)-1-(3,3-dimethylbut-1-en-1-yl)-3,5-bis(trifluoromethyl)benzene (**5h**)

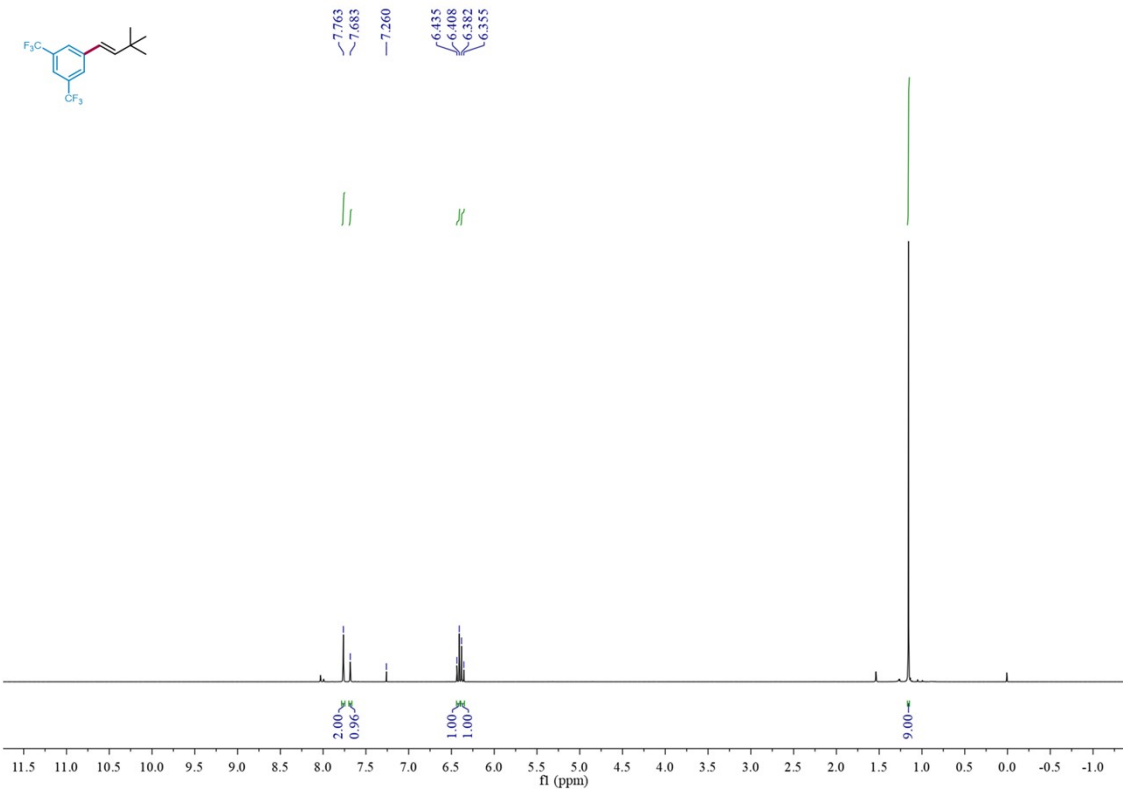

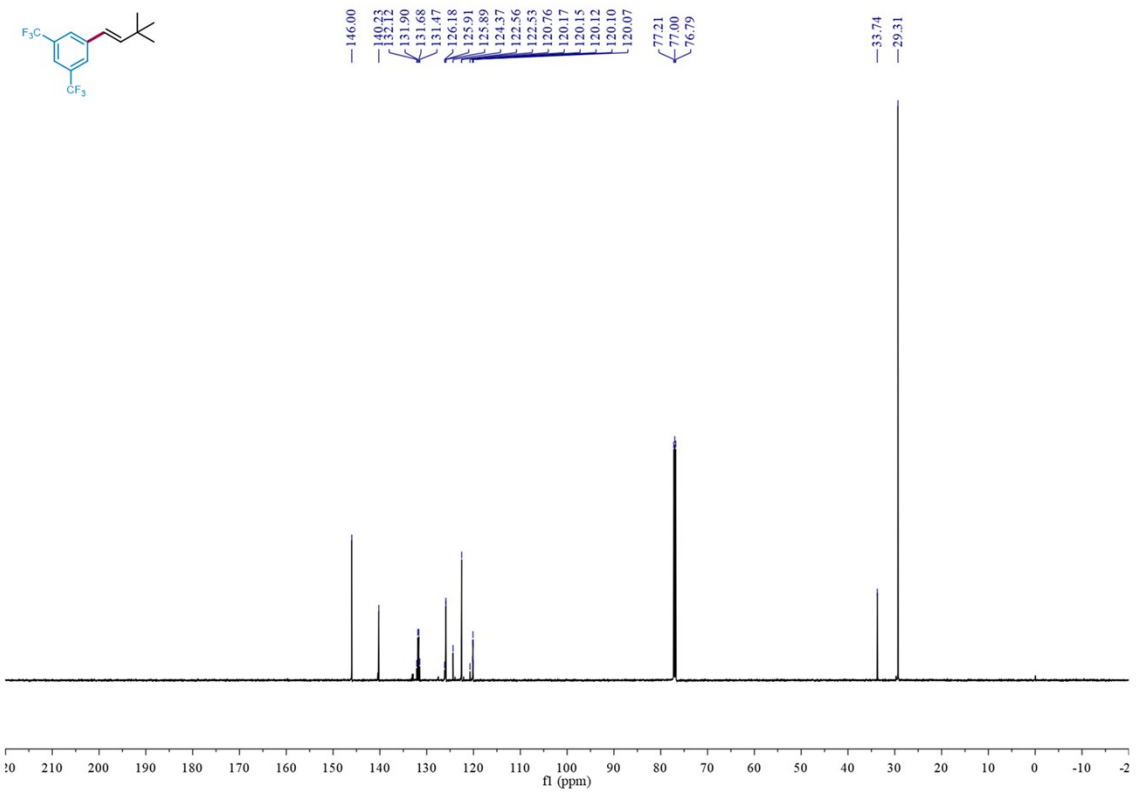

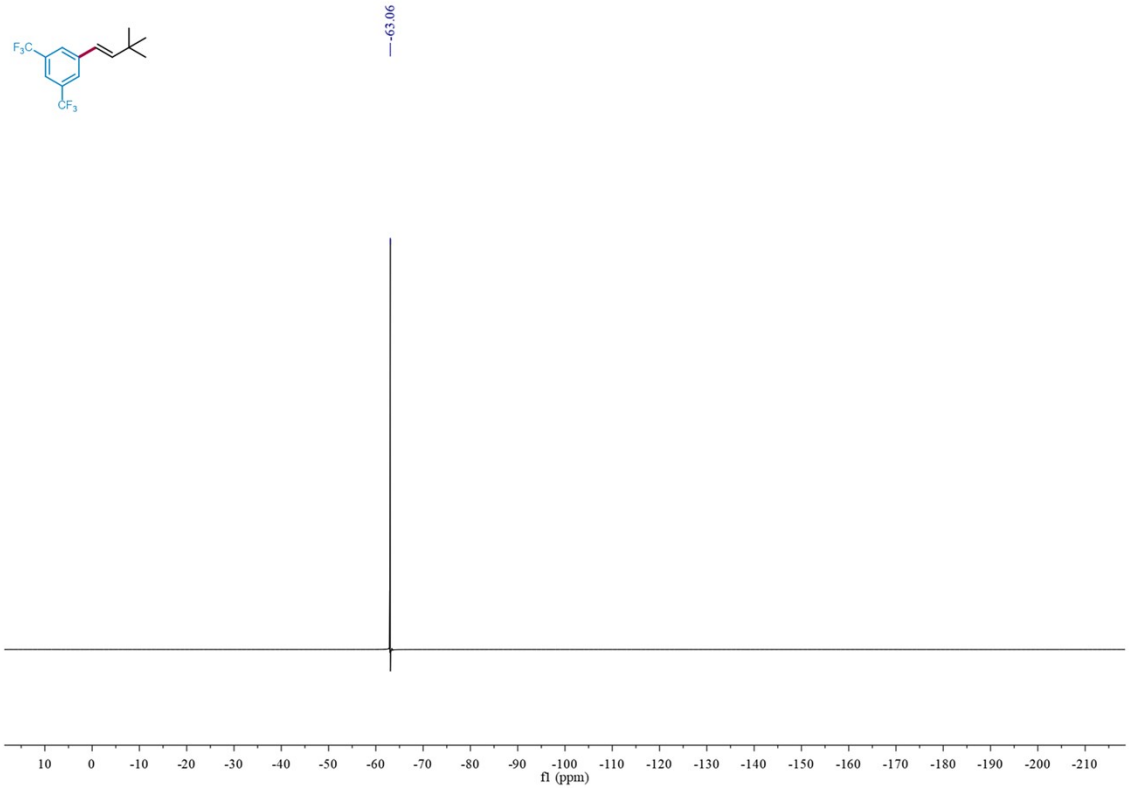
-63.06
10
0
-10
-20
-30
-40
-50
-60
-70
-80
-90
-100
-110
-120
-130
-140
-150
-160
-170
-180
-190
-200
-210
f1 (ppm)

(*E*)-3-benzylidene-2,2-dimethylbicyclo[2.2.1]heptane (**5i**)

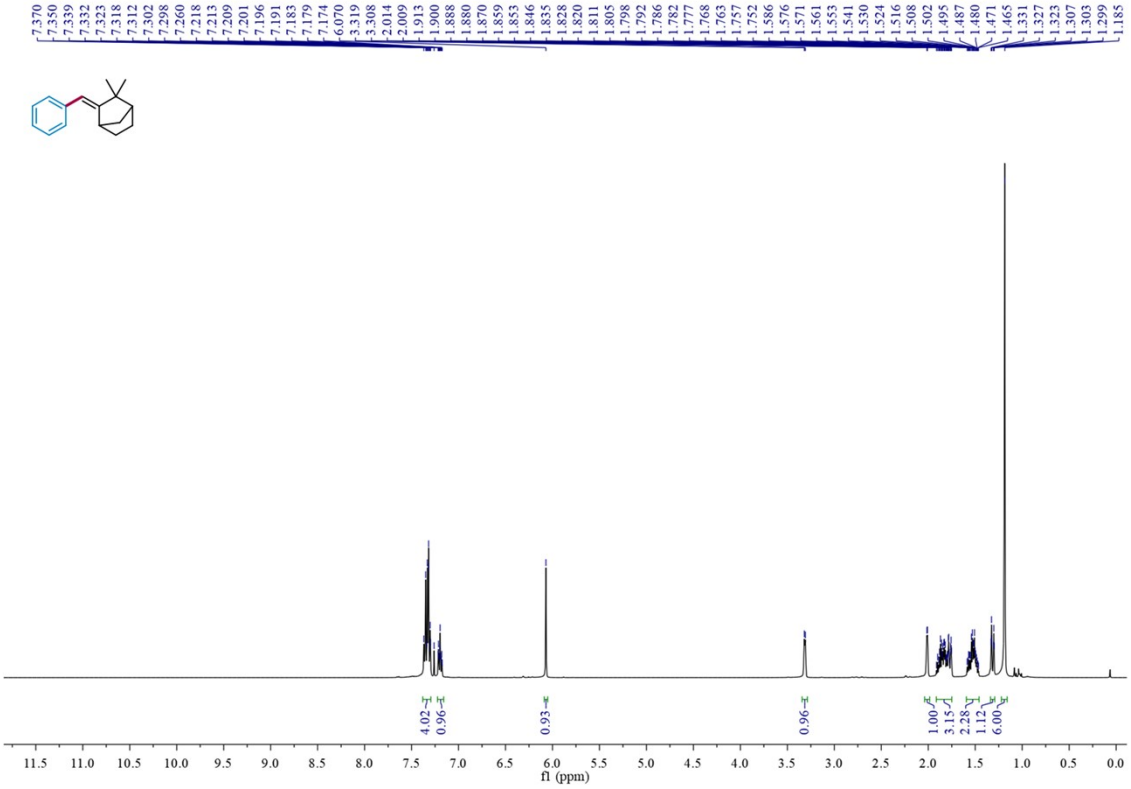

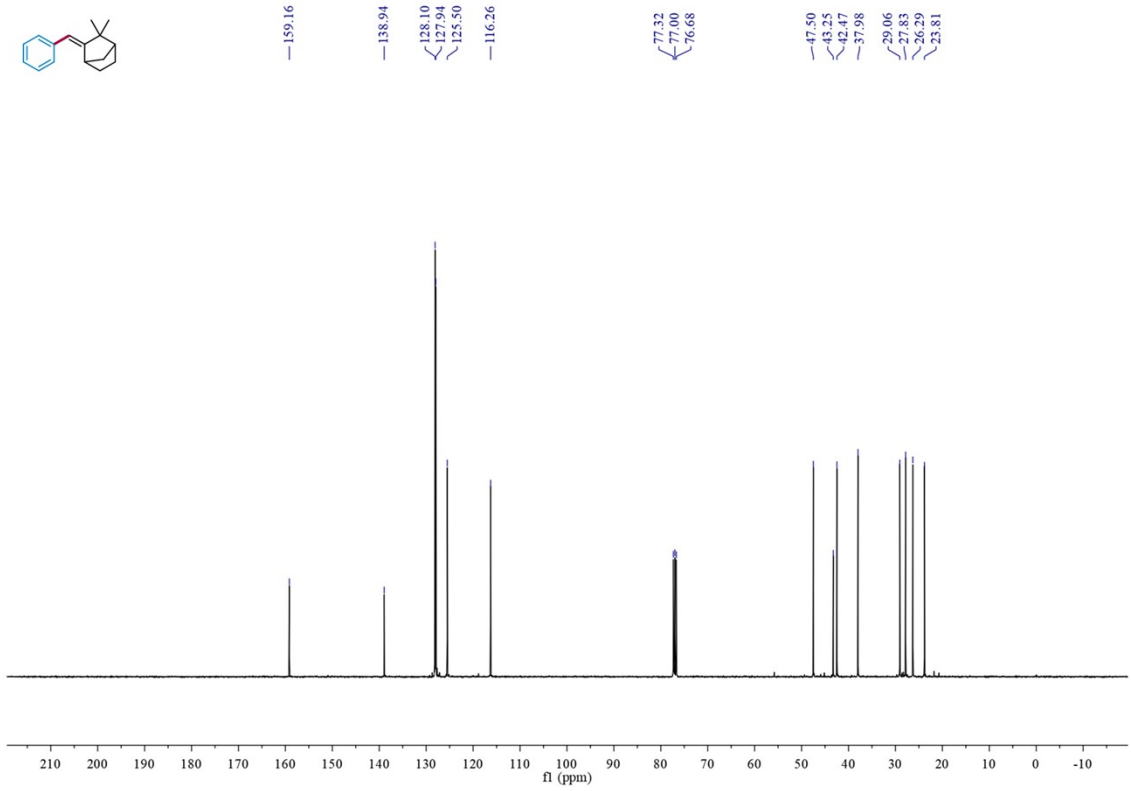

(*E*)-(2,4,4-trimethylpent-1-en-1-yl)benzene (**5j**)

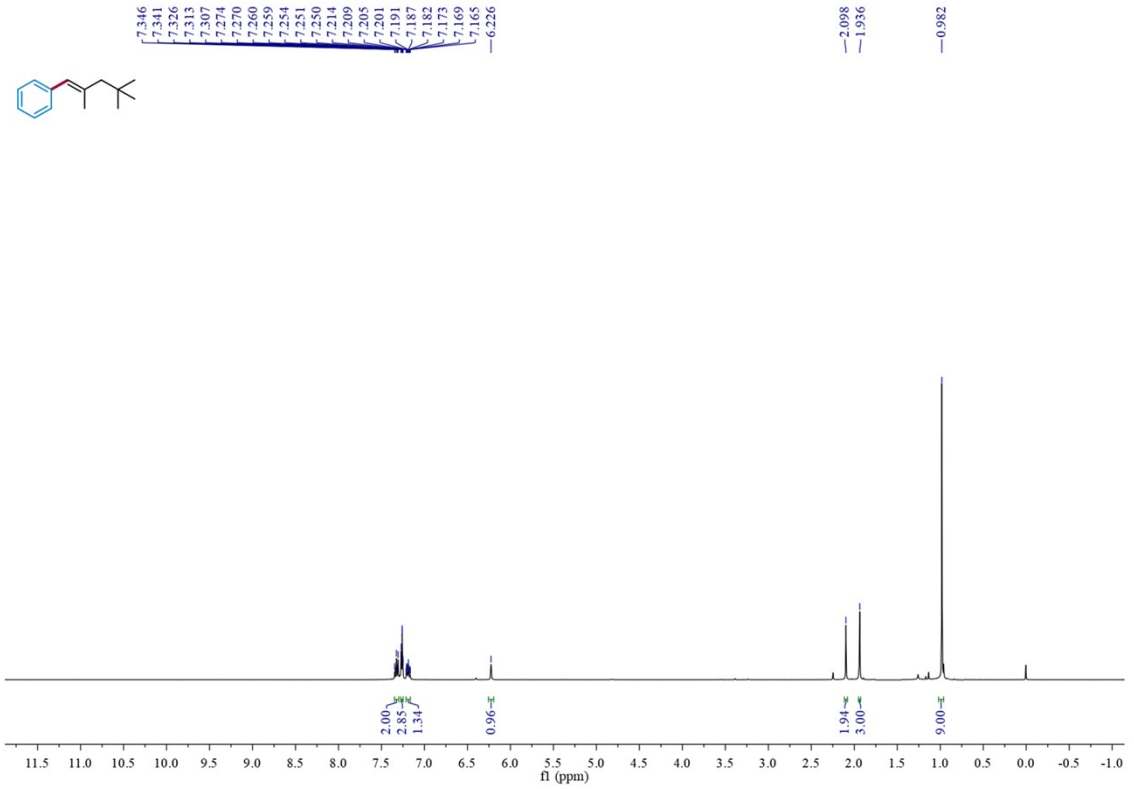

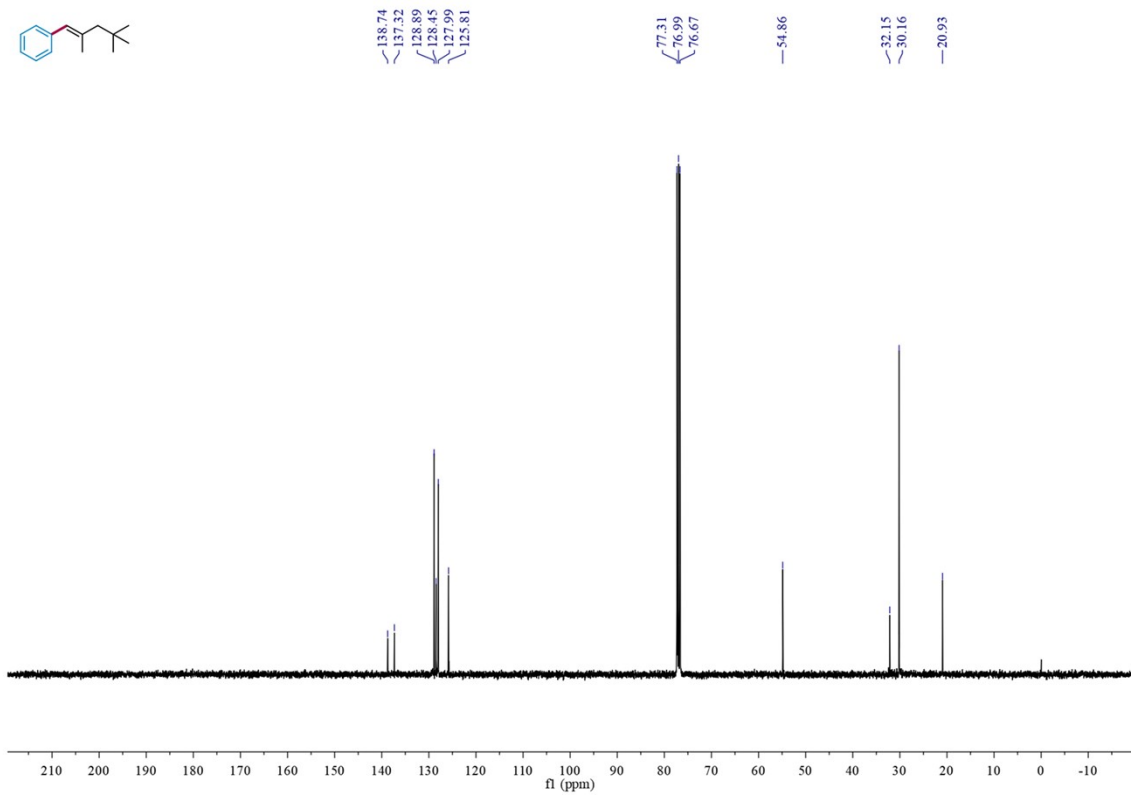

(*E*)-(2-cyclohexylvinyl)benzene (**5k**)

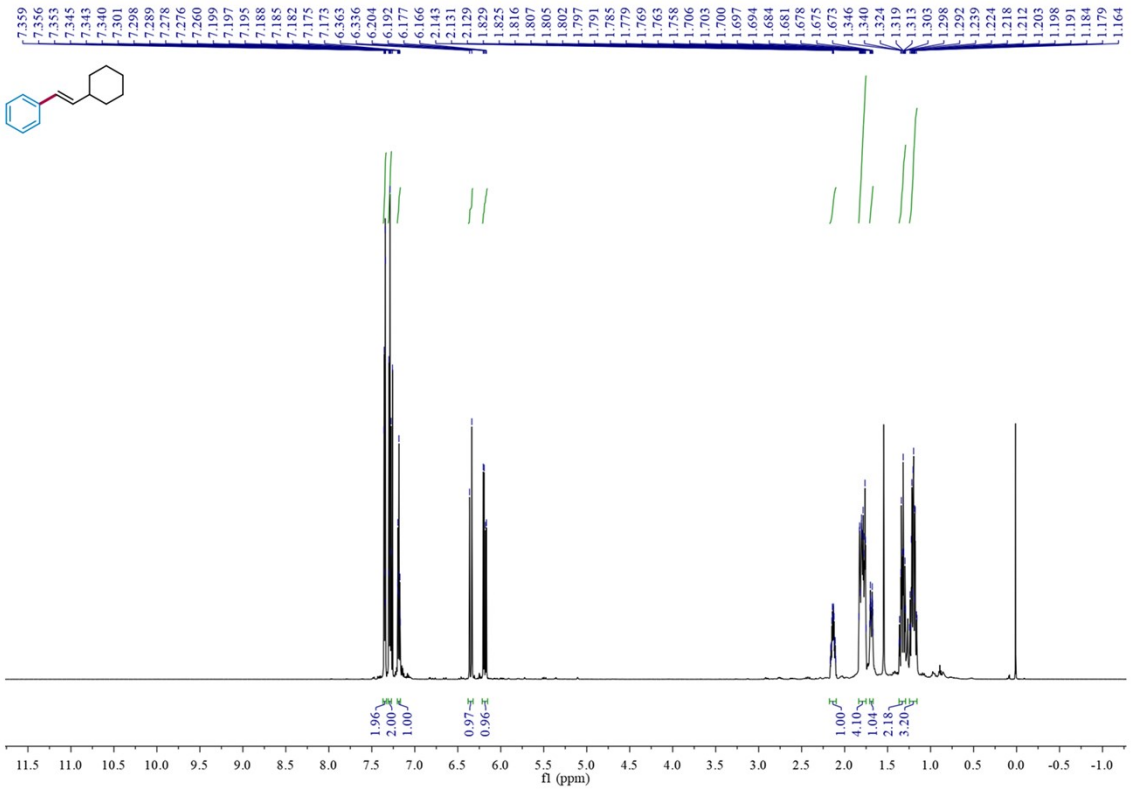

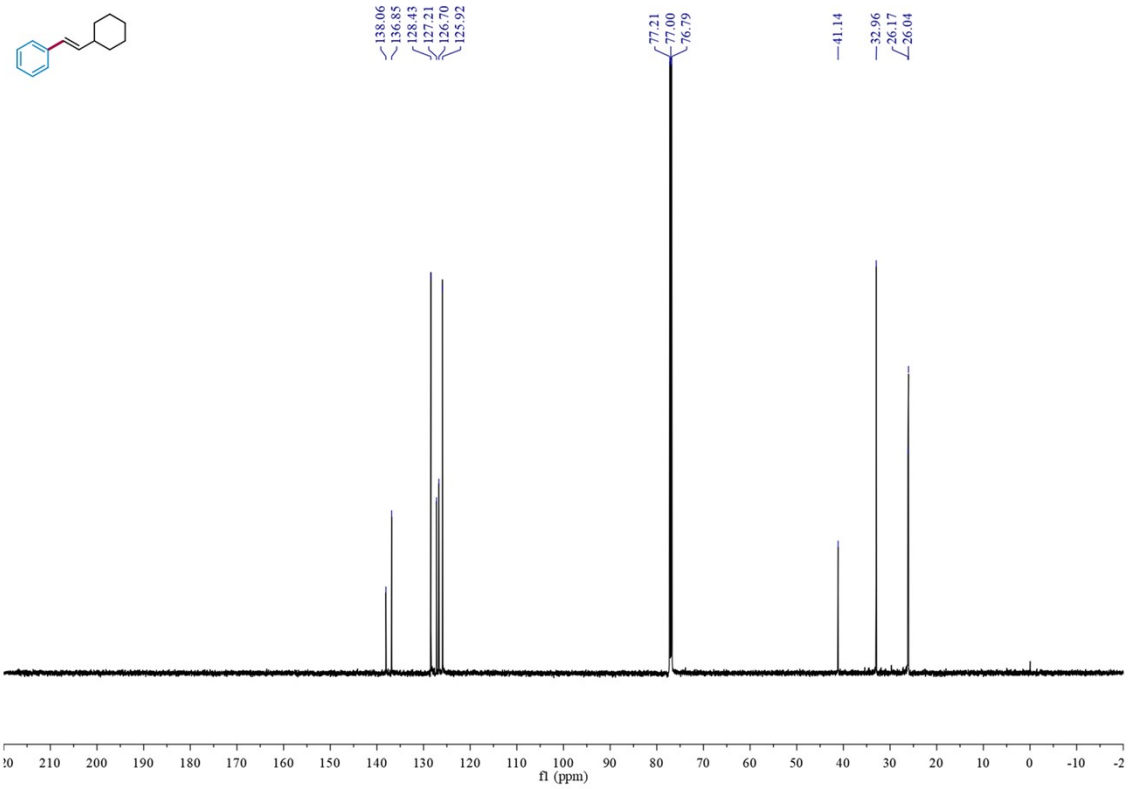

3-Phenylcyclopentene (**5l**)

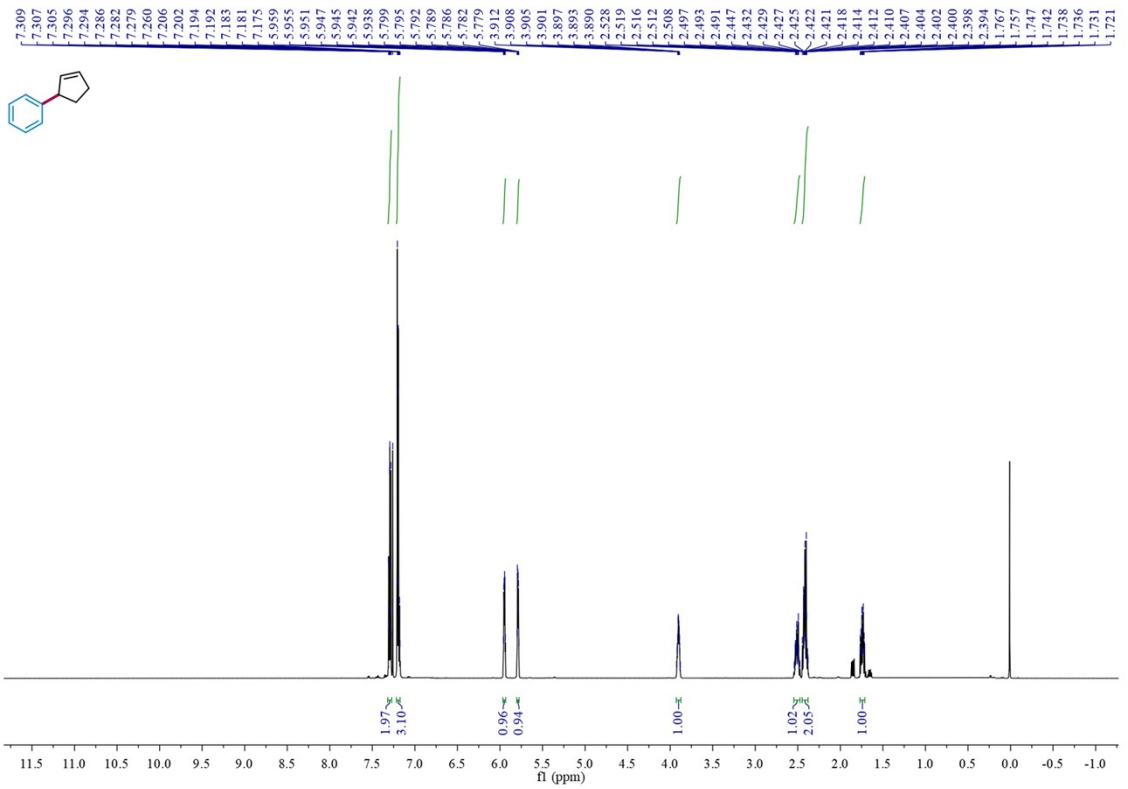

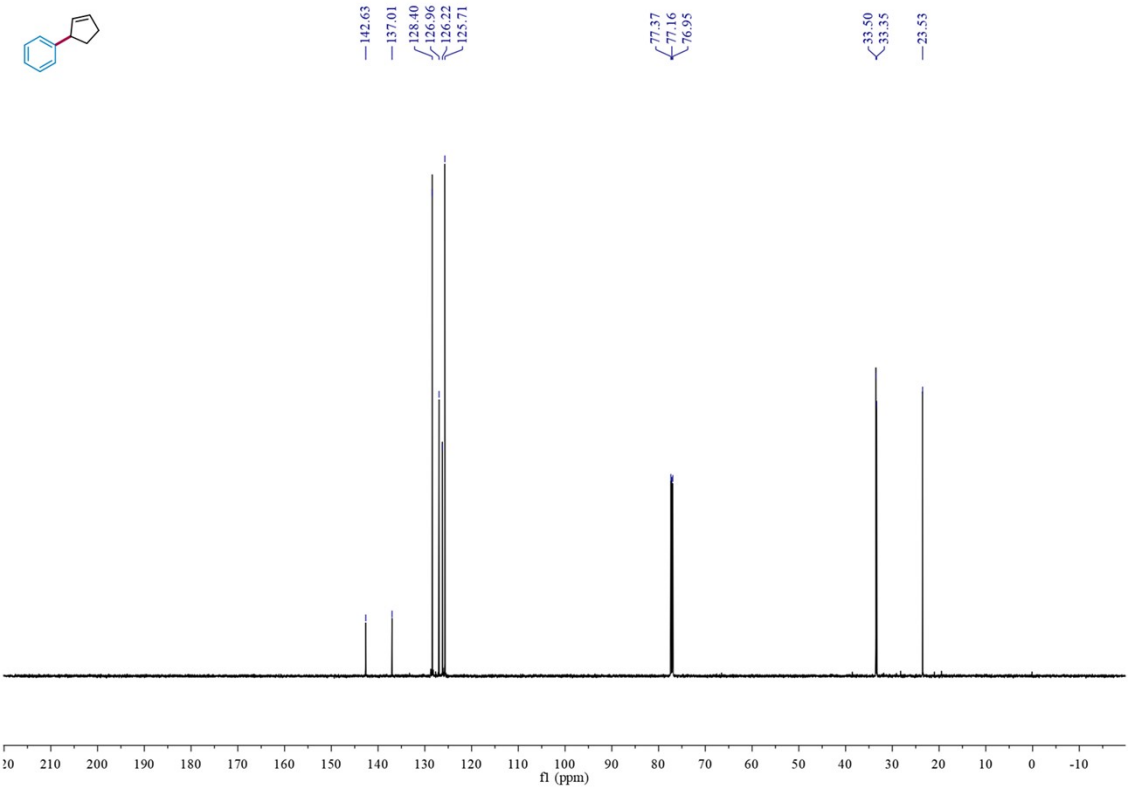

3-phenylcyclohexene (**5m**)

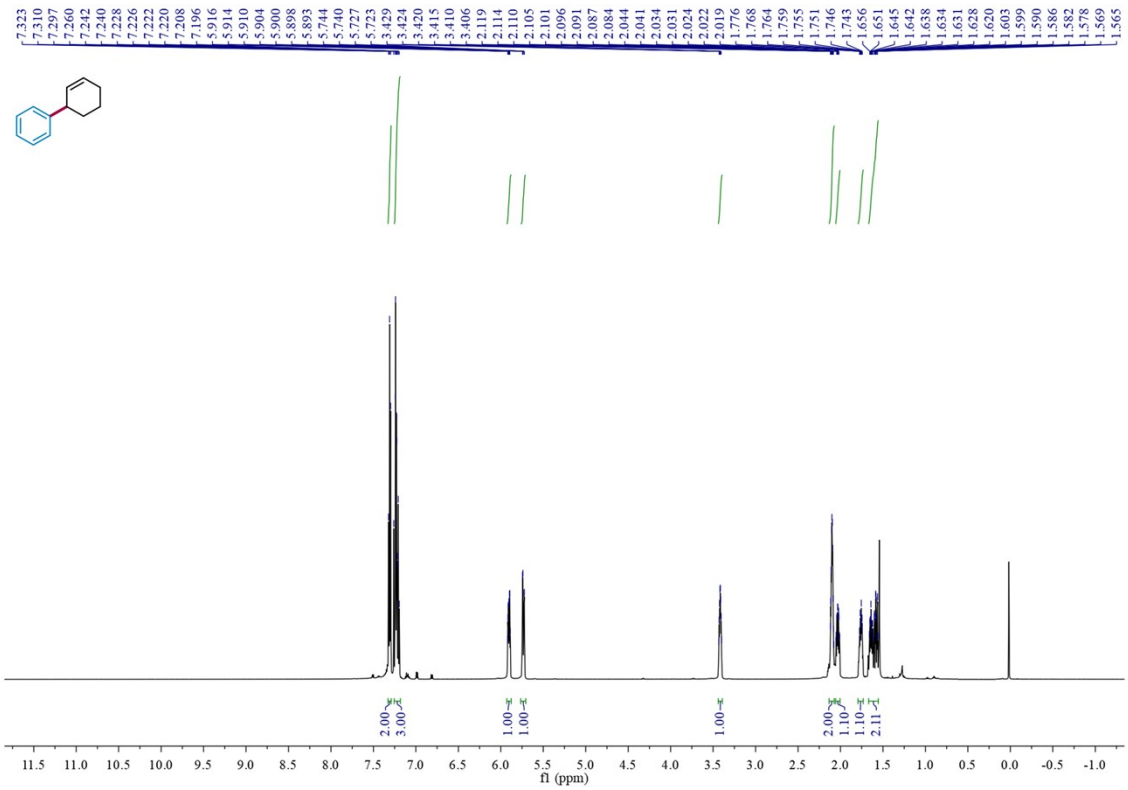

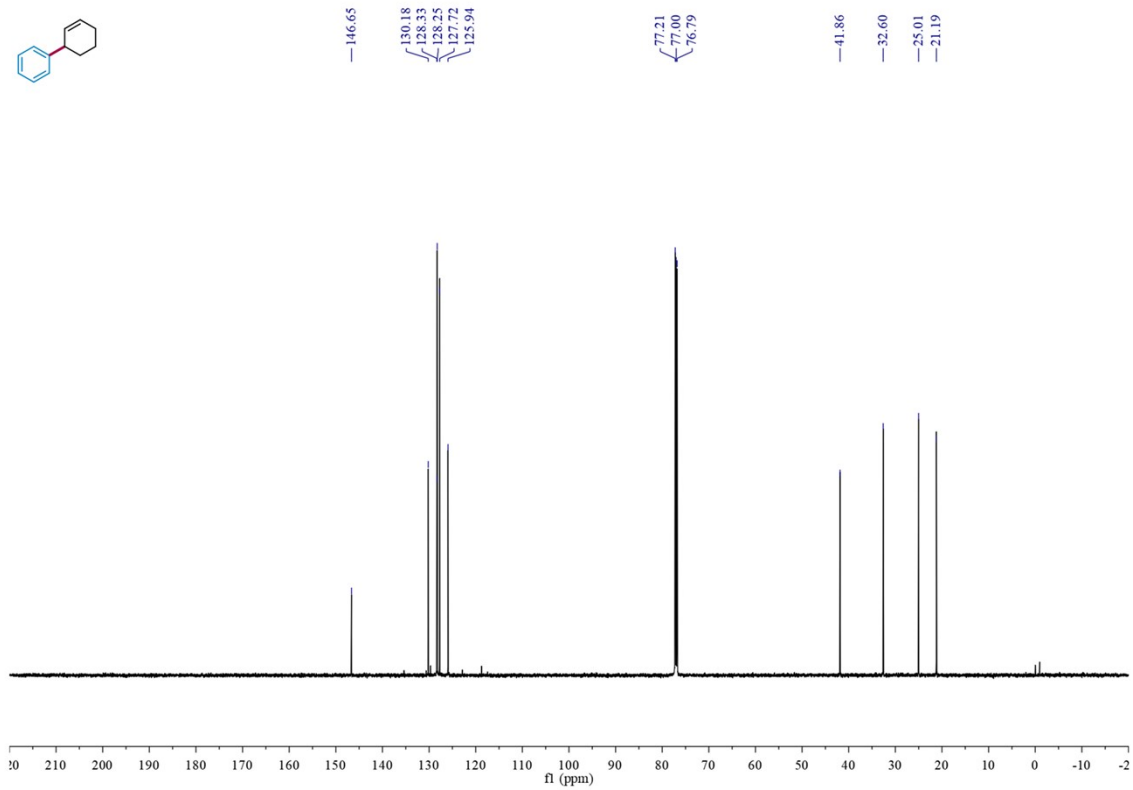

3-Phenyl-1-cyclooctene (**5n**)

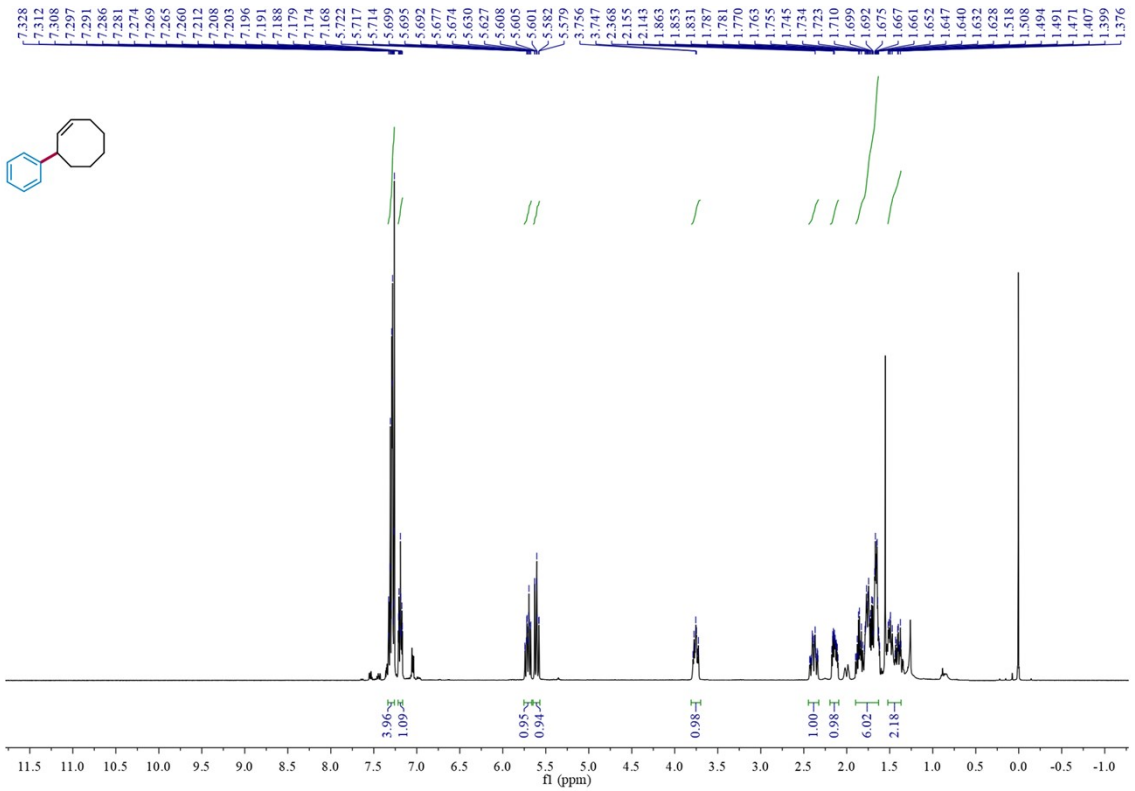

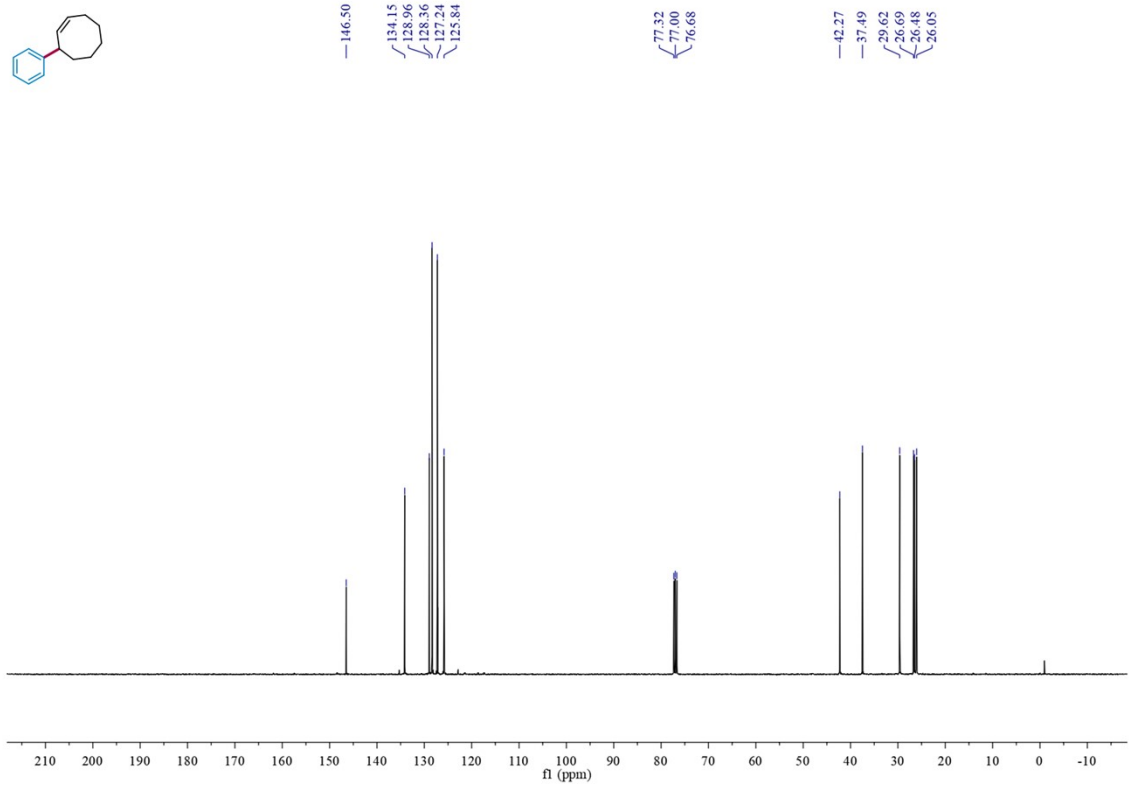

8. References

[1] B. Du, Y. Ouyang, Q. Chen and W. Yu, *J. Am. Chem. Soc*. **2021**, *143*, 14962–14968.

[2] J. Bauer, W. Frey and R. Peters, *Angew. Chem. Int. Ed*. **2014**, *53*, 7634–7638.

[3] E. Li, O. Apolinar, R. Deng and K. Engle, *Chem. Sci*. **2021**, *12*, 11038–11044.

[4] D. Taber, J. Berry and T. Martin, *J. Org. Chem*. **2008**, *73*, 9334–9339.

[5] S. Maity, R. Kancherla, U. Dhawa, E. Hoque, S. Pimparkar and D. Maiti, *ACS Catal*. **2016**, *6*, 5493–5499.

[6] H. Clavier, J. Broggi and S. Nolan, *Eur. J. Org. Chem*. **2010**, 937–943.

[7] K. Bian, D. Nemoto Jr., S. Kao, et al, *J. Am. Chem. Soc*. **2022**, *144*, 11810–11821.

[8] E. Falk, S. Makai, T. Delcaillau, et al, *Angew. Chem. Int. Ed*. **2020**, *59*, 21064–21071.

[9] A. Tomer, B. Kusema, J. Paul, et al. *J. Catal*. **2018**, *368*, 172−189.

[10] E. Werner and M. Sigman, *J. Am. Chem. Soc*. **2011**, *133*, 9692−9695.

[11] Y. Zou and J. Zhou, *Chem. Commun*. **2014**, *50*, 3725−3728.

[12] A. Mikhaylov, A. Dilman, R. Novikov, et al, *Tetrahedron Lett*. **2016**, *57*, 11−14.

[13] N. Thiel, B. Kaewmee, T. Ngoc, et al. *Chem. Eur. J*. **2020**, *26* 1597−1603.

[14] F. Singh and T. Wirth, *Org. Lett*. **2011**, *13*, 6504−6507.

[15] E. Alacid and C. Nájera, *Org. Lett*. **2008**, *10*, 5011−5014.

[16] J. Cotter, A. Hogan, and D. O'Shea, *Org. Lett*. **2007**, *9*, 1493−1496.

[17] J. Yu, H. Shou, W. Yu, H. Chen and W. Su, *Adv. Synth. Catal*. **2019**, *361*, 5133−5139.

[18] J. Han, X. Sun, X. Wang, et al. *Org. Lett*. **2020**, *22*, 1480−1484.

[19] K. Bojaryn, S. Fritsch and C. Hirschhäuser, *Org. Lett*. **2019**, *21*, 2218–2222.

[20] G. Hilt and C. Hengst, *Synlett* **2006**, *19*, 3247−3250.

[21] X. Han, Y. Zhang and J. Wu, *J. Am. Chem. Soc*. **2010**, *132*, 4104–4106.

[22] A. Fürstner, R. Martin, H. Krause, G. Seidel, et al, *J. Am. Chem. Soc*. **2008**, *130*, 8773–8787.